Evolution of Circumstellar Disks and Planet Formation

Wladimir Lyra

New Mexico State University

UNSAM – Buenos Aires - Aug 8th, 2024

Quick Bio

Wladimir Lyra

Interests: Planet formation, accretion disks, hydrodynamics, computational methods.

Faculty
New Mexico State University, NM 2019 – (tenured 2022).
California State University, Northridge **CA,** 2015-2019.

Visiting Faculty
Nagoya University, Nagoya, **Japan** 2015.
Max-Planck Institute for Astronomy, Heidelberg **Germany** 2018, 2019.

Postdocs
Hubble Fellow @ Jet Propulsion Laboratory – Caltech, 2011-2015.
American Museum of Natural History (New York **NY**), 2009-2011.

Ph.D.
Uppsala University (Uppsala, **Sweden**), 2004-2009.
Nordic Institute for Theoretical Physics (Stockholm, **Sweden**).
Max-Planck Institute for Astronomy (Heidelberg, **Germany**).

Research Assistant
European Southern Observatory (Garching, **Germany**, 2003).
Cerro Tololo Interamerican Observatory (La Serena, **Chile**, 2003-2004).
Lisbon Observatory, **Portugal** (2003).
Space Telescope Science Institute (Baltimore **MD**, 2002).

B.Sc.
Federal University of Rio de Janeiro (**Brazil**), Astronomy, 1999-2003.

The PFITS+ Collaboration

Planet Formation in the Southwest

PI

Wladimir Lyra – *New Mexico State University*

Co-Is

Andrew Youdin – *University of Arizona*

Jake Simon – *Iowa State University*

Chao-Chin Yang – *University of Nevada, Las Vegas*

(now University of Alabama)

Orkan Umurhan – *NASA Ames*

Postdocs

Debanjan Sengupta - *Ames -> NMSU*

Leonardo Krapp - *UA -> Universidad Concepción*

Daniel Carrera - *ISU -> NMSU*

Rixin Li - *UA -> UC Berkeley*

Tabassum Tanvir - *ISU*

Graduate Students

NMSU - Daniel Godines, Victoria de Cun, Manuel Cañas.

ISU – Jeonghoon Lim, David Rea, Olivia Brouillette

UNLV – Alex Mohov, Stanley Baronett, Sricharan Balaji

UA – Eonho Chang

Current Funding

Astronomy and Astrophysics grants '20, '21, '24

Exoplanet Research Program – '23
Emerging Worlds – '21, '22, '23, '24
Future Investigators in NASA Earth and Space Science and Technology – '23,'24
Theoretical and Computational Astrophysics Networks – '20

NMSU Computational Astrophysics group

Postdoctoral Scholars

Debanjan Sengupta
Dust growth, meteoritics,
Turbulence and accretion.

Daniel Carrera
Planetesimal formation,
pebble accretion

Graduated and former members

Ali Hyder
Jupiter’s atmospheric
dynamics and geochemistry.

Manuel Cañas
Formation of Kuiper
belt objects.

Victoria de Cun
Planets in AGN disks

Graduate Students

Harrison Cook
5th year
Black hole mergers
Transients in AGN

Sarah Chinski
3rd year
Europa’s ice shell
convection

Daniel Godines
3rd year
Observational signatures of
streaming instability

Incoming graduate students

Eleanor Serviss
(U Montana)
Gravitational Instability

Leopold Hutnik
(U Wisconsin)
Kuiper belt objects

Olivia Brouilette
(Iowa State)
Early planet formation

Planet Formation

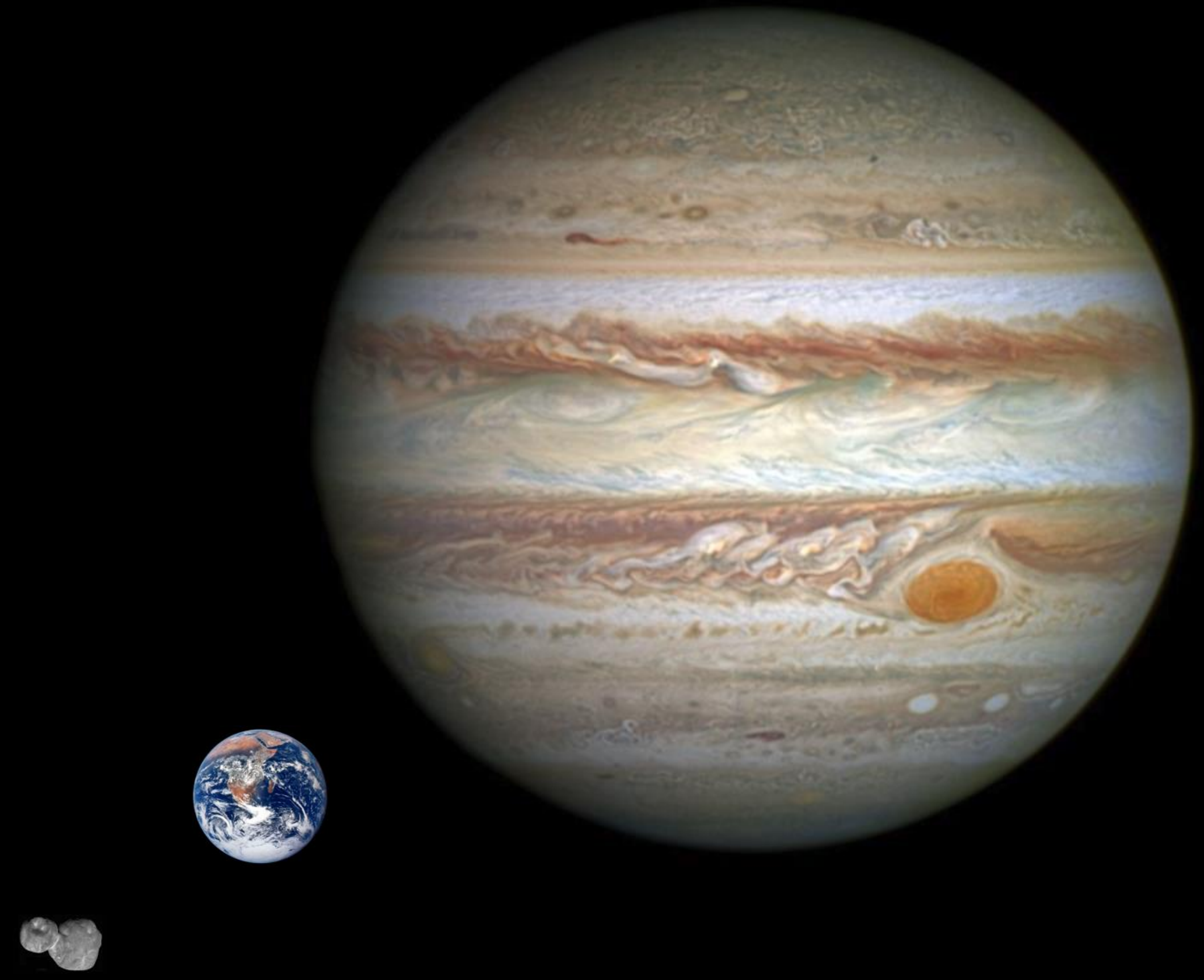

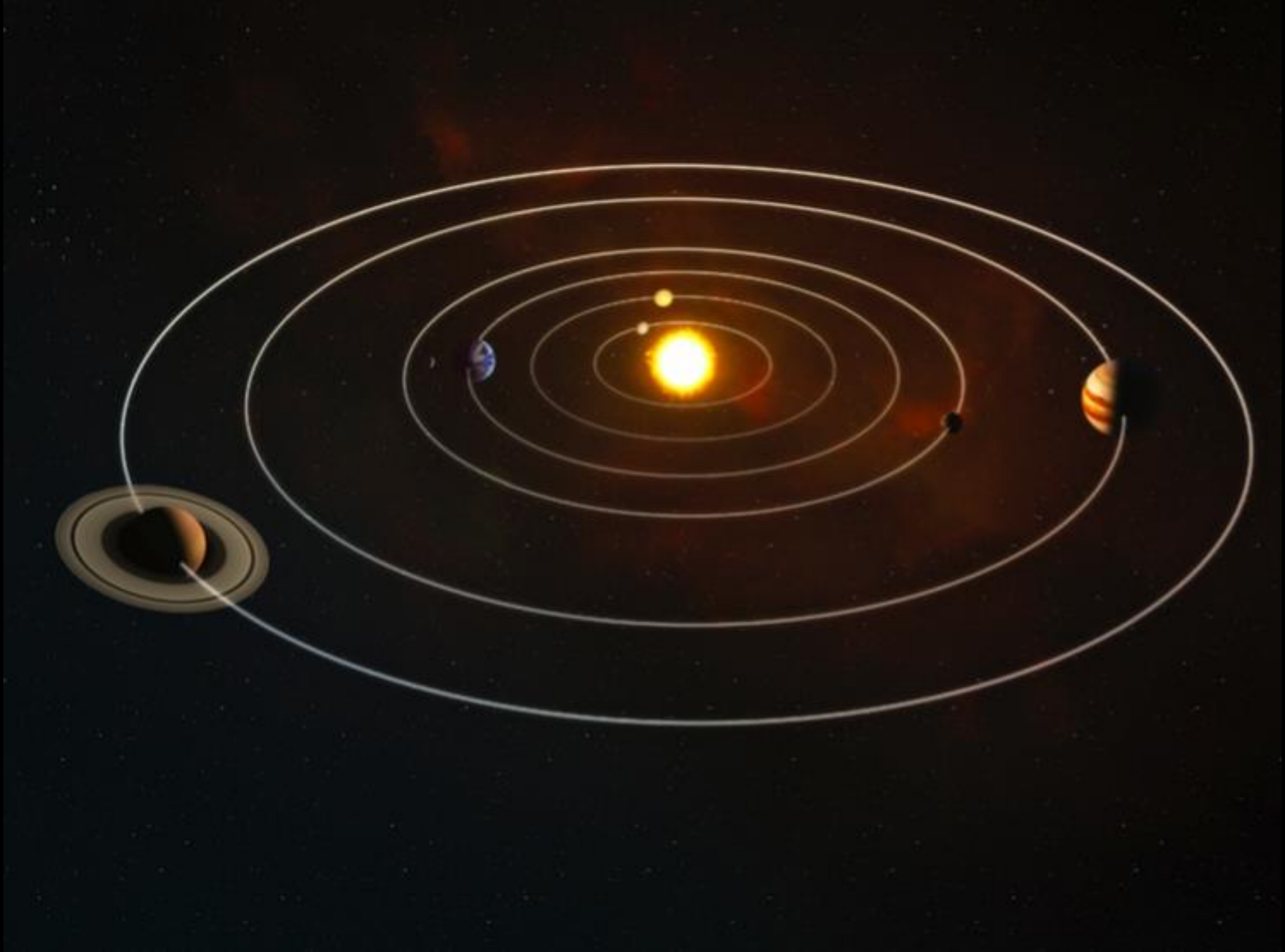

UK Astrophysical
Fluids Facility

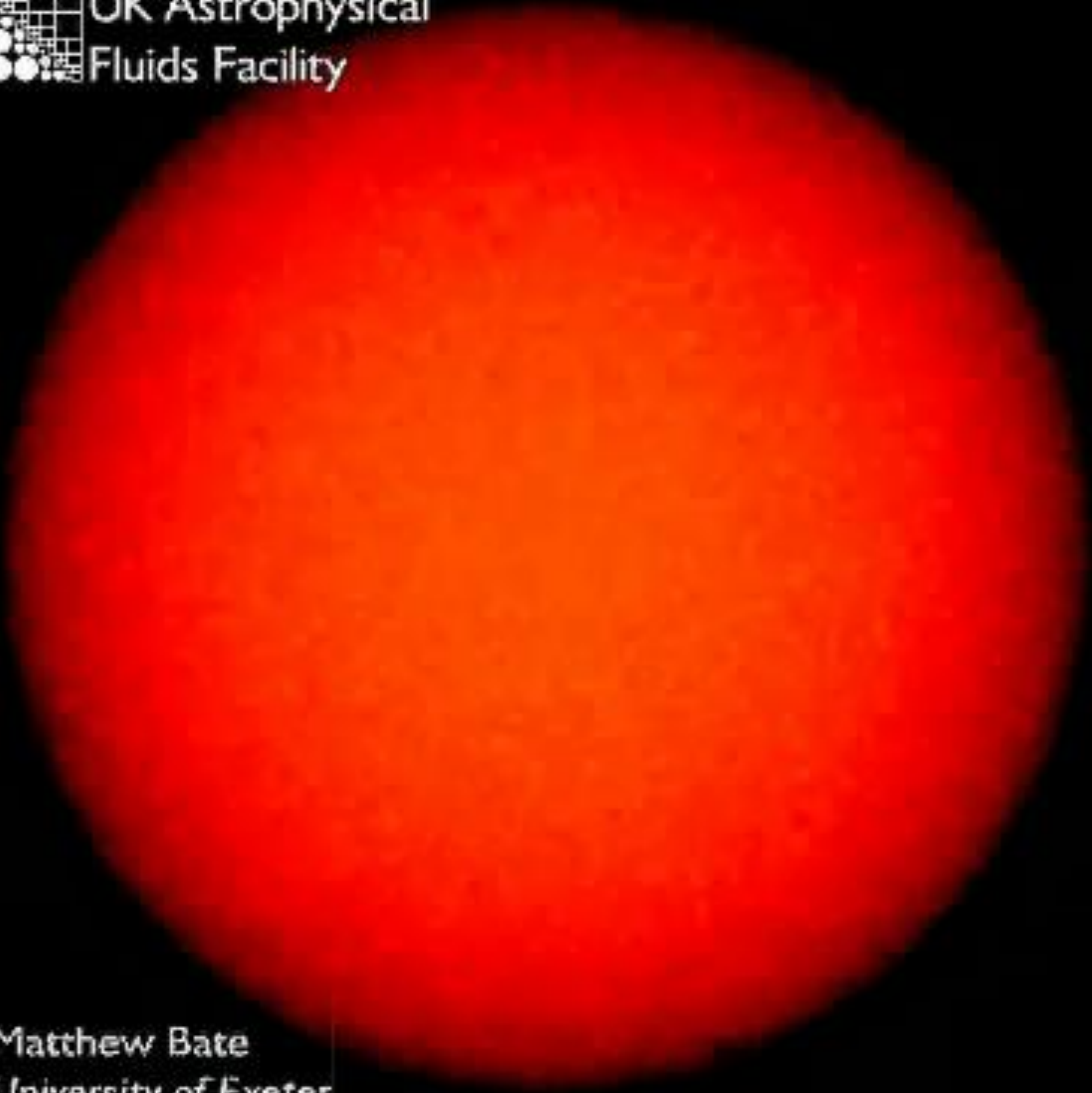

Matthew Bate
University of Exeter


Betelgeuse
Bellatrix
Orion's Belt
Orion Nebula
Rigel
Saiph

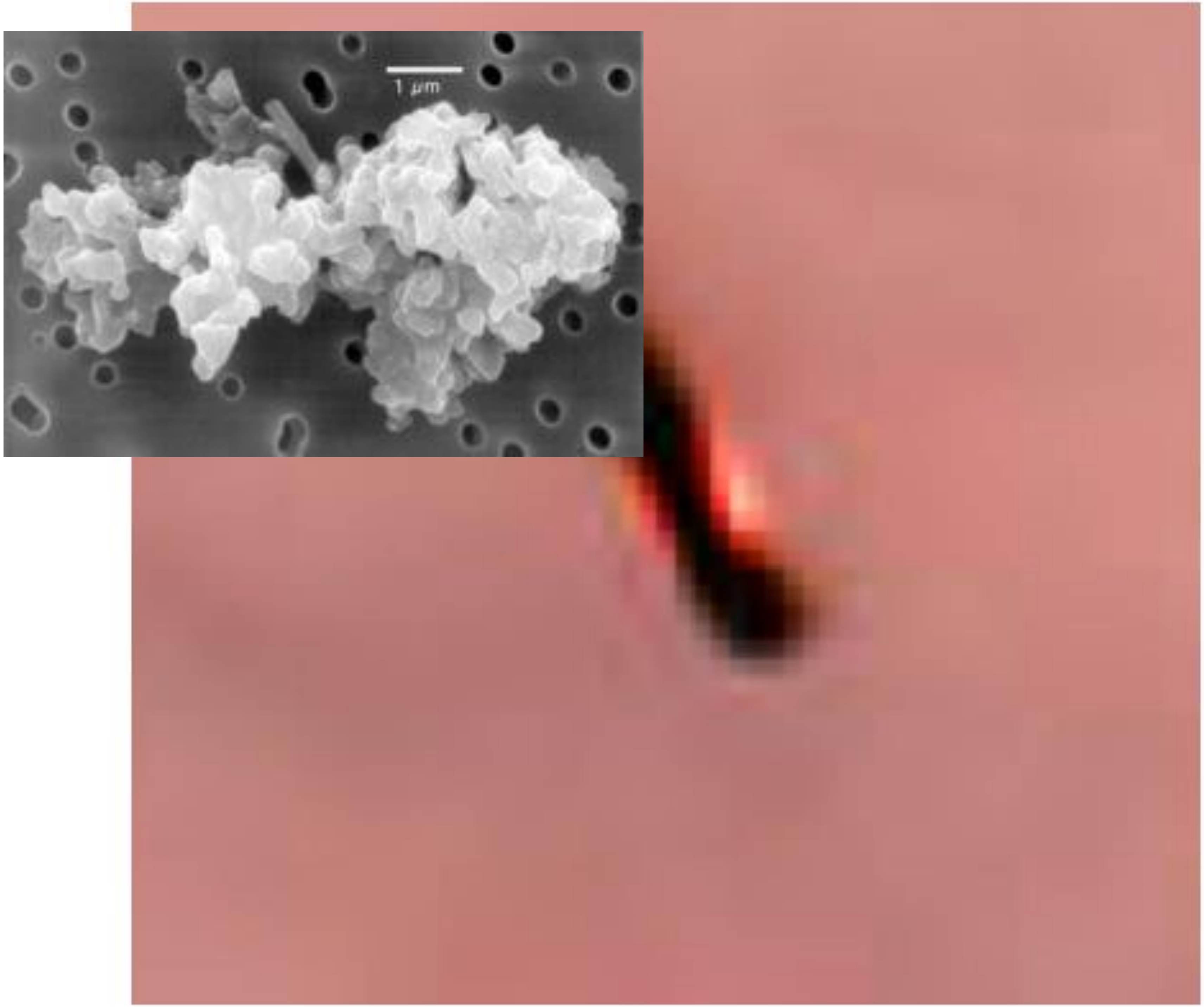
1 μm

Circumstellar/Protoplanetary Disks

PP disk fact sheet

Density: $10^{13} – 10^{15}$ cm^{-3}
(Air: 10^{21} cm^{-3})

Temperature: 10-1000 K

Scale: 0.1-100AU

Mass: $10^{-3} – 10^{-1}$ M_{sun}

Composition: 5:2 H_2-He mixture. 1% metals.

The Astronomer’s Periodic Table

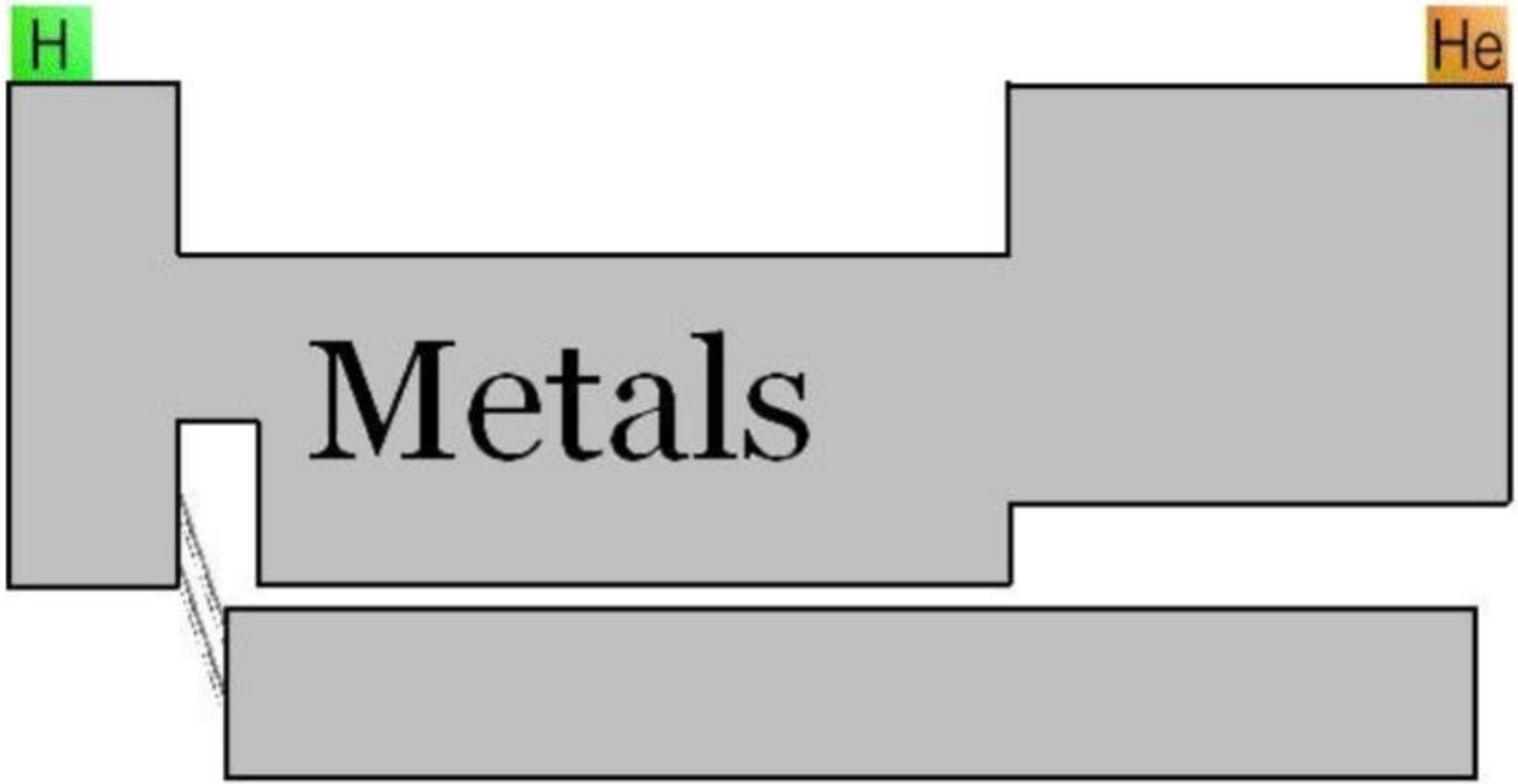

Planet Formation

"Planets form in disks of gas and dust"

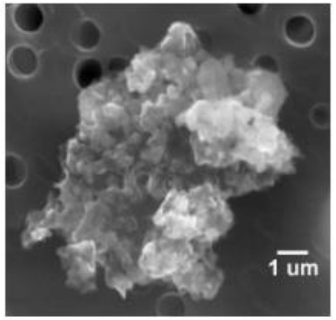

A miracle happens →

Dust evolution

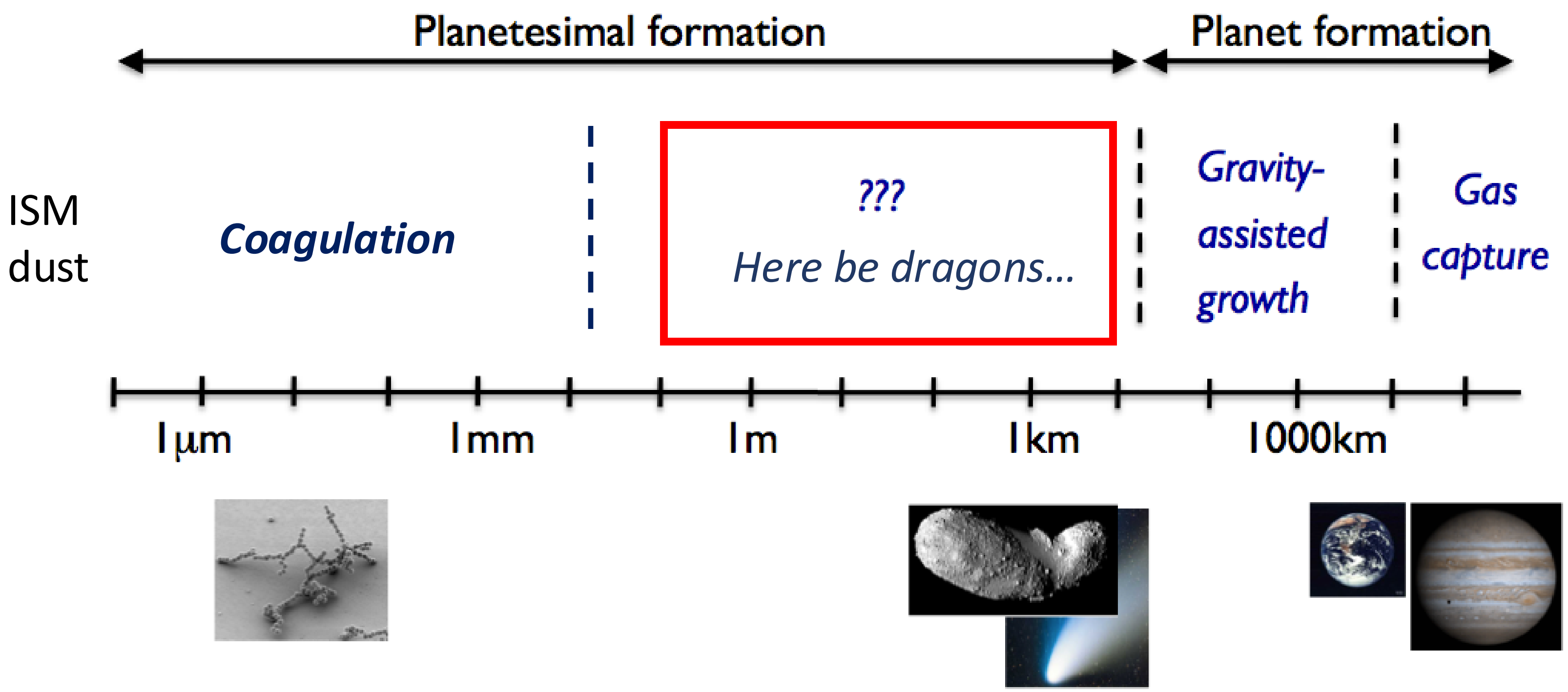

Headwind and Dust Drift

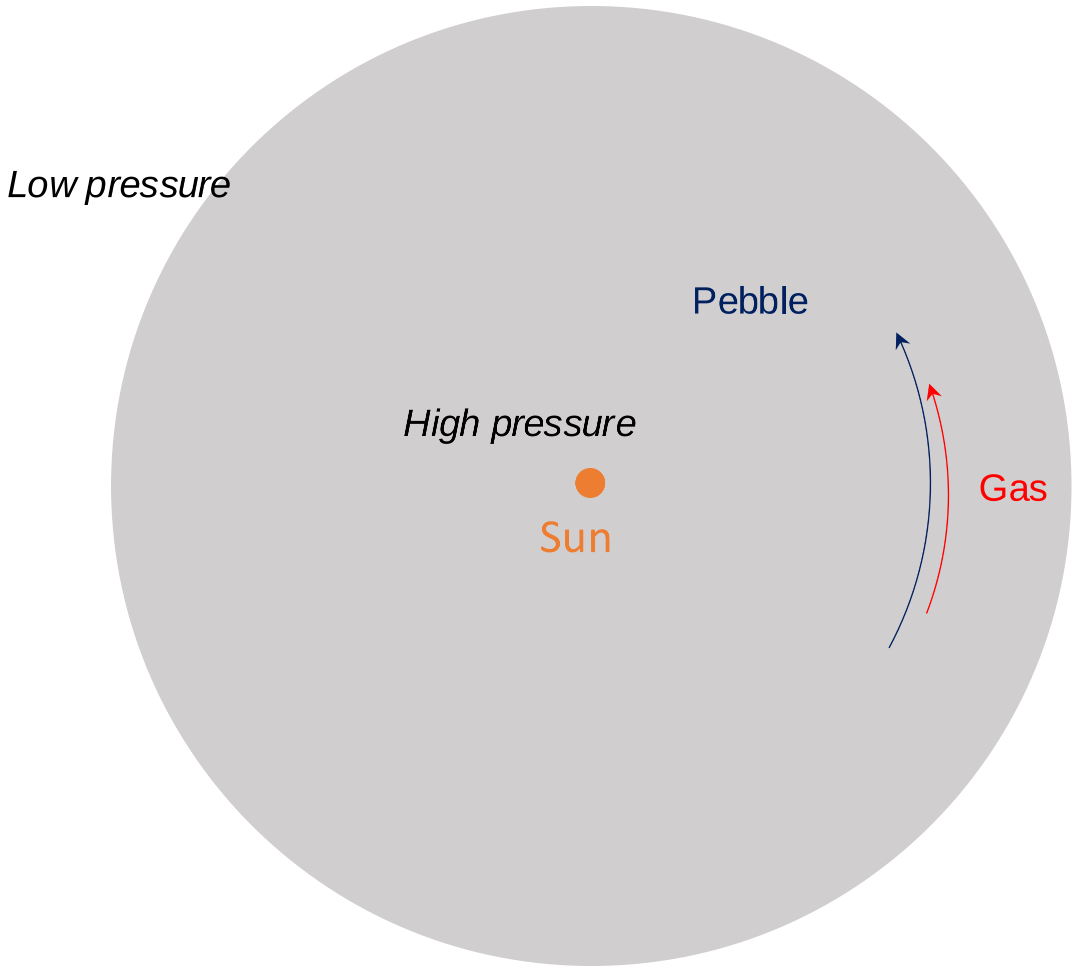

The gas has some pressure support (sub-Keplerian).

The pebbles do not feel gas pressure (Keplerian).

Dust coagulation and drift

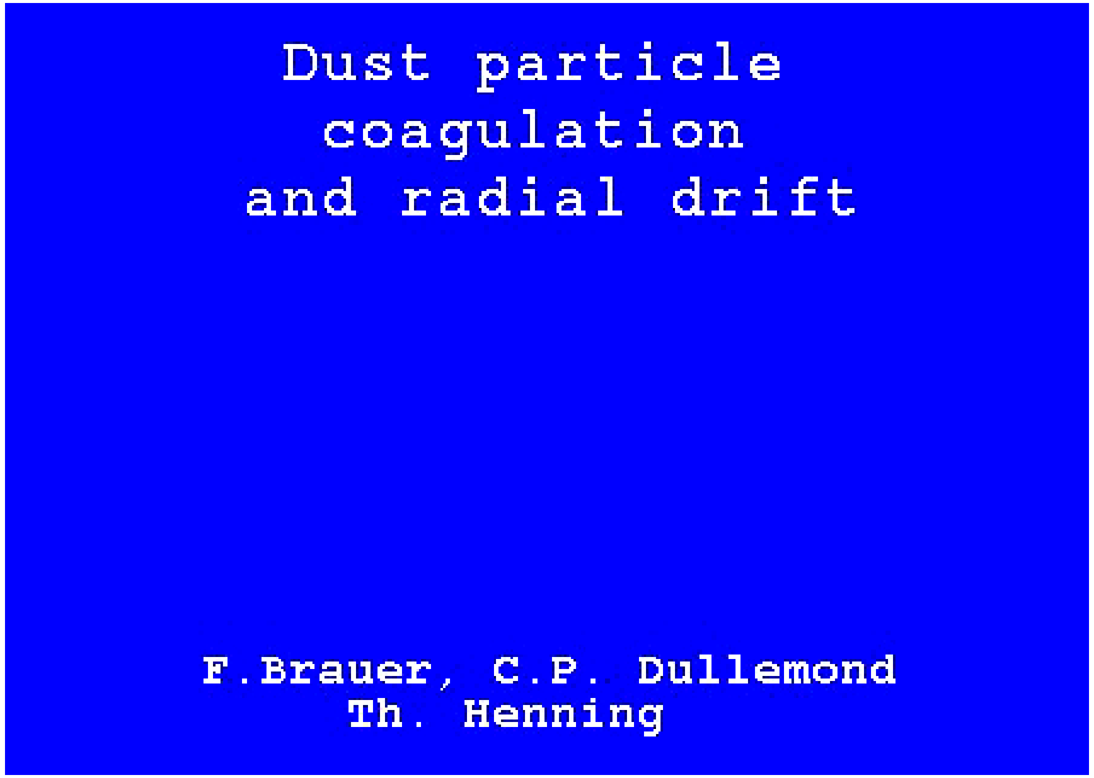

Brauer et al. (2008)

Streaming Instability

The dust drift is hydrodynamically unstable

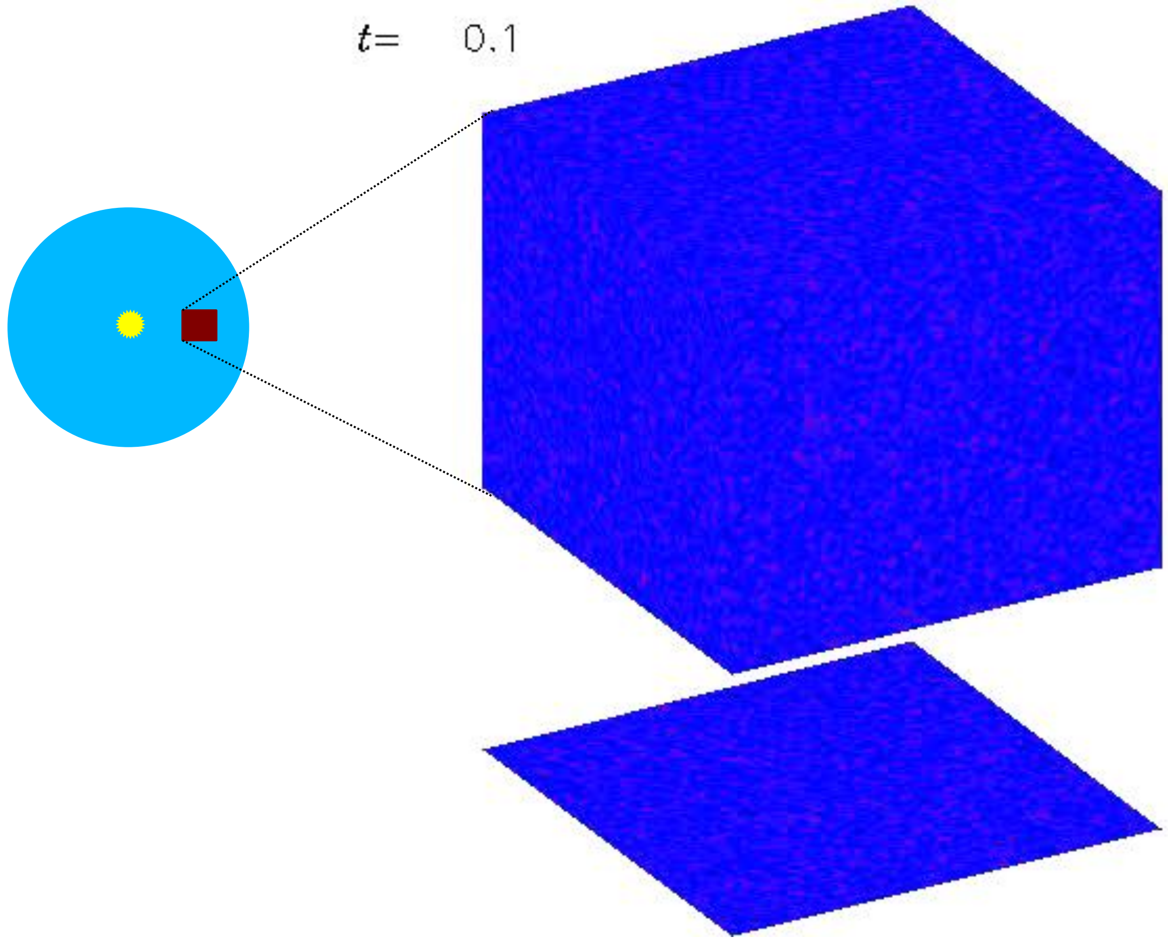

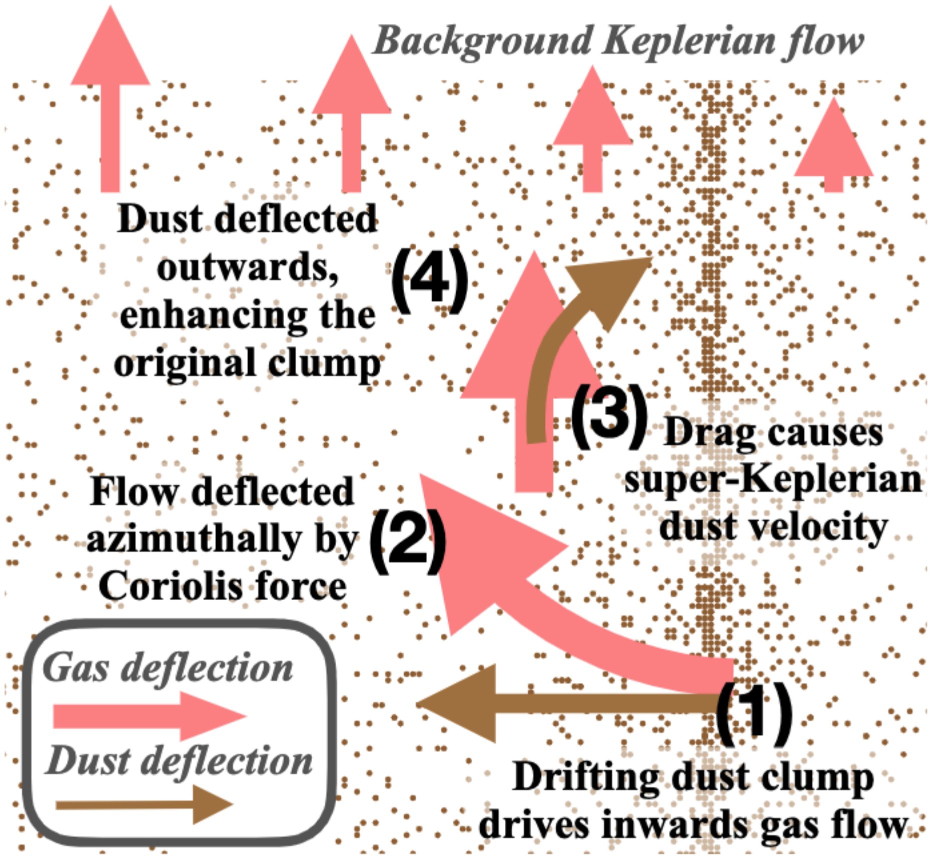

Lesur et al. (2022)

Youdin & Goodman ‘05, Johansen & Youdin ‘07, Youdin & Johansen+ ‘07, Kowalik+ ’13, Lyra & Kuchner ‘13, Schreiber+ ‘18, Klahr & Schreiber ’20, Simon+ ‘16, ‘17, Carrera+ ‘15, ‘17, ‘20, Gole+ ’20, Li+ ‘18, ‘19, Abod+ ’19, Nesvorny+ ’19

Gravitational collapse into planetesimals

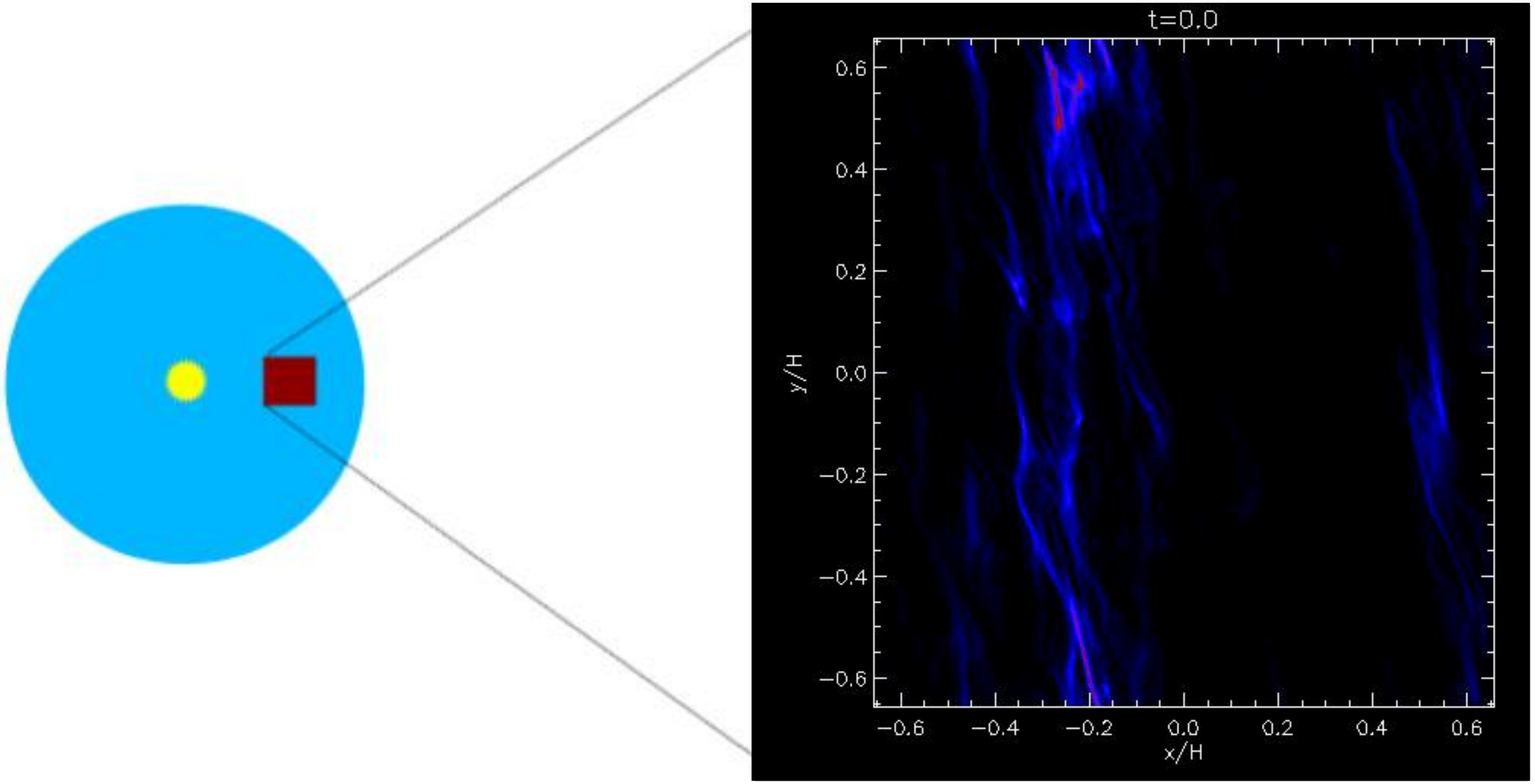

Johansen et al. (2007)

How can we verify the streaming instability hypothesis?

Planetesimal Formation

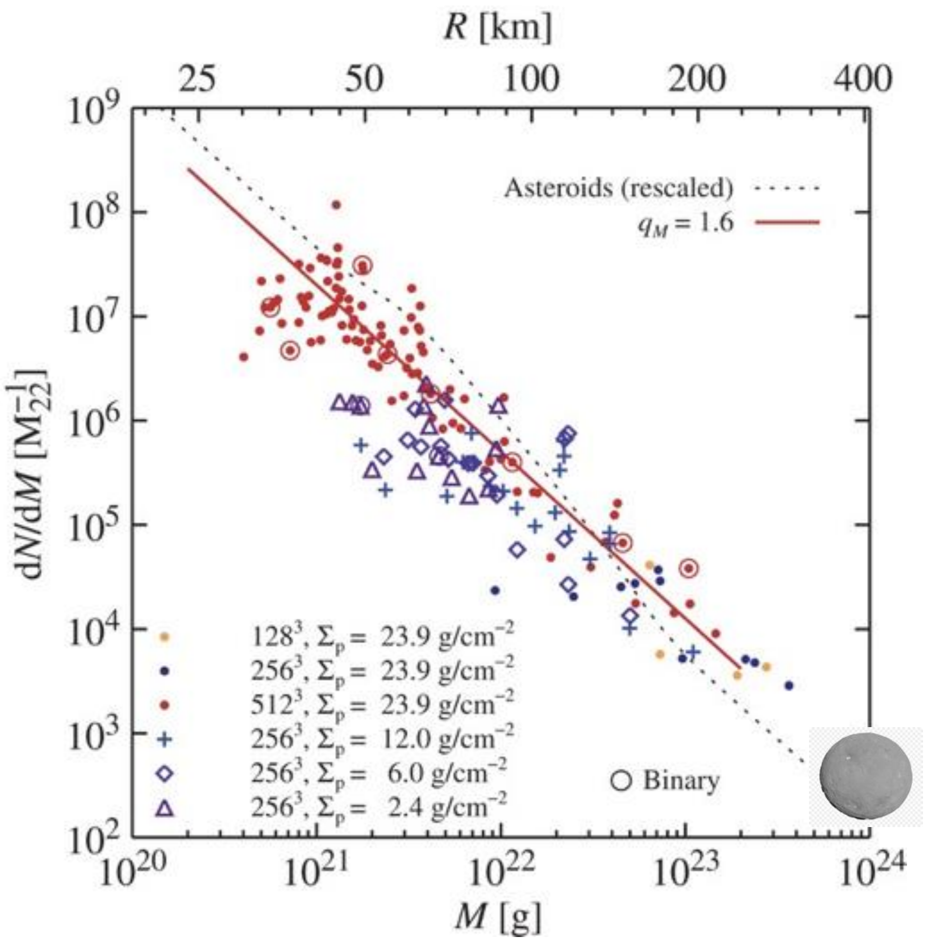

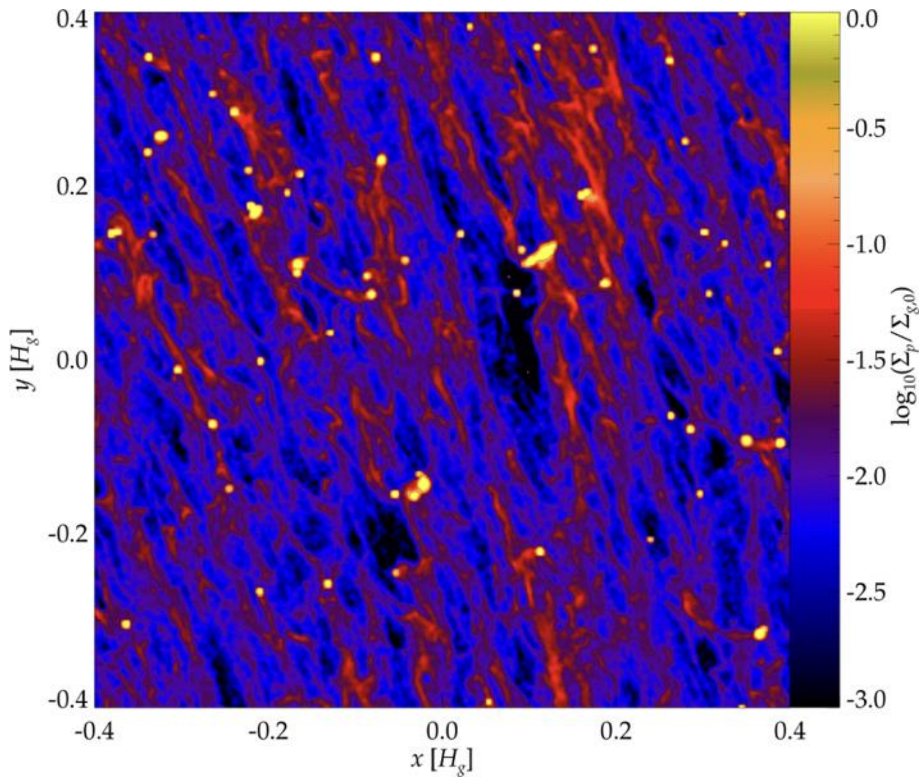

Initial mass function consistent with mass distribution of asteroid belt. Slope 1.6

Yang & Johansen (2014); Schäfer, Yang, & Johansen (2017)

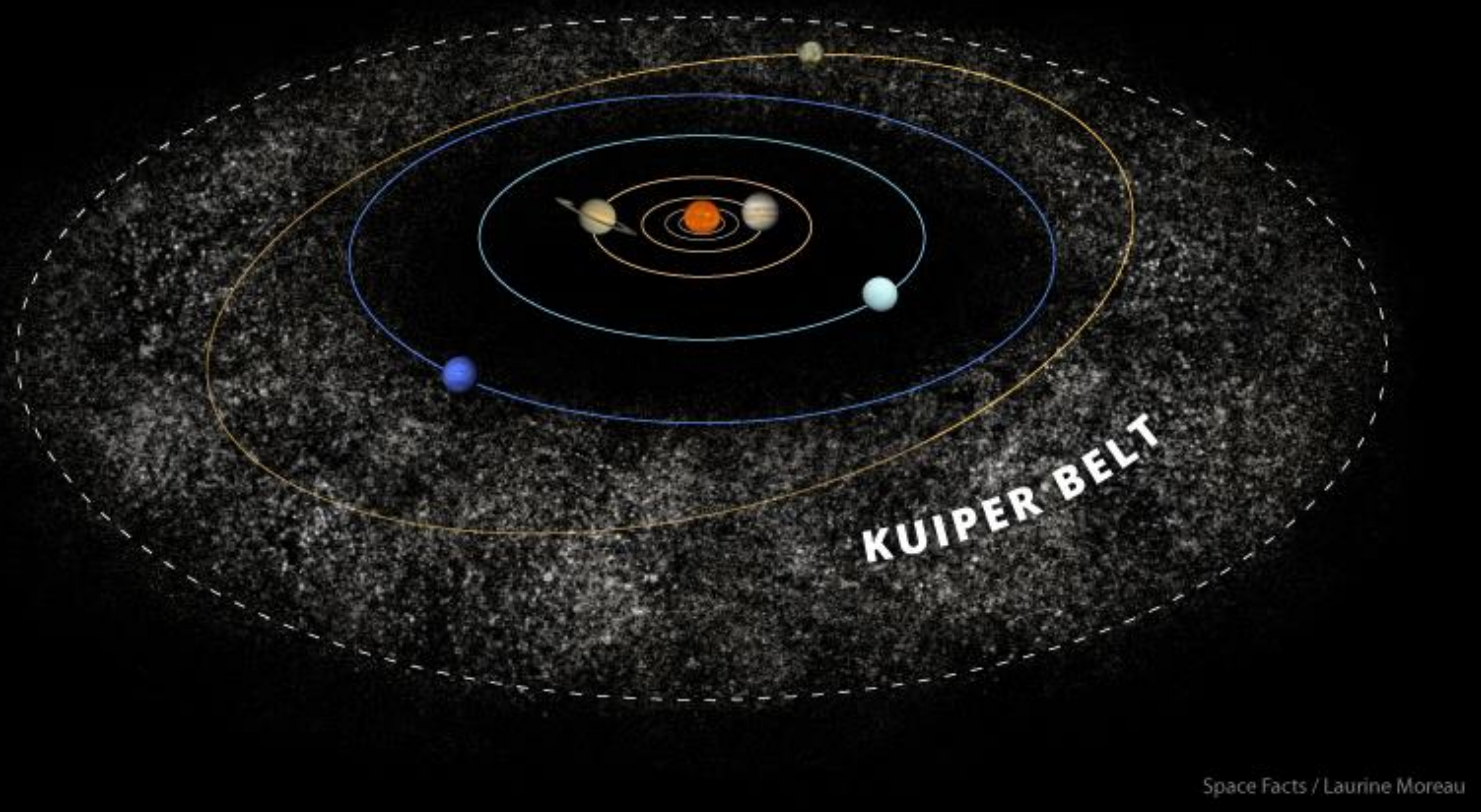
KUIPER BELT
Space Facts / Laurine Moreau

Structure of the Kuiper Belt

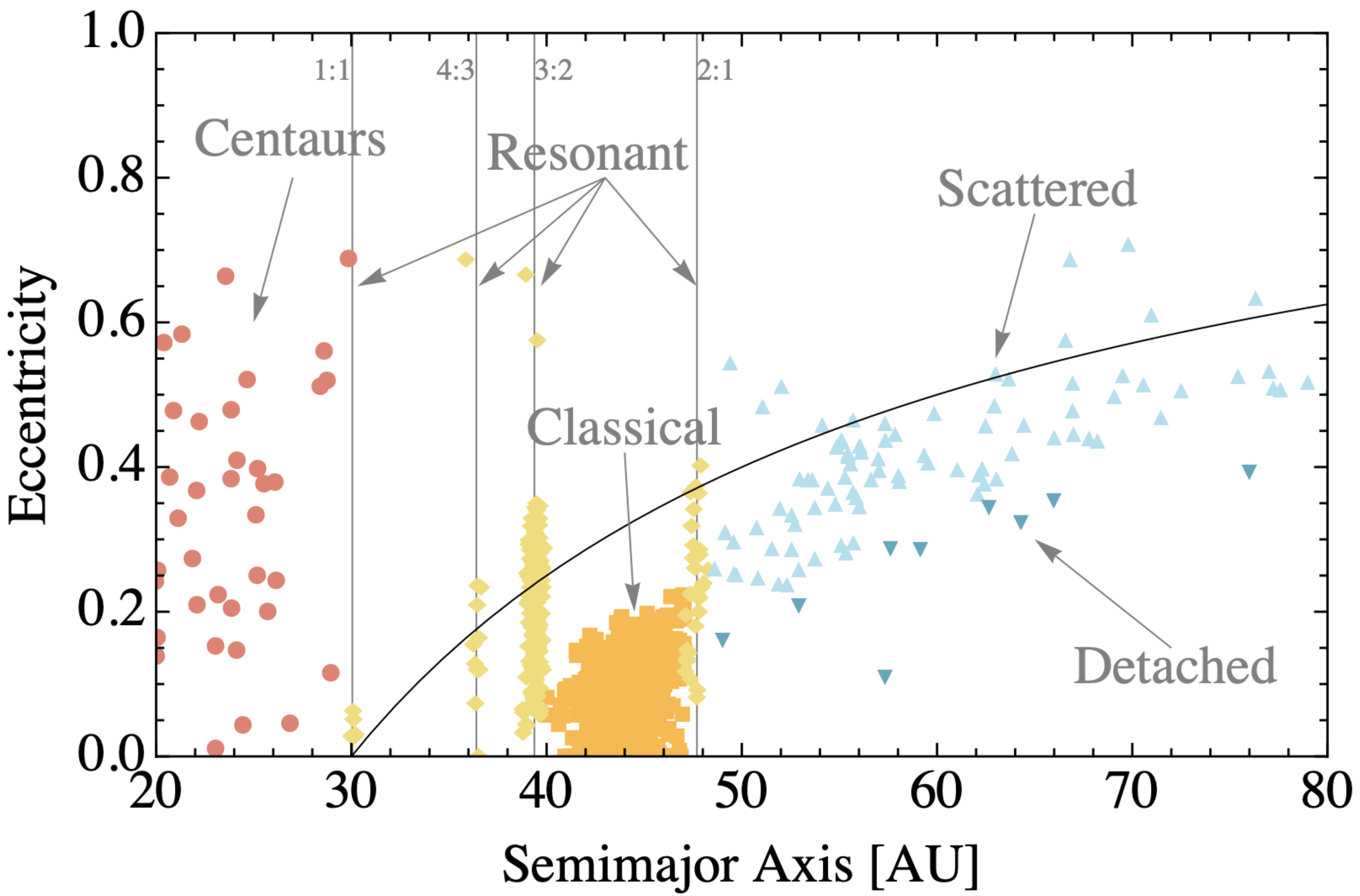

Classicals: Presumably pristine planetesimals

Gladman+ ‘08, Lacerda ‘09, Batygin+ ’10

New Horizons Trajectory

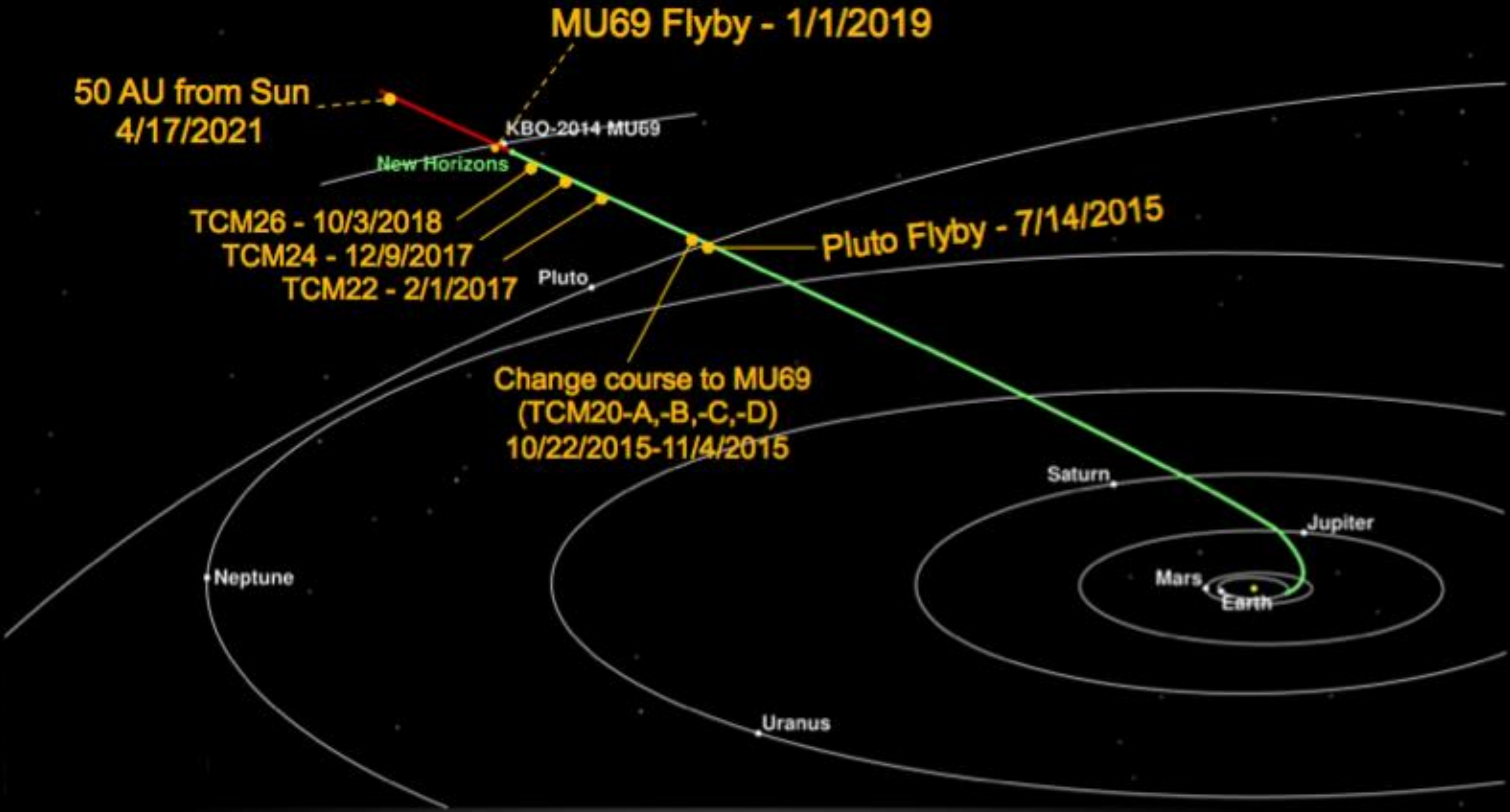

Arrokoth (MU_{69})

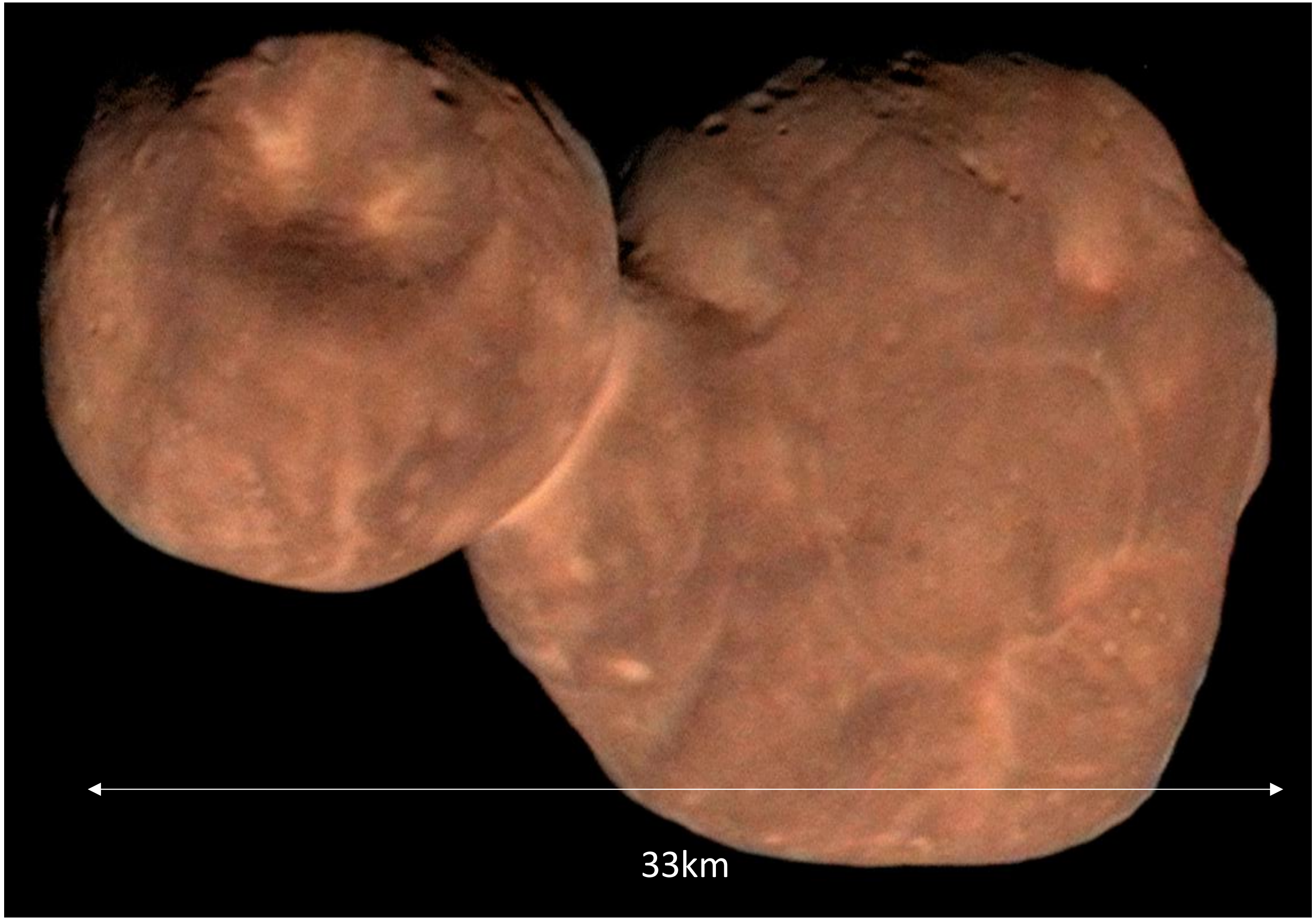

New Horizons Flyby, Jan 2019

Classical KBOs: Preference for Prograde

Cold TNOs

Resonant

Centaurs / Scattered

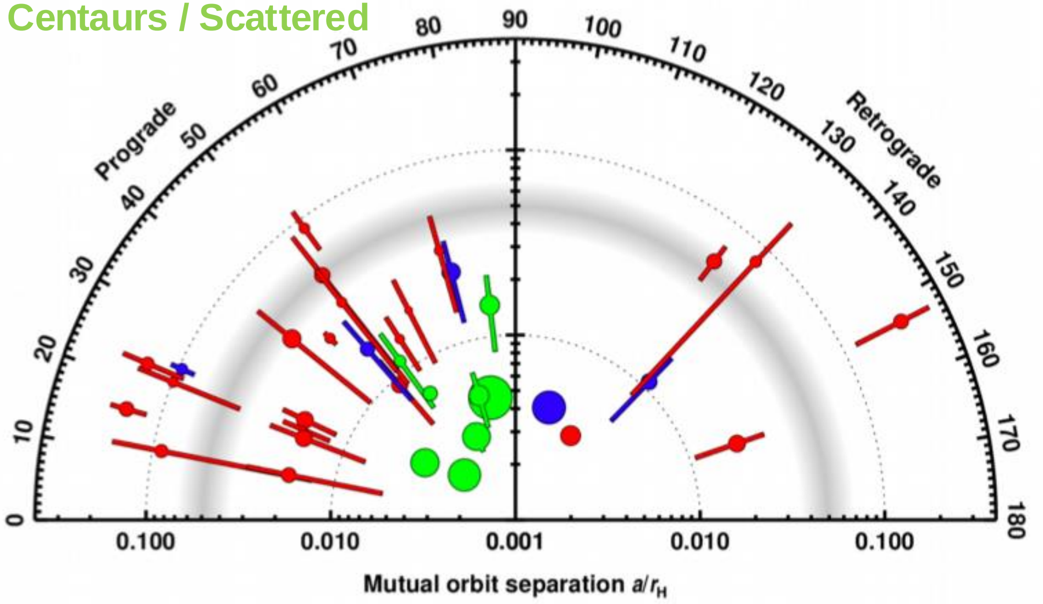

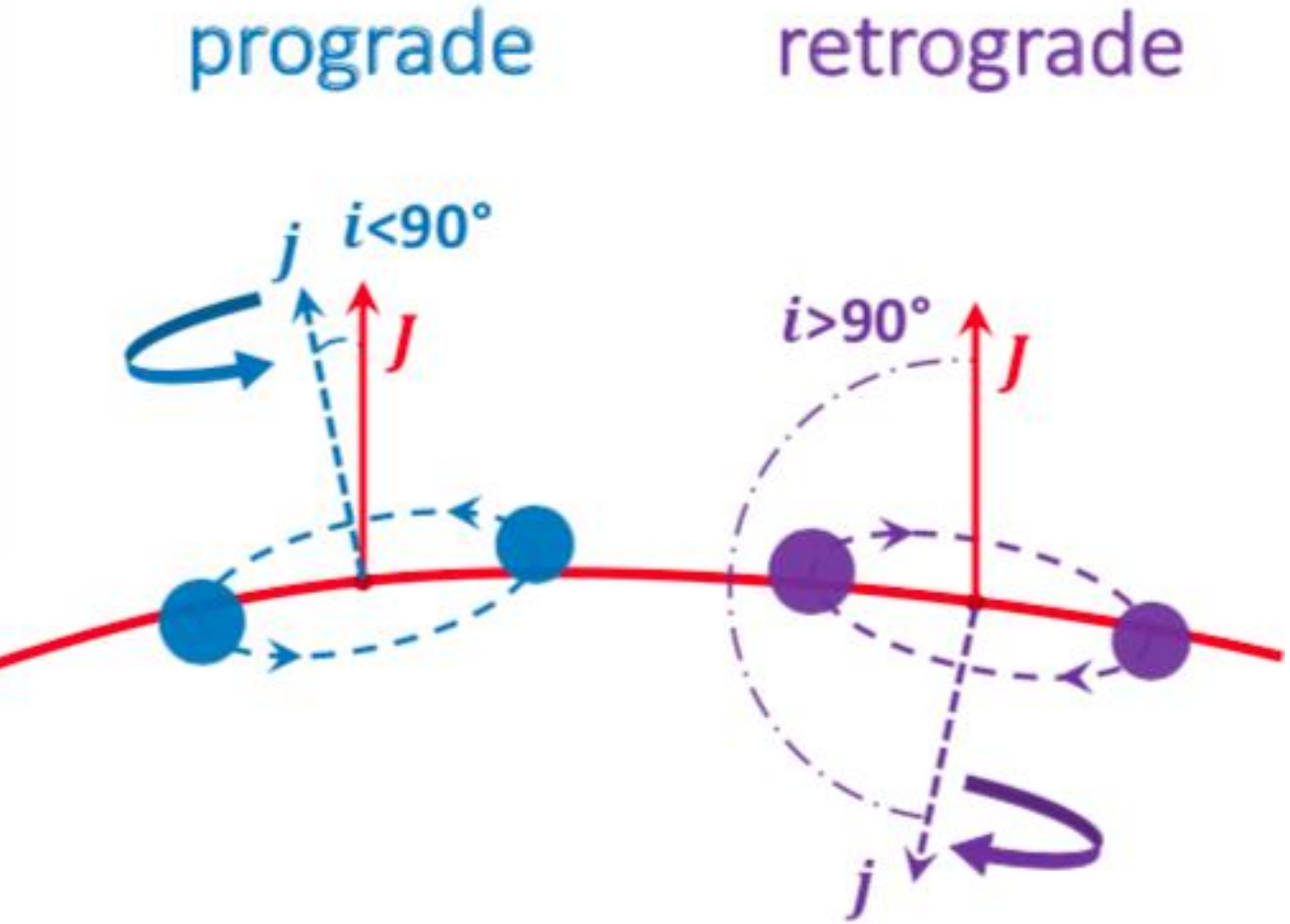

Grundy+2019

Counting binaries: Preference for Prograde (~80%)

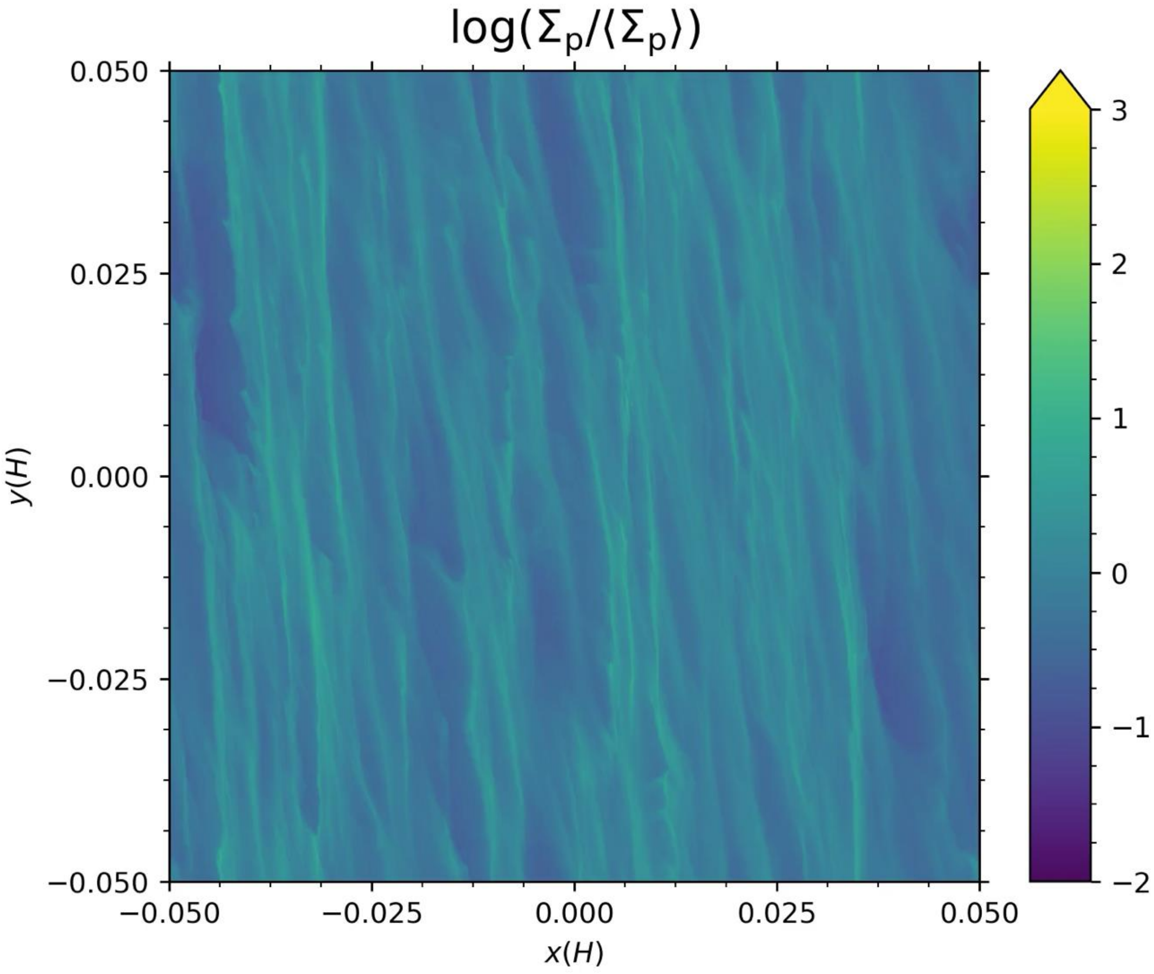

SI Model (solid)
KBOs (dashed)

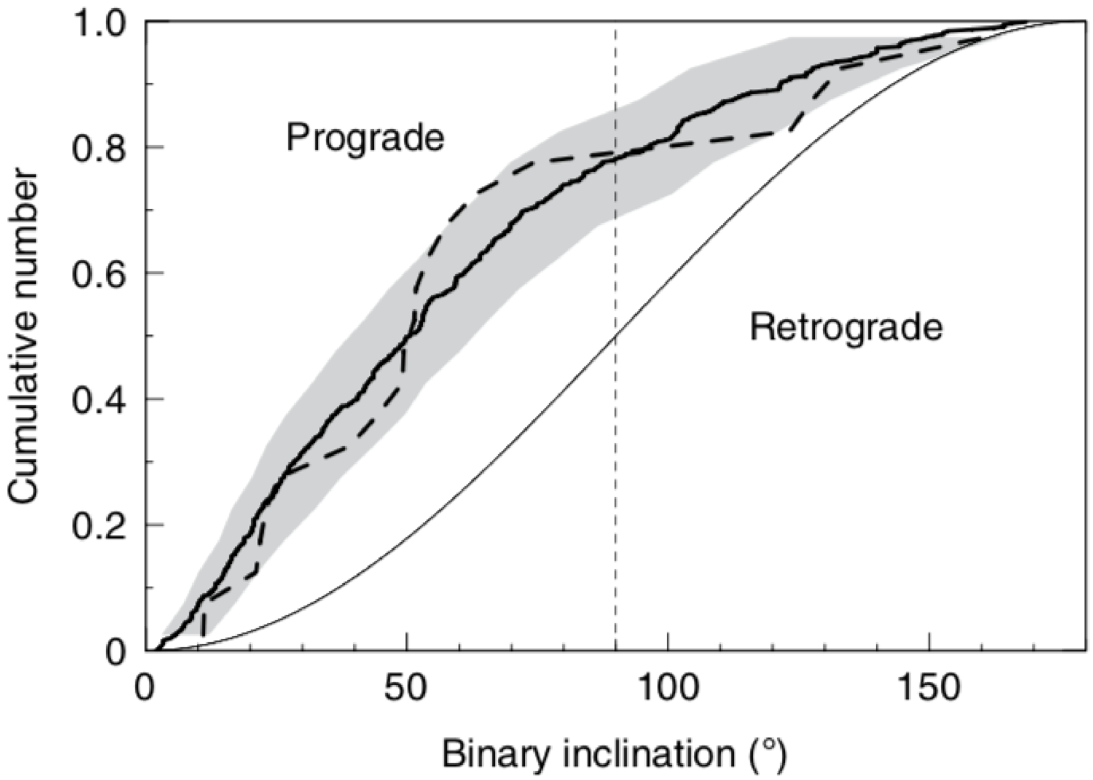

W. Lyra

Nesvorny+'19, model by Rixin Li

Preference for Prograde (~80%)

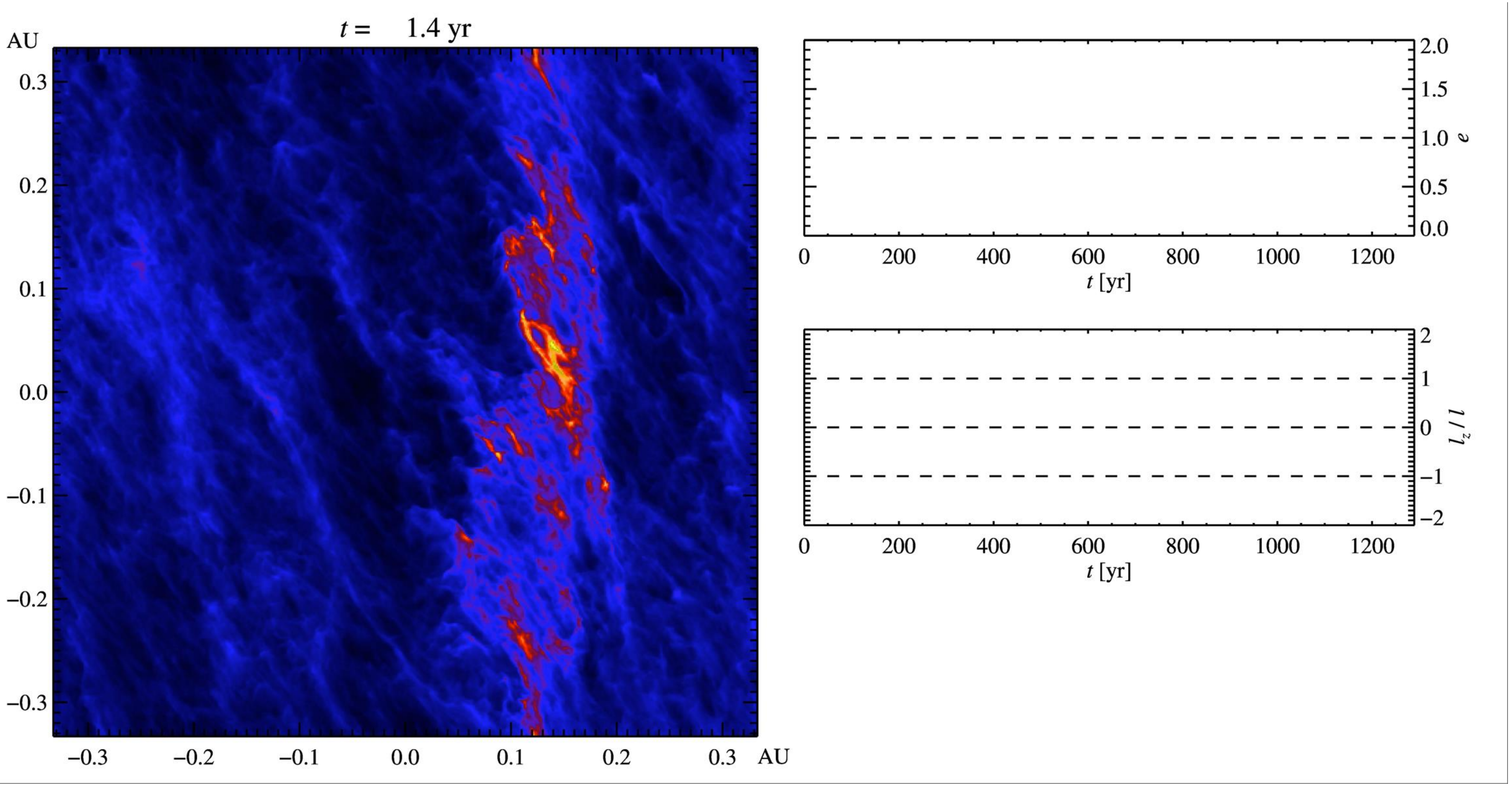

Data from A. Johansen (private communication)

Exponential tapering at high mass end of IMF

Simulations

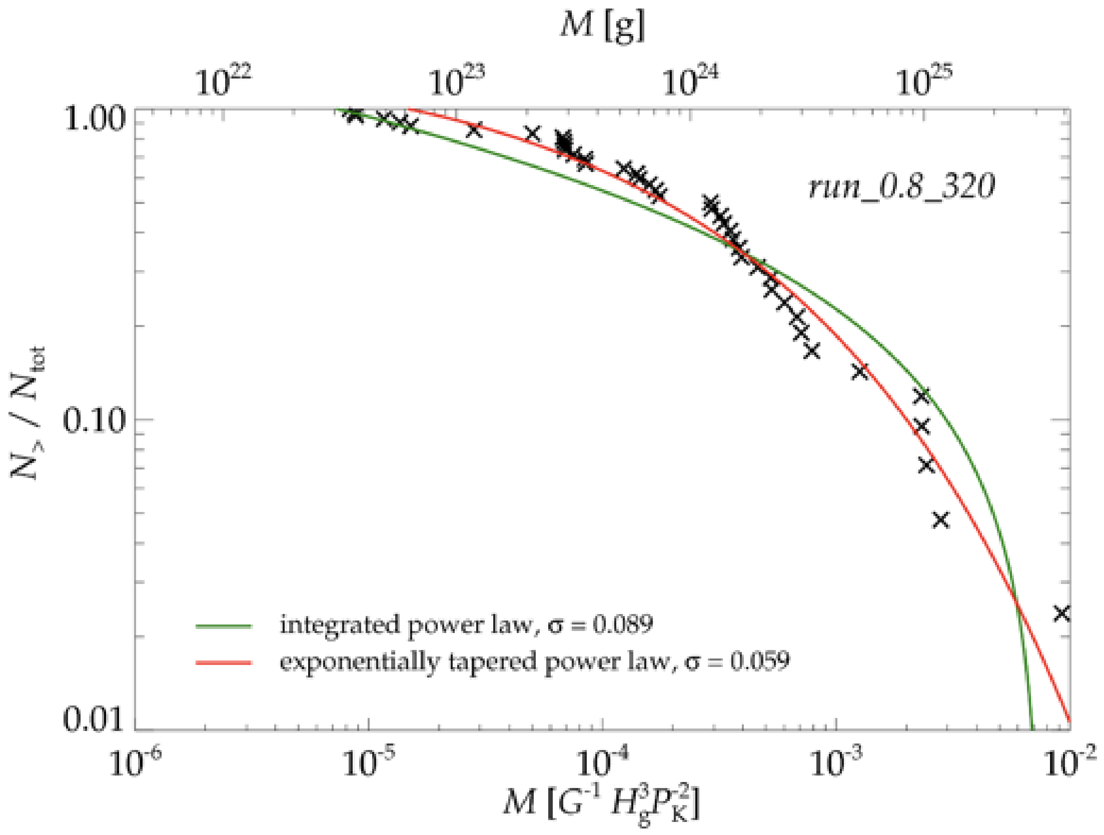

Schäfer et al. 2017

Observations (OSSOS survey)

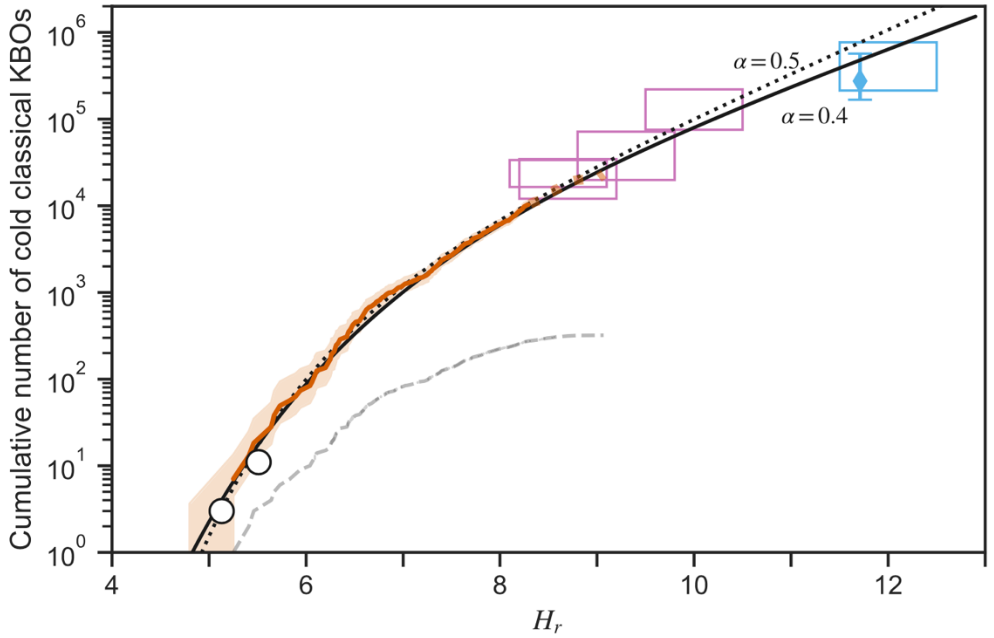

Figure 1. The H_r distribution of the cold main Kuiper Belt. The gray dashed line represents the distribution of raw detections in the OSSOS++ sample. The orange curve (shown as a dotted line for $H_r > 8.3$, where our sample debiasing is less secure) represents the debiased OSSOS++ sample, with the shading indicating the Poisson 95% confidence range. The black lines represent two exponentially tapered functions matched (see Section 3) to the debiased OSSOS++ data with forced large-H_r (small object) asymptotic slopes (dotted: $\alpha = 0.5$; solid: $\alpha = 0.4$). For $H_r < 9$, the two model curves are nearly identical. The debiased OSSOS++ measurements are well matched by the exponential taper form. The boxes represent literature-derived estimates; see Table 1 and Section 2.2.1. The cyan diamond with uncertainty represents a direct debiasing of detected cold classicals in B04. The black open circles are located where the MPC database indicates a cumulative total of 3 ($H_r \sim 5.13$) and 11 ($H_r \sim 5.51$) main-belt cold objects.

Kavelaars et al. 2021

The mass-density relationship of Kuiper Belt objects

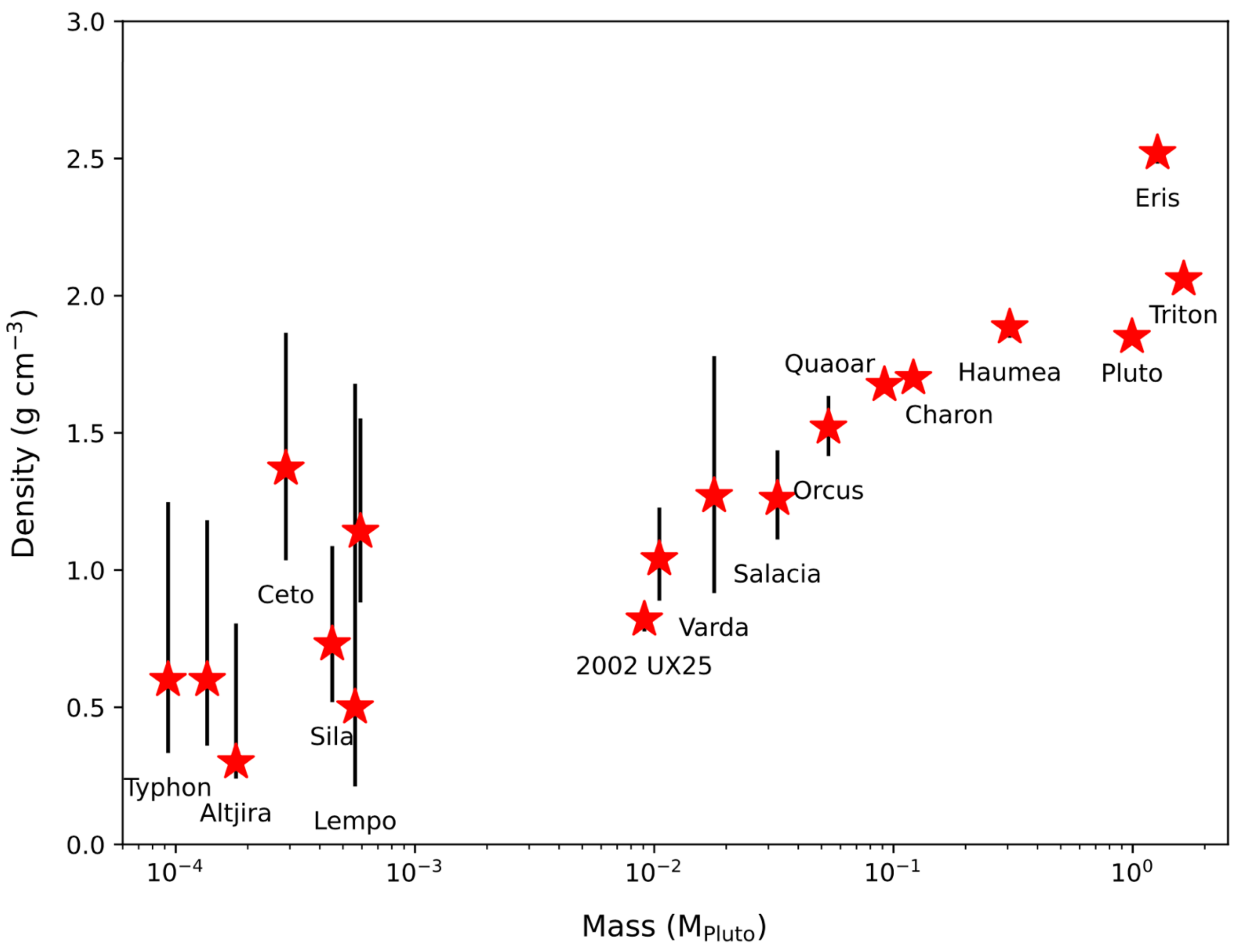

The Astronomer's Periodic Table

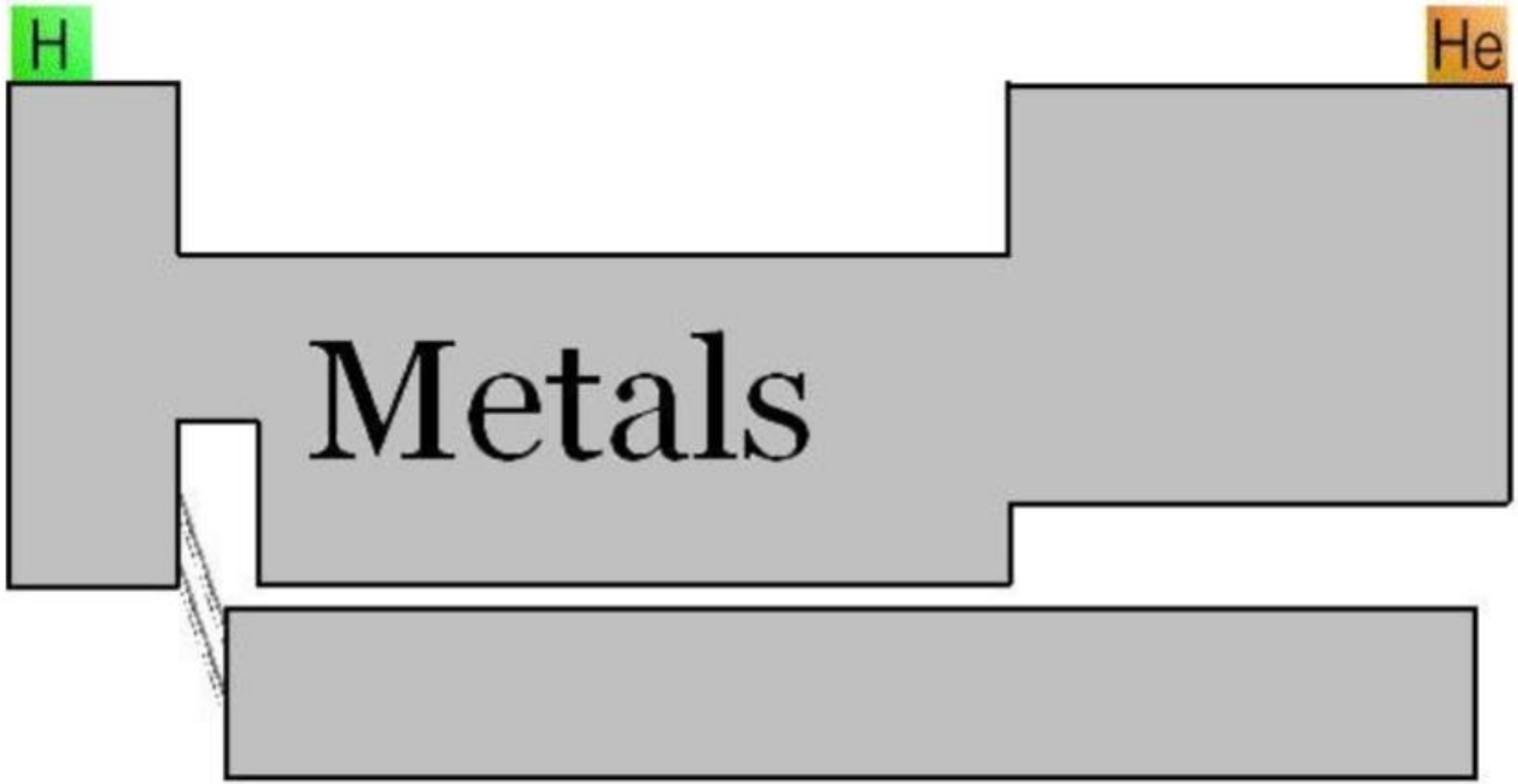

The Astronomer's Periodic Table

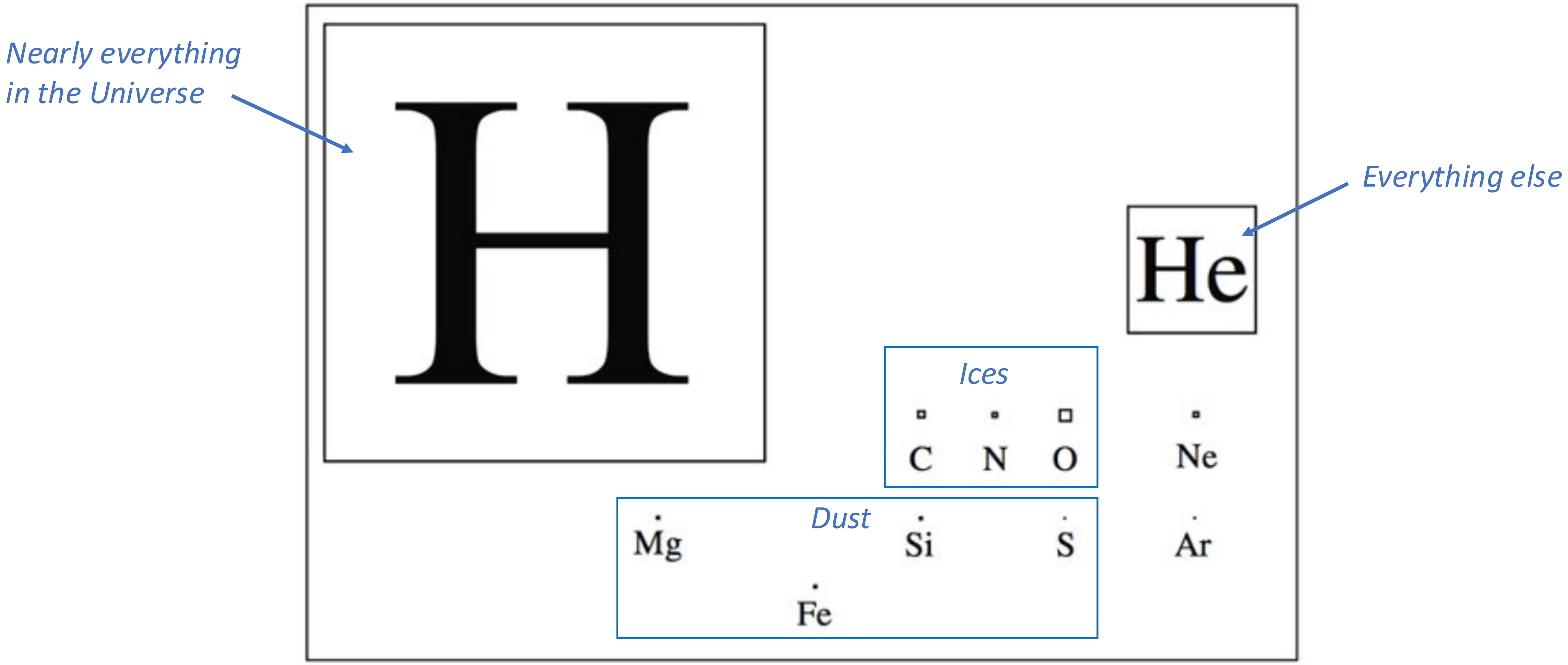

Bimodal pebble composition

Heating and UV irradiation remove ice on Myr timescales (Harrison & Schoen 1967)

- Small grains lofted in the atmosphere lose ice
- Big grains are shielded and remain icy.

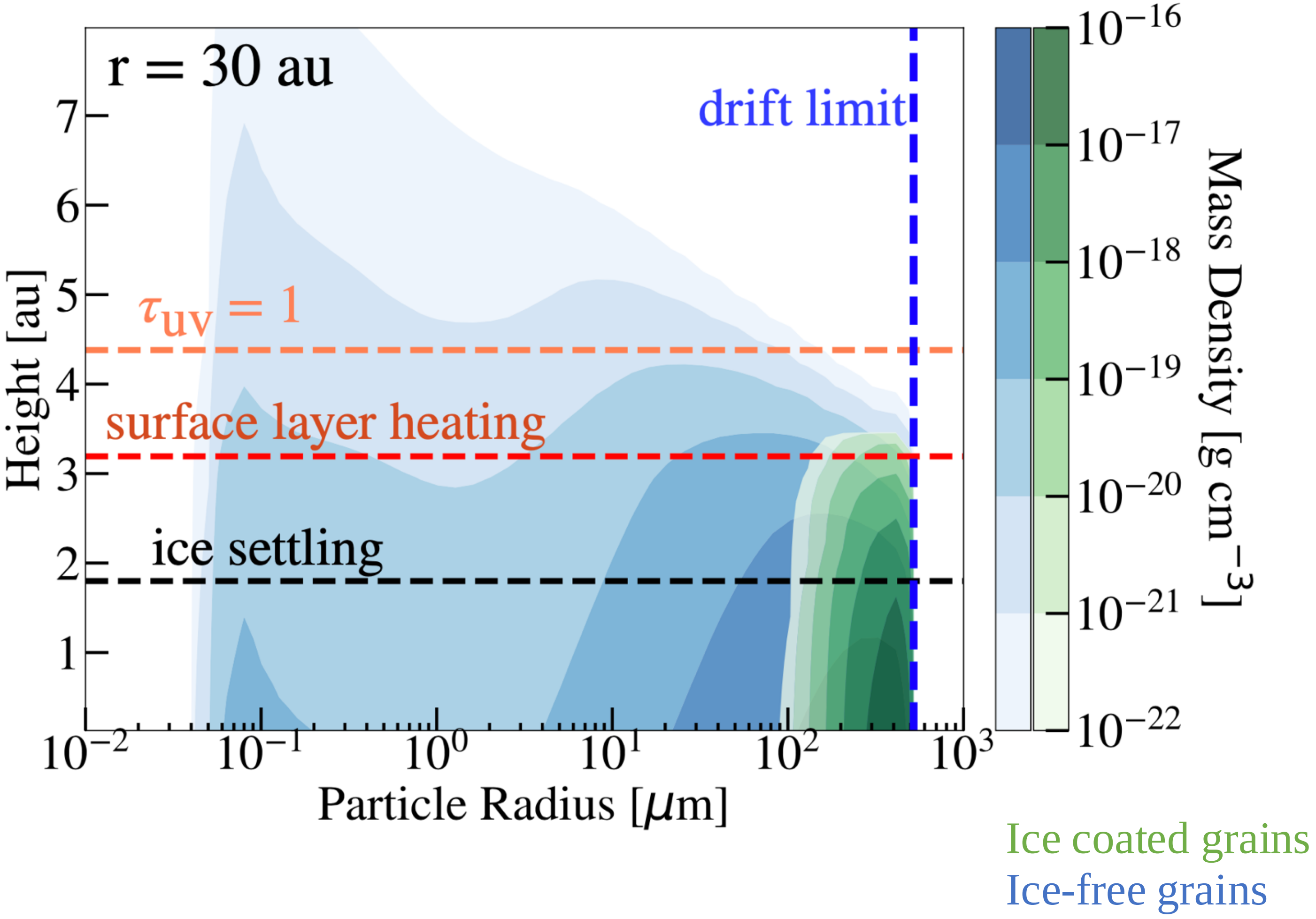

Powell et al. (2022)

Split into icy and silicate pebbles

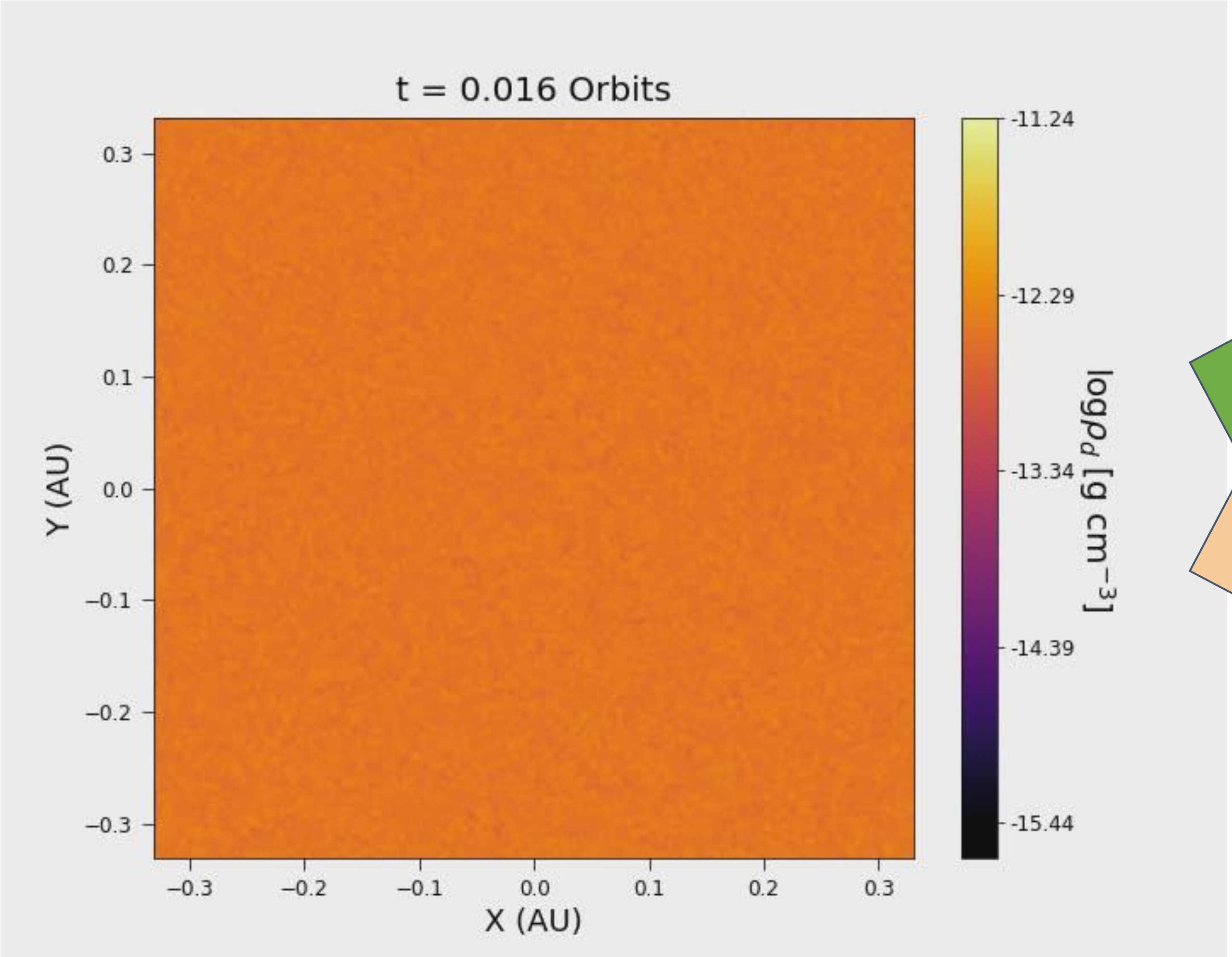

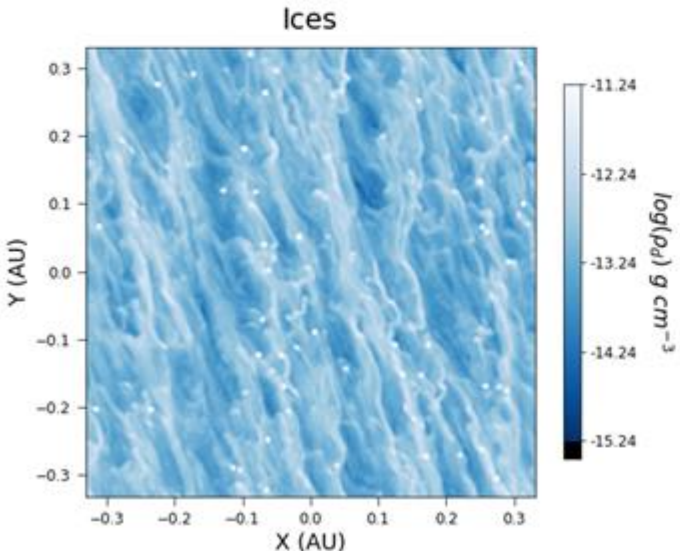

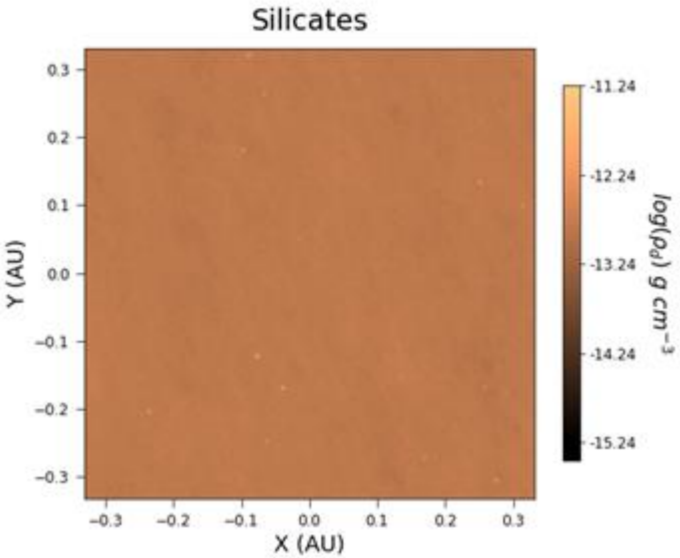

Canas+Lyra et al. 2024

The first planetesimals are icy

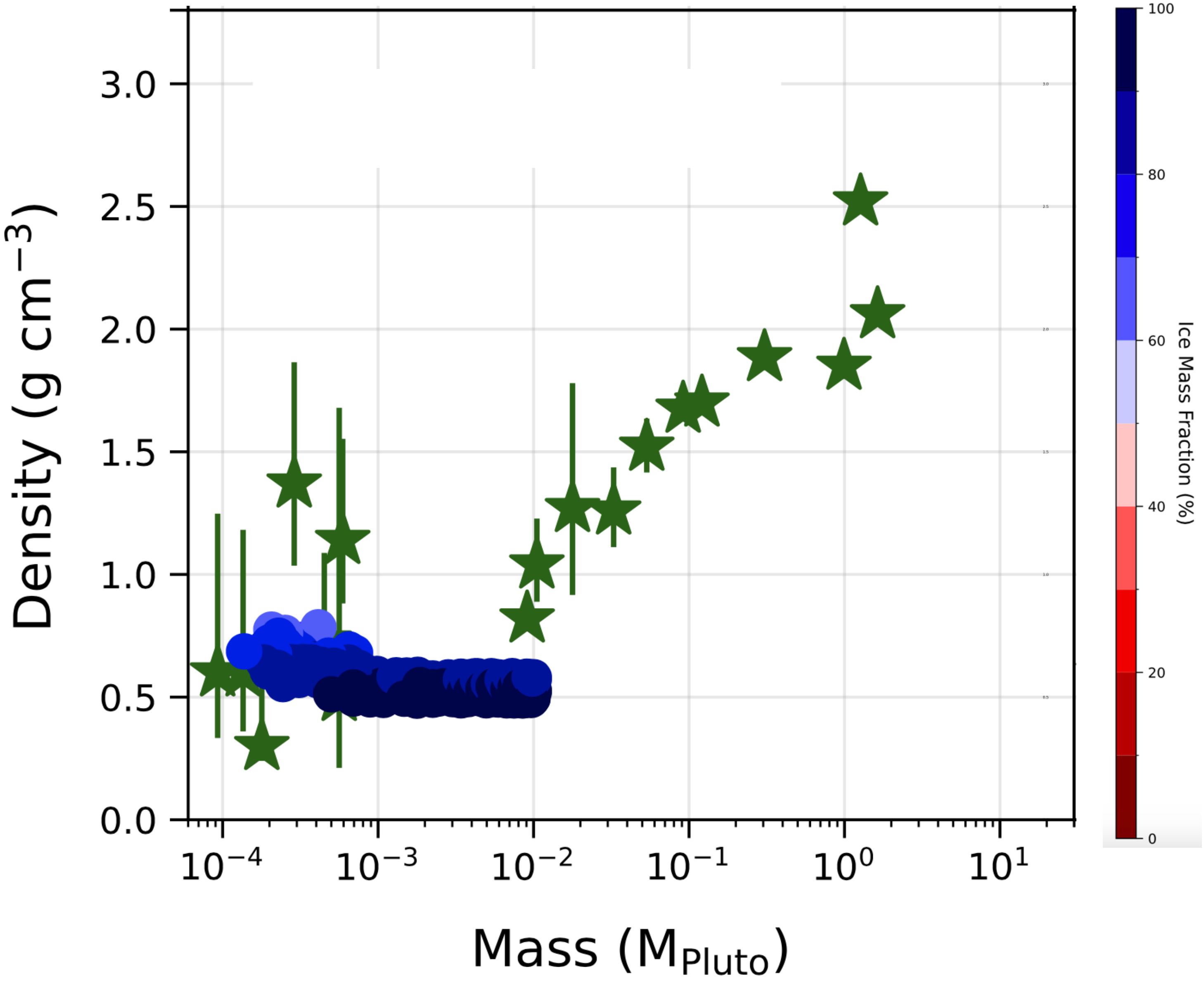

Canas+Lyra et al. 2024

Pebble Accretion

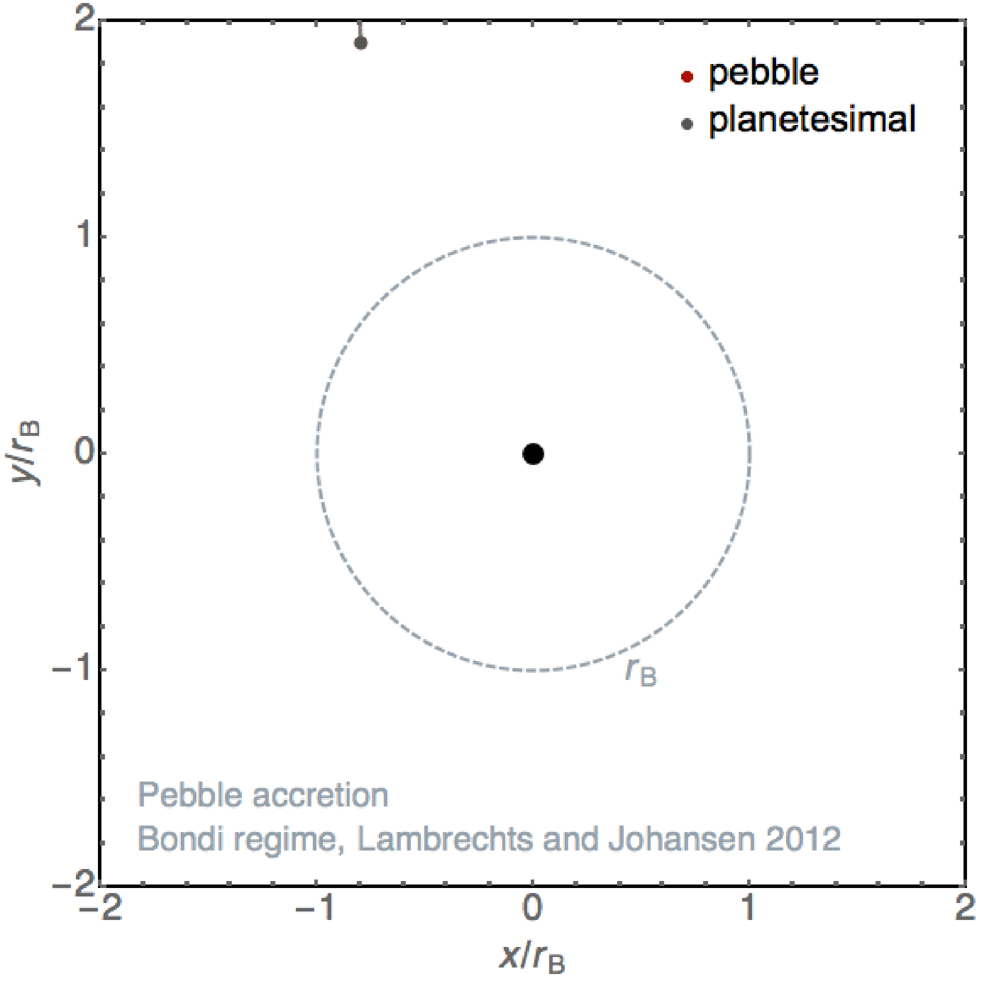

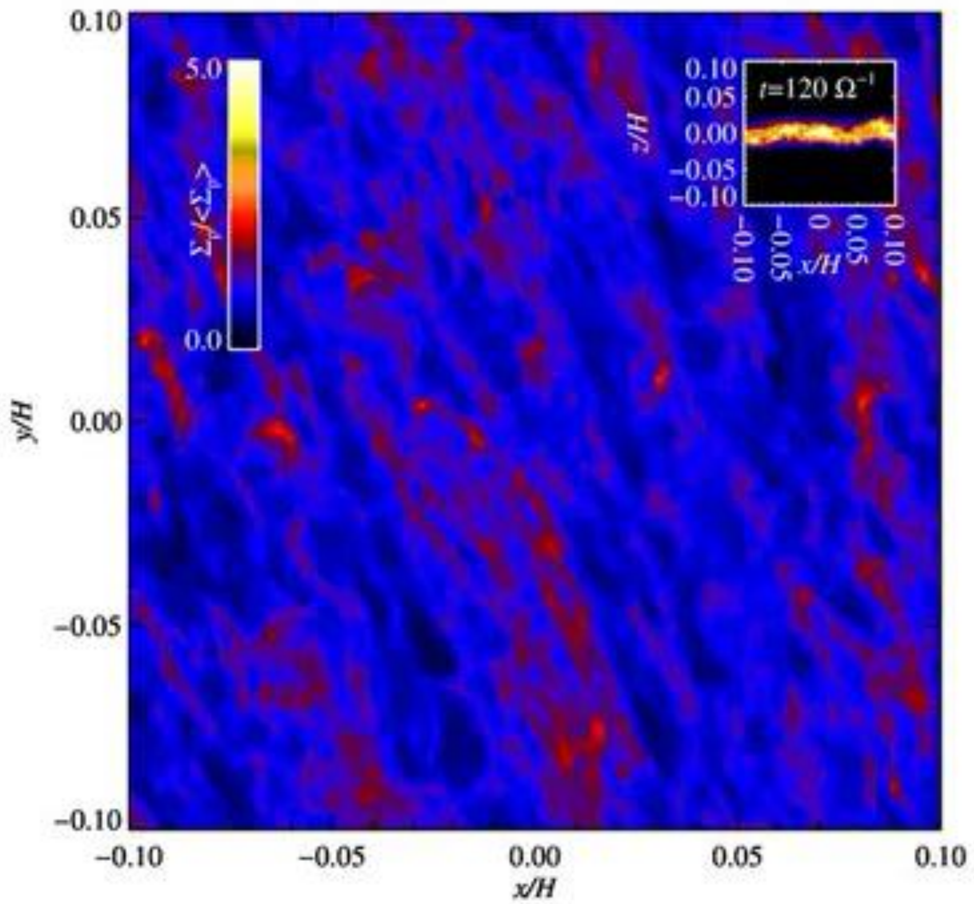

Klahr & Henning '97, Klahr '06, Lyra+ '08, '09, '23, Inaba & Barge '08,
Ormel & Klahr '10, **Lambrechts & Johansen '12**
See Johansen & Lambrechts '17 for a review

Pebble Accretion

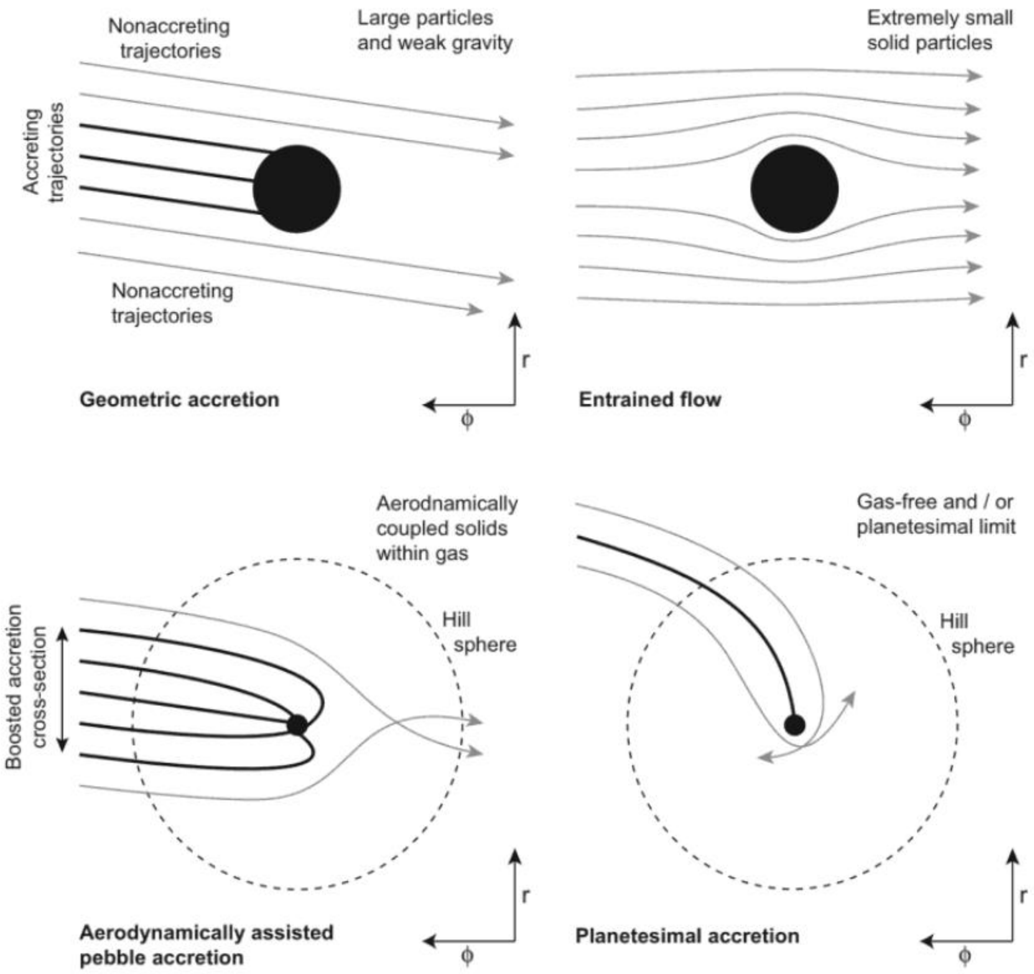

Bondi Accretion

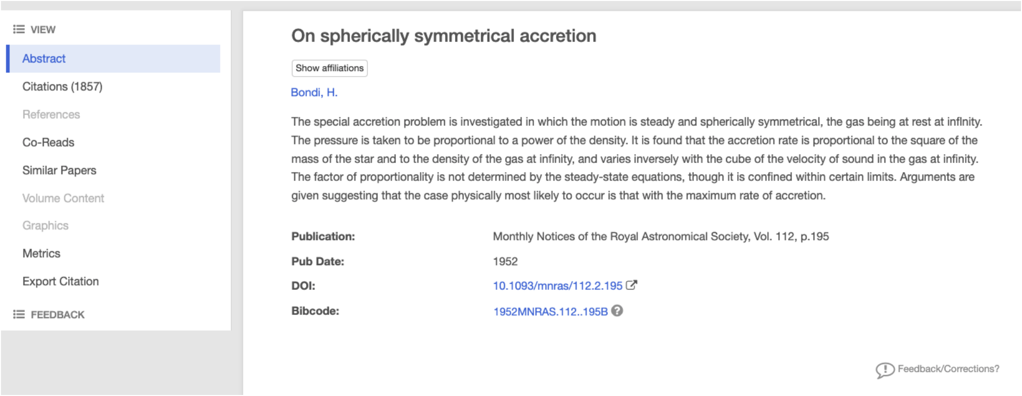

VIEW
Abstract
Citations (1857)
References
Co-Reads
Similar Papers
Volume Content
Graphics
Metrics
Export Citation
FEEDBACK

On spherically symmetrical accretion

Show affiliations

Bondi, H.

The special accretion problem is investigated in which the motion is steady and spherically symmetrical, the gas being at rest at infinity. The pressure is taken to be proportional to a power of the density. It is found that the accretion rate is proportional to the square of the mass of the star and to the density of the gas at infinity, and varies inversely with the cube of the velocity of sound in the gas at infinity. The factor of proportionality is not determined by the steady-state equations, though it is confined within certain limits. Arguments are given suggesting that the case physically most likely to occur is that with the maximum rate of accretion.

Publication:	Monthly Notices of the Royal Astronomical Society, Vol. 112, p.195
Pub Date:	1952
DOI:	10.1093/mnras/112.2.195
Bibcode:	1952MNRAS.112..195B

Feedback/Corrections?

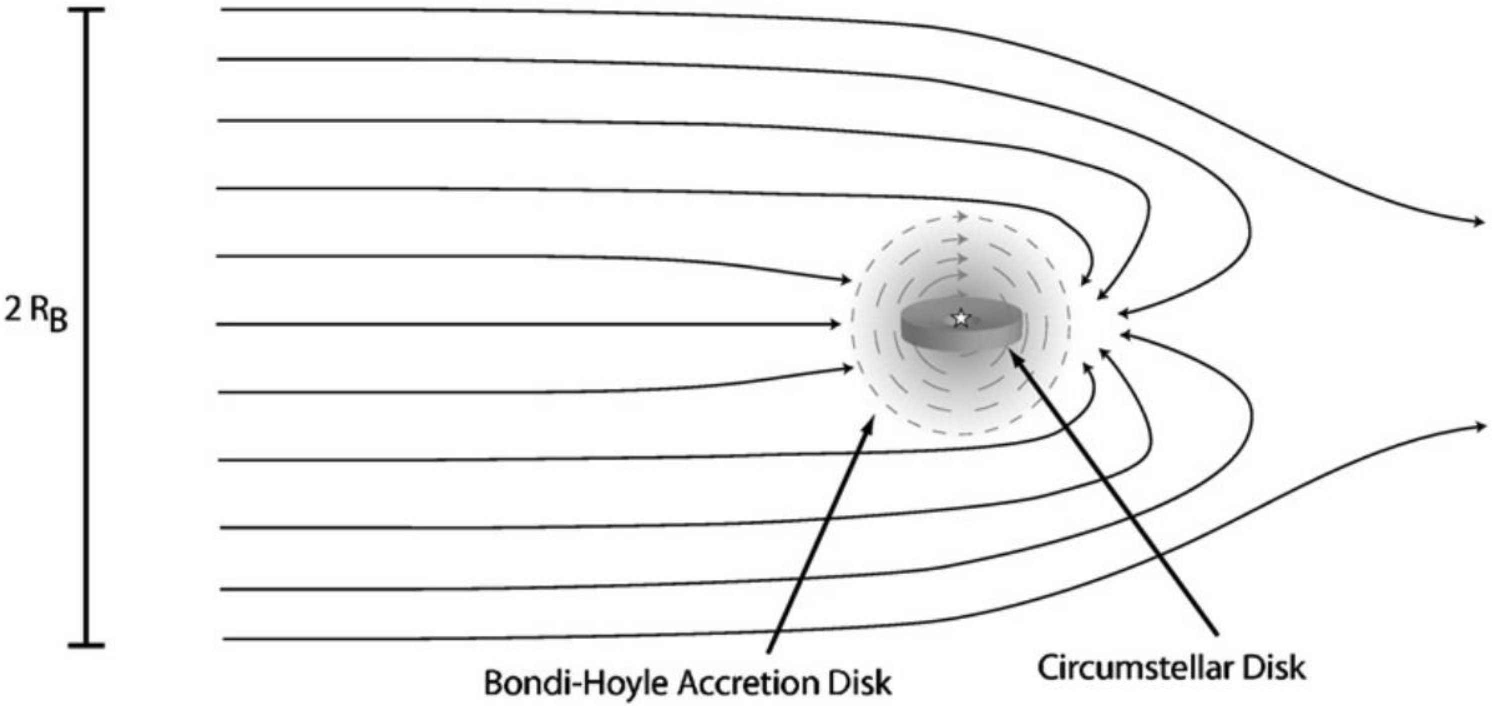

Pebble Accretion: Geometric, Bondi, and Hill regime

Bondi accretion - Bound against thermal (dynamic) kinetic energy

Hill accretion - Bound against stellar tide

$$\xi \equiv \left(\frac{R_{\rm acc}}{2H_d}\right)^2 \qquad \dot{M}_{\rm 3D} = \lim_{\xi\to 0} \dot{M} = \pi R_{\rm acc}^2 \rho_{d0} \delta v, \qquad \dot{M}_{\rm 2D} = \lim_{\xi\to\infty} \dot{M} = 2R_{\rm acc} \Sigma_d \delta v,$$

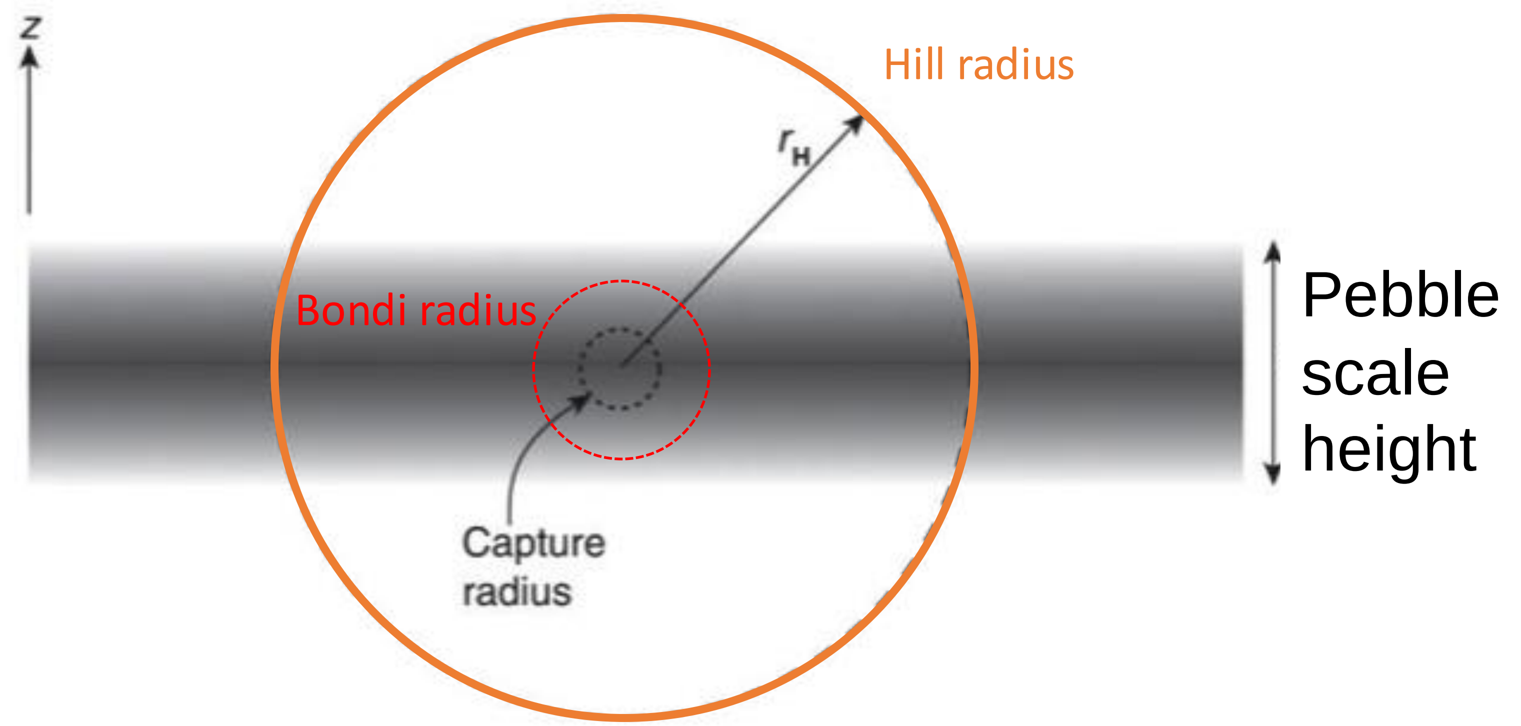

Mass Accretion rates

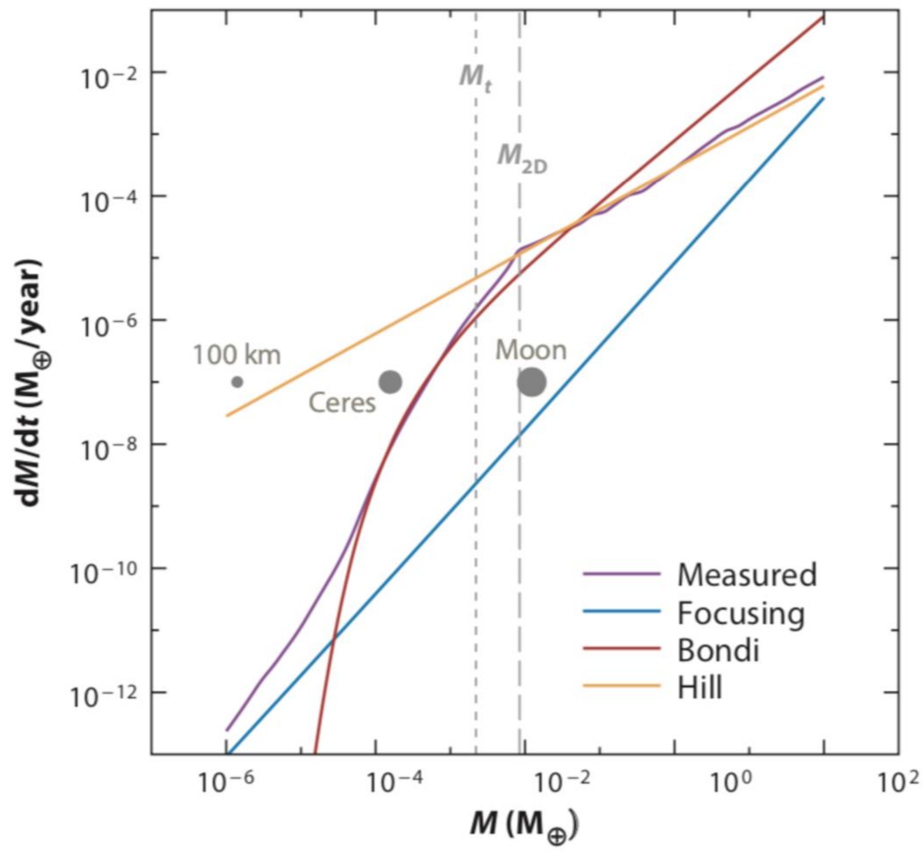

Johansen & Lambrechts '17

Integrate pebble accretion

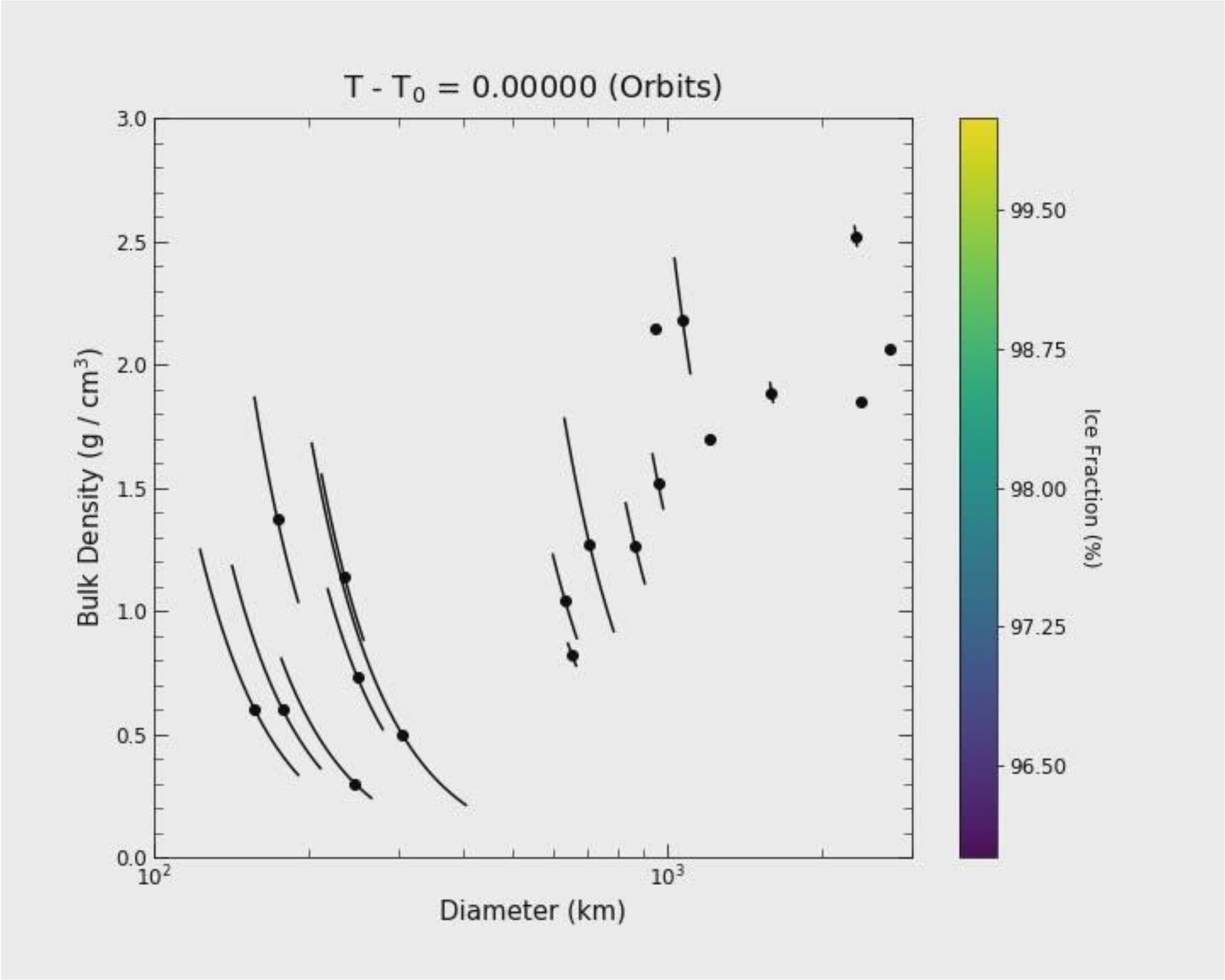

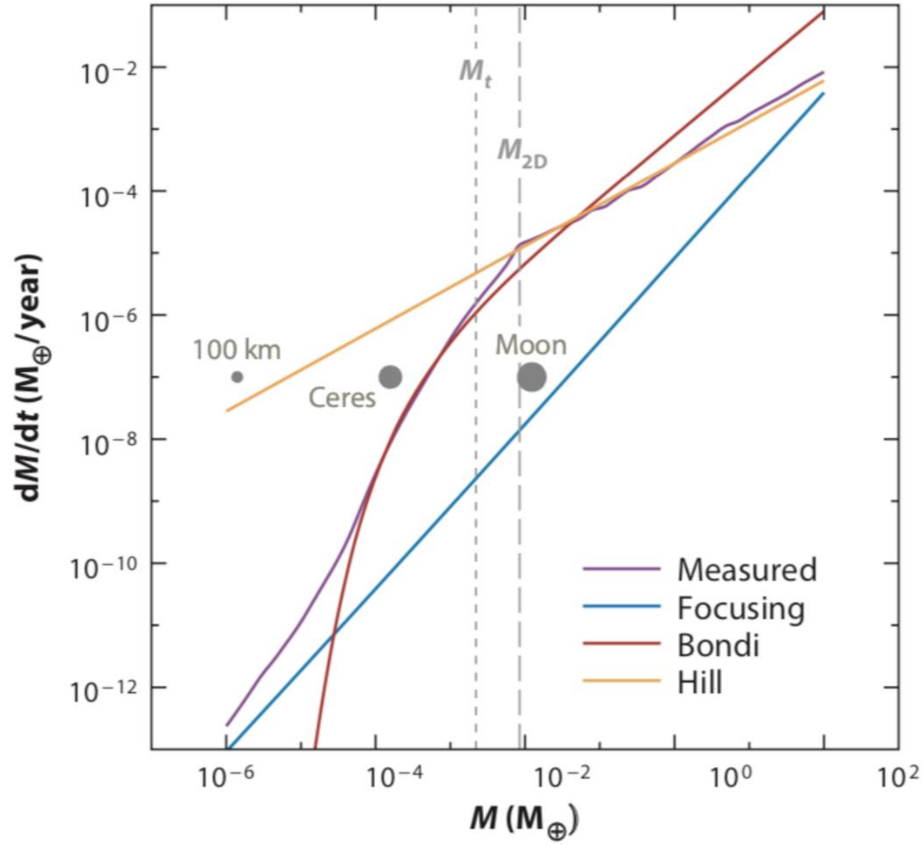

Pebble Accretion: Pebbles of different size accrete differently

Bondi Regime

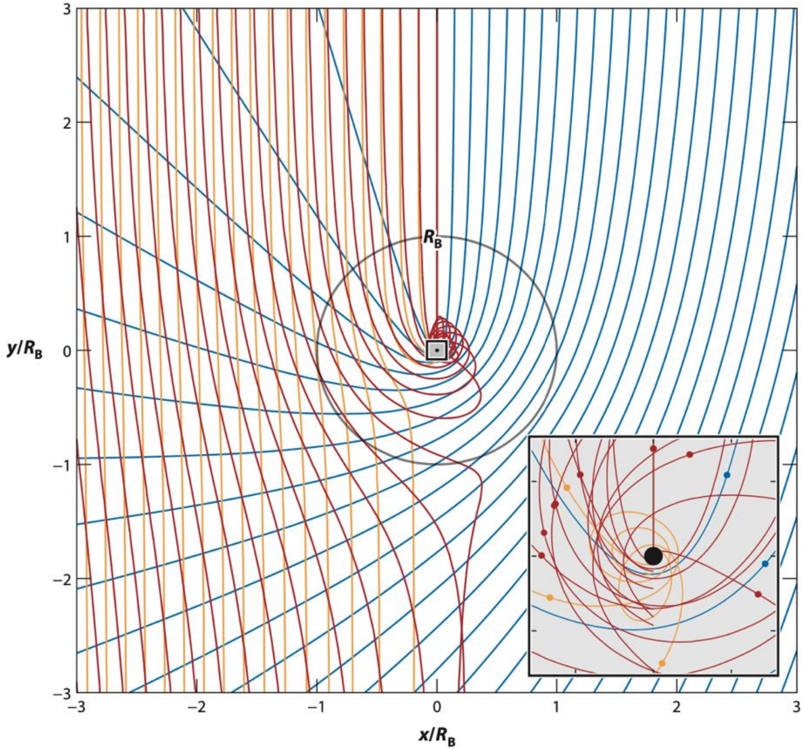

Best accreted
Drag time = Time to cross Bondi sphere

Hill Regime

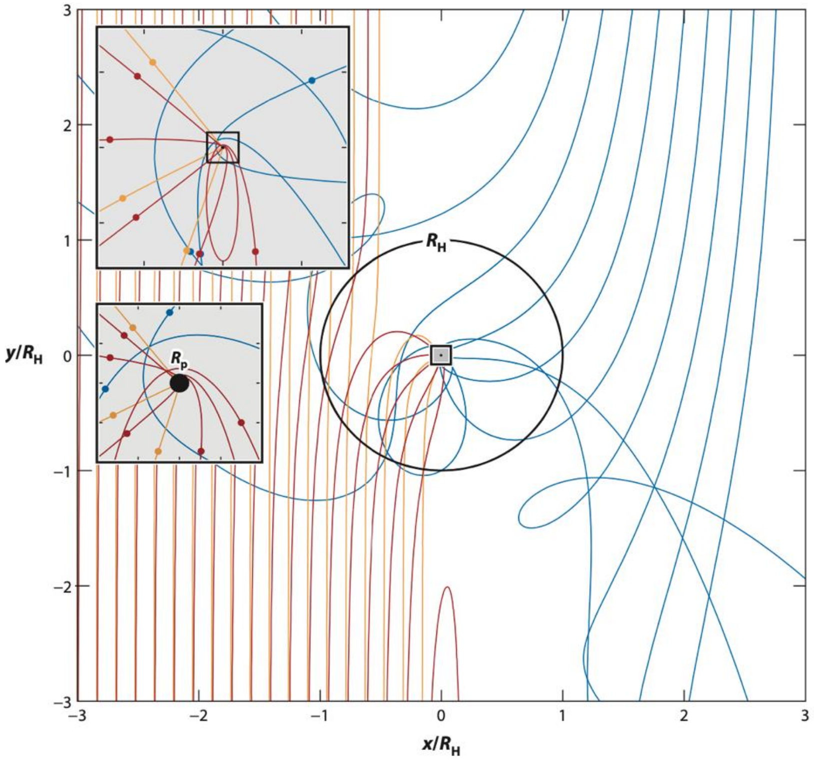

Best accreted
Drag time ~ Orbital Time

Polydisperse (Multi-Species) Pebble Accretion

$$\rho_d(a,z) = \int_0^a m(a')\,F(a',z)\,da'.$$

$$F(a,z) \equiv f(a)\,e^{-z^2/2H_d^2},$$

$$f(a) = \frac{3(1-p)Z\Sigma_g}{2^{5/2}\pi^{3/2}H_g\rho_\bullet^{(0)}a_{\max}^{4-k}}\sqrt{1+a\frac{\pi}{2}\frac{\rho_\bullet(a)}{\Sigma_g\alpha}}\;a^{-k}.$$

$$S \equiv \frac{1}{\pi R_{\rm acc}^2}\int_{-R_{\rm acc}}^{R_{\rm acc}} 2\sqrt{R_{\rm acc}^2-z^2}\,\exp\left(-\frac{z^2}{2H_d^2}\right)dz,$$

$$W(a) = \frac{3(1-p)Z\Sigma_g}{4\pi\rho_\bullet^{(0)}a_{\max}^{4-k}}\,a^{-k},$$

$$\delta v \equiv \Delta v + \Omega R_{\rm acc},$$

$$R_{\rm acc} \equiv \hat{R}_{\rm acc}\exp[-\chi(\tau_f/t_p)^\gamma],$$

$$\hat{R}_{\rm acc}^{(\rm Bondi)} = \left(\frac{4\tau_f}{t_{\rm B}}\right)^{1/2}R_{\rm B},$$

$$\hat{R}_{\rm acc}^{(\rm Hill)} = \left(\frac{\rm St}{0.1}\right)^{1/3}R_{\rm H},$$

$$\frac{\partial\Sigma_d(a)}{\partial a} \propto a^{-p};$$

$$\rho_\bullet \propto a^{-q};$$

$$t_p \equiv \frac{GM_p}{(\Delta v + \Omega R_{\rm H})^3}$$

$$\dot{M}(a) = \int_0^a \frac{\partial\dot{M}(a')}{\partial a'}da',$$

$$\frac{\partial\dot{M}(a)}{\partial a} = \pi R_{\rm acc}^2(a)\,\delta v(a)\,S(a)\,m(a)\,f(a).$$

$$\dot{M}_{\rm 2D,\,Hill} = 2\times 10^{2/3}\Omega R_H^2\int_0^{a_{\max}}{\rm St}(a)^{2/3}\,m(a)\,W(a)\,da.$$

$$\dot{M}_{\rm 3D,\,Bondi} = \frac{4\pi R_{\rm B}\Delta v^2}{\Omega}\times \int_0^{a_{\max}}{\rm St}\,e^{-2\psi}m(a)f(a)\left[1+2\left({\rm St}\frac{\Omega R_{\rm B}}{\Delta v}\right)^{1/2}e^{-\psi}\right]da,$$

$$\psi \equiv \chi[{\rm St}/(\Omega t_p)]^\gamma.$$

Lyra et al. (2023)

Analytical theory of polydisperse (multi-species) pebble accretion

Monodisperse (single species)

$$\dot{M}_{3D} = \lim_{\xi \to 0} \dot{M} = \pi R_{acc}^2 \rho_{d0} \delta v,$$

$$\dot{M}_{2D} = \lim_{\xi \to \infty} \dot{M} = 2 R_{acc} \Sigma_d \delta v,$$

Lambrechts & Johansen (2012)

Polydisperse (multiple species)

$$\dot{M}_{2D,Hill} = \frac{6(1-p)}{14-5q-3k} \left(\frac{\mathrm{St}_{max}}{0.1} \right)^{2/3} \Omega R_H^2 Z \Sigma_g.$$

$$\dot{M}_{3D,Bondi} \approx C_1 \frac{\gamma_l\left(\frac{b_1+1}{s}, j_1 a_{max}^s\right)}{s\, j_1^{(b_1+1)/s}} + C_2 \frac{\gamma_l\left(\frac{b_2+1}{s}, j_2 a_{max}^s\right)}{s\, j_2^{(b_2+1)/s}} + C_3 \frac{\gamma_l\left(\frac{b_3+1}{s}, j_3 a_{max}^s\right)}{s\, j_3^{(b_3+1)/s}} + C_4 \frac{\gamma_l\left(\frac{b_4+1}{s}, j_4 a_{max}^s\right)}{s\, j_4^{(b_4+1)/s}},$$

Lyra et al. (2023)

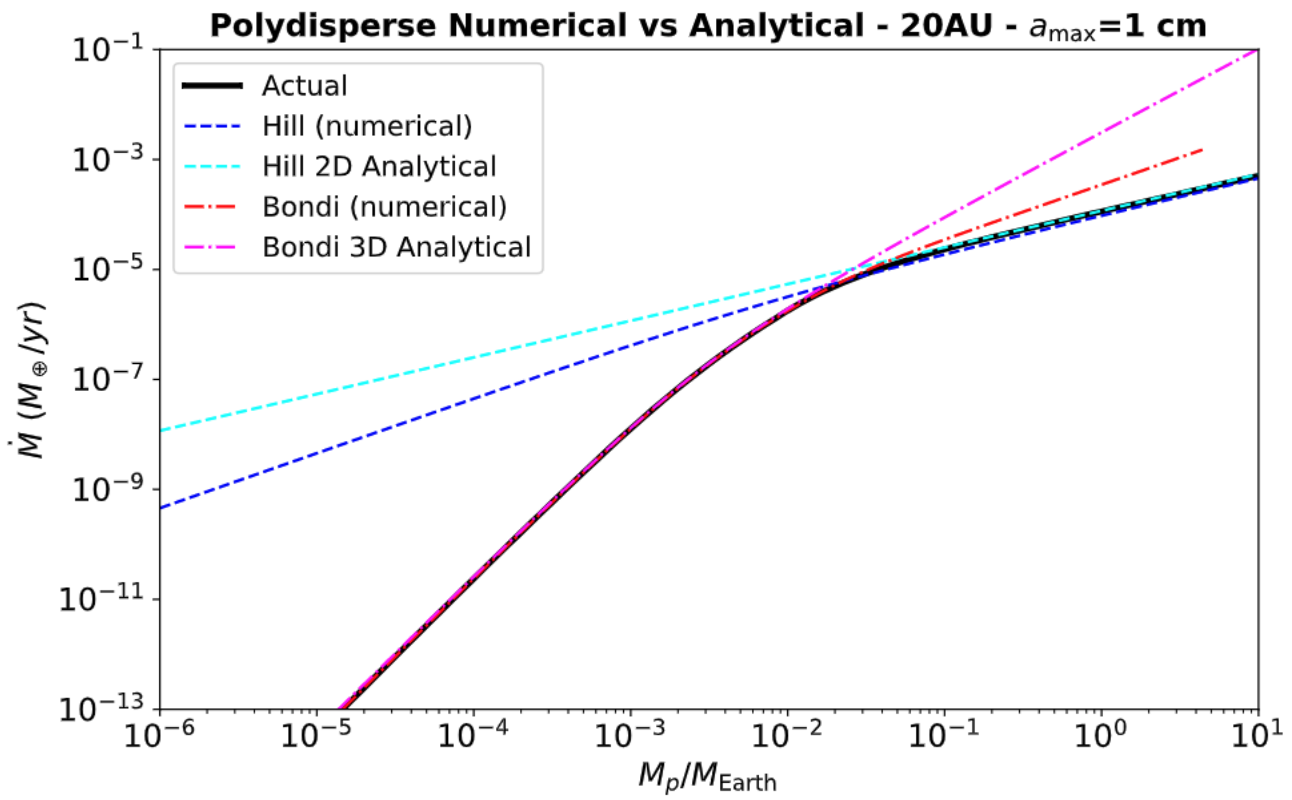

Lyra et al. 2023

Accretion Rates

Bondi (low-mass) regime is 1-2 orders of magnitude more efficient than monodisperse

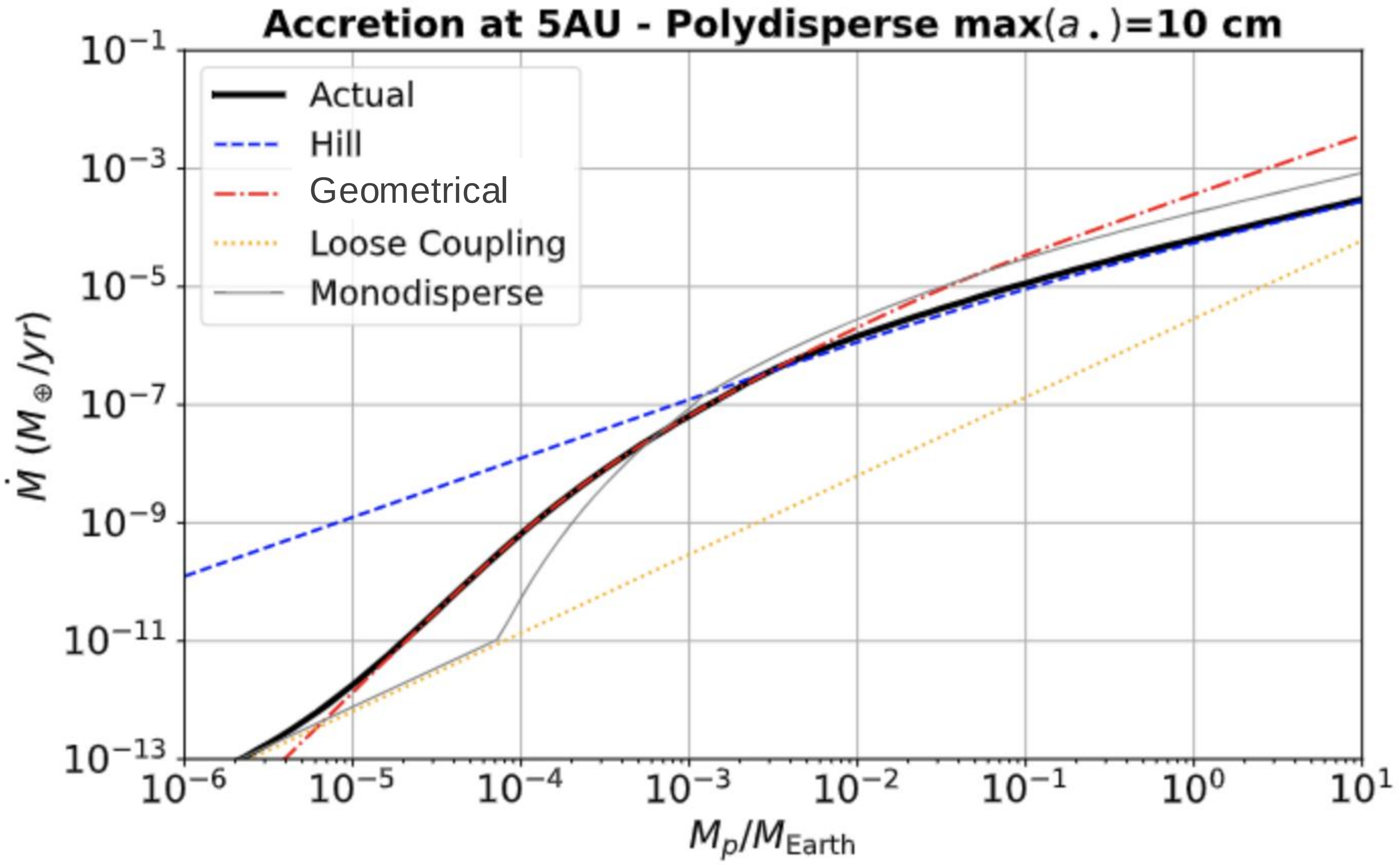

Lyra et al. 2023

Growing Pluto by silicate pebble accretion

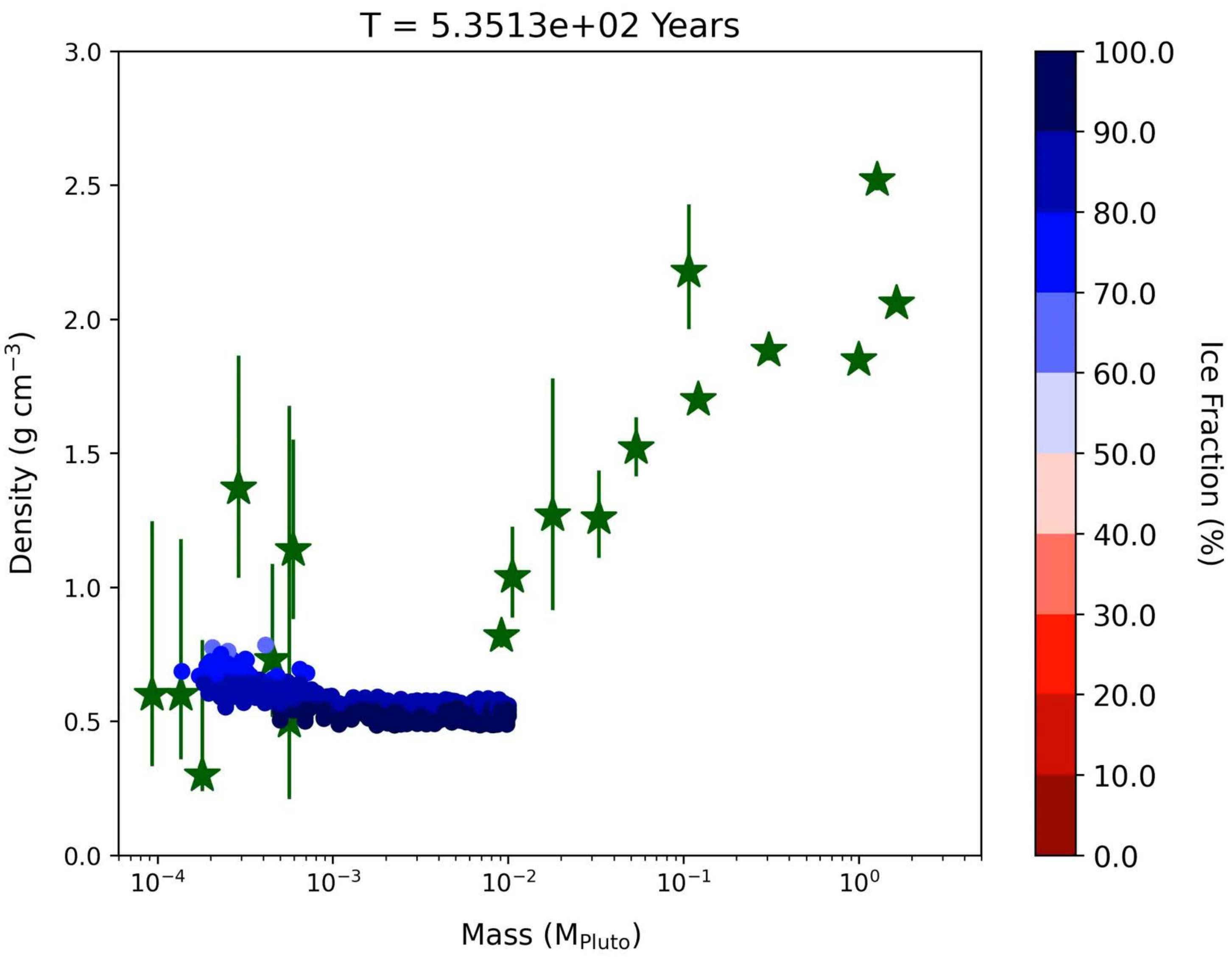

Canas+Lyra et al. 2024

Pebble Density

Ice Fraction

Mass Accretion rate

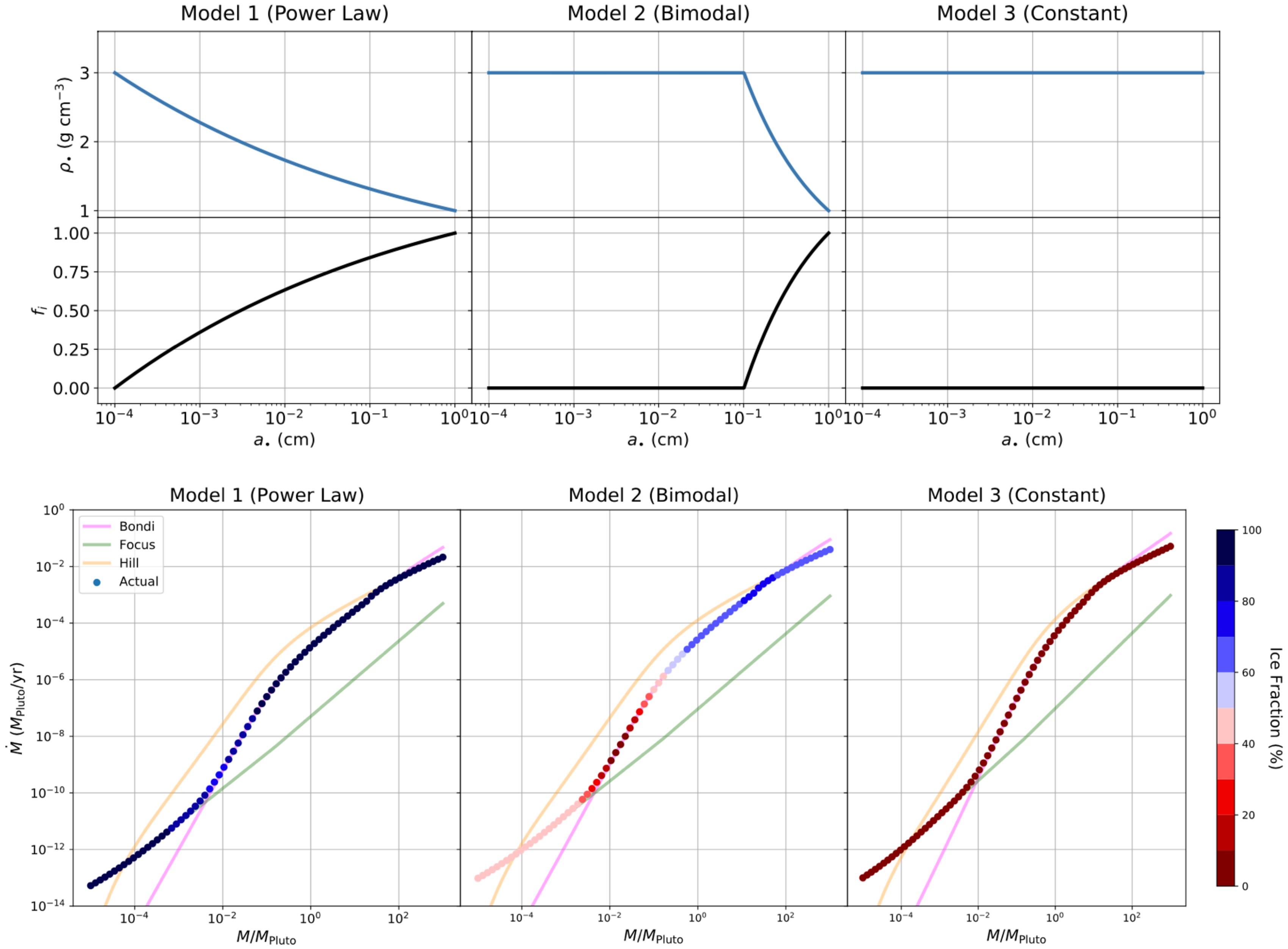

Canas+Lyra et al. 2024

Growing Pluto by silicate pebble accretion

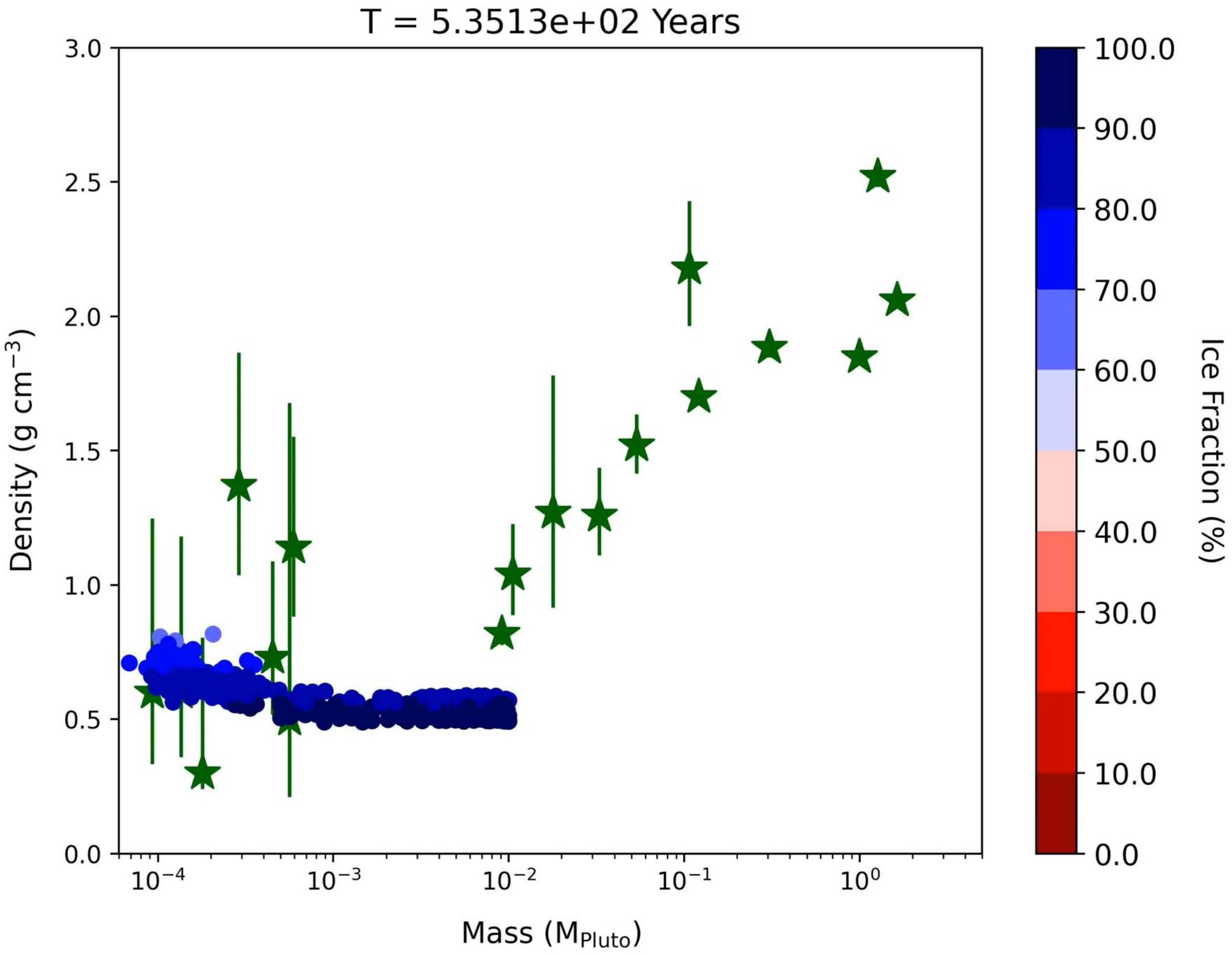

Canas+Lyra et al. 2024

Resulting Densities vs Mass relations

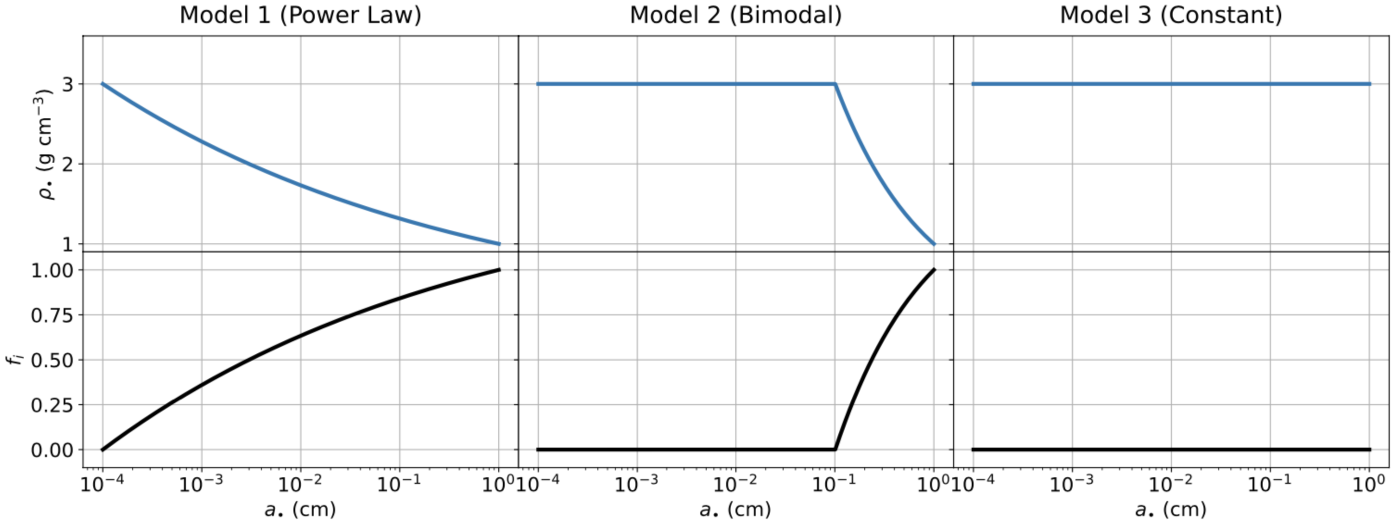

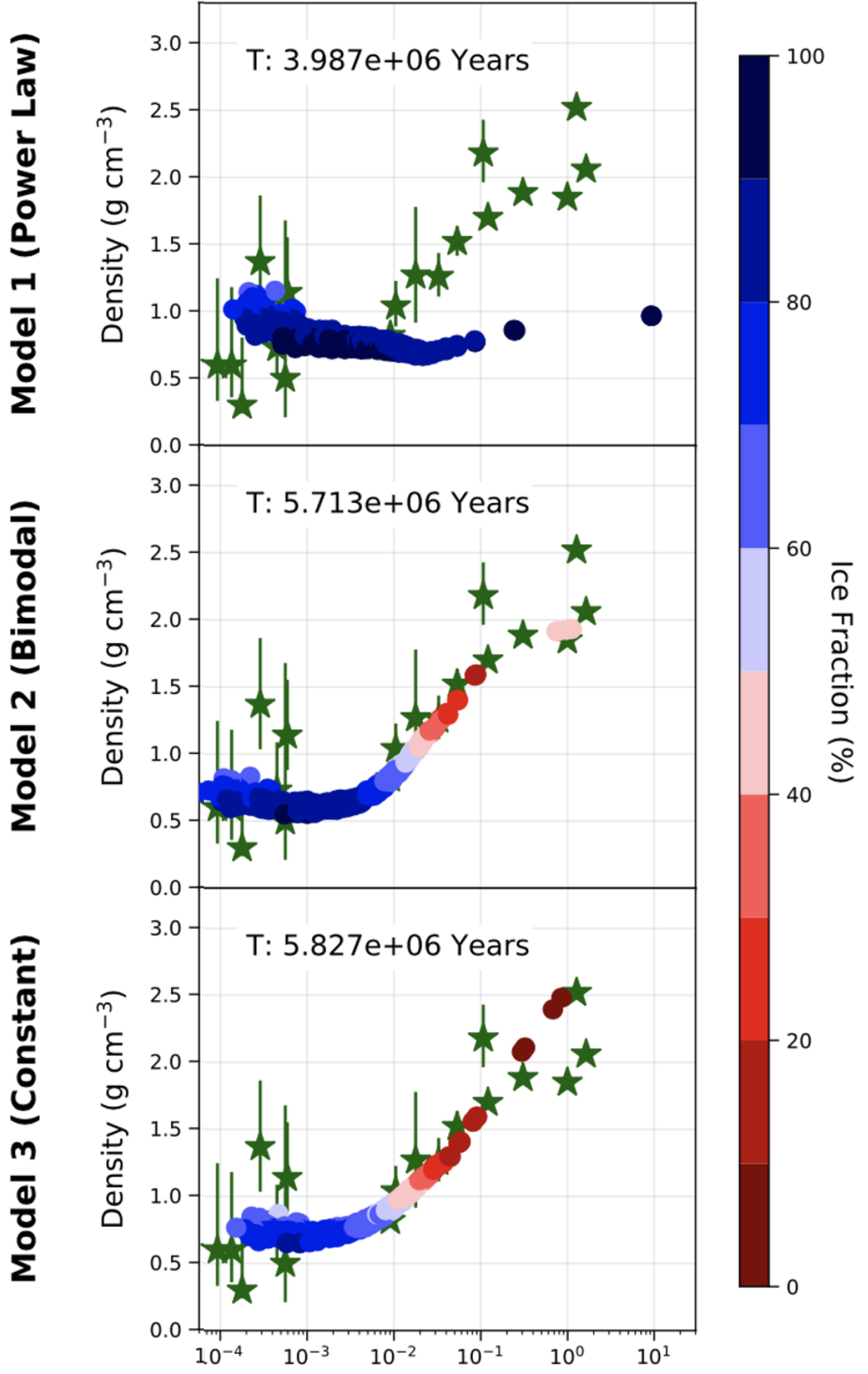

Problem: wrong number density

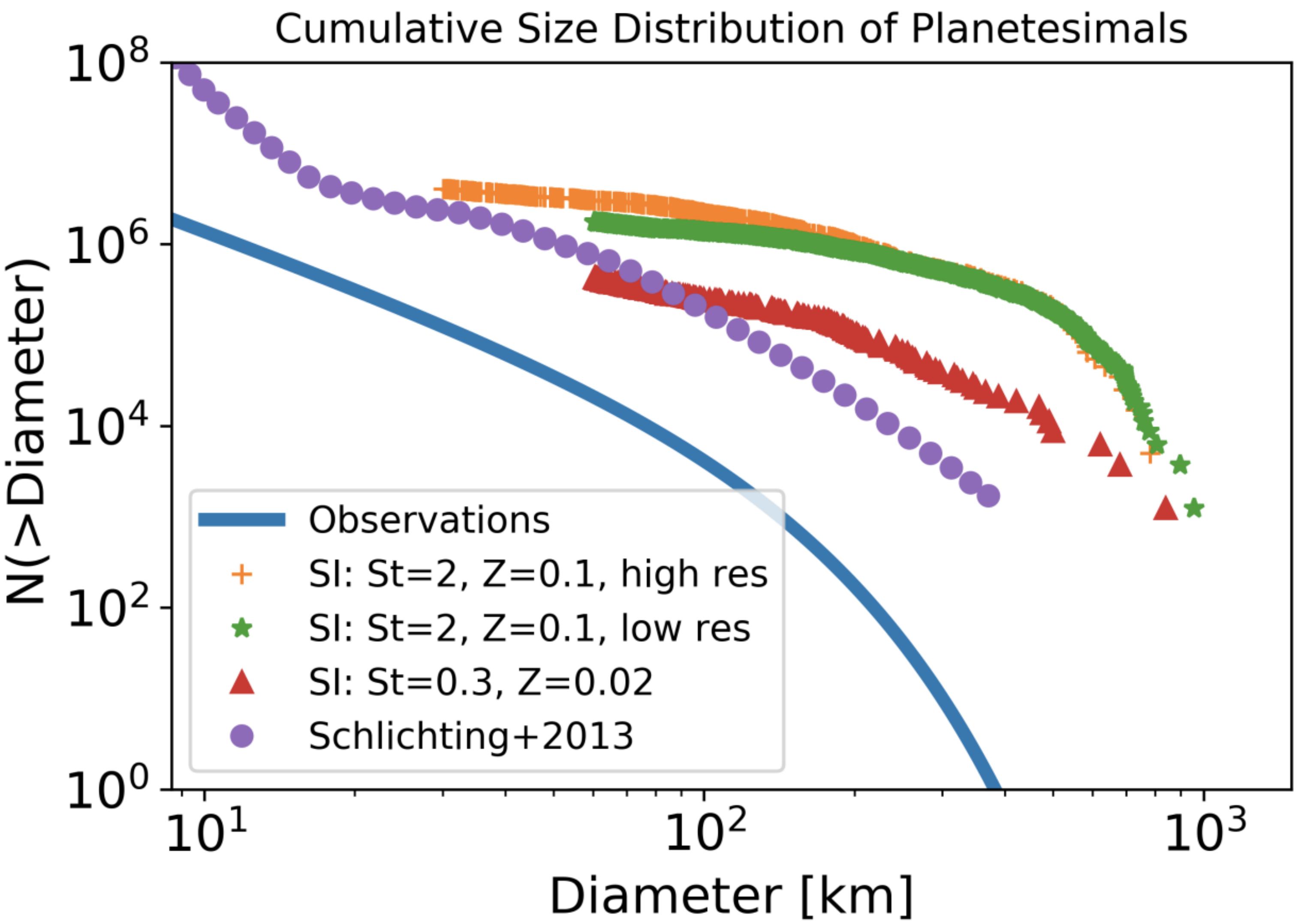

Simon et al. 2023

Vortices – an ubiquitous fluid mechanics phenomenon



Von Kármán *vortex street*


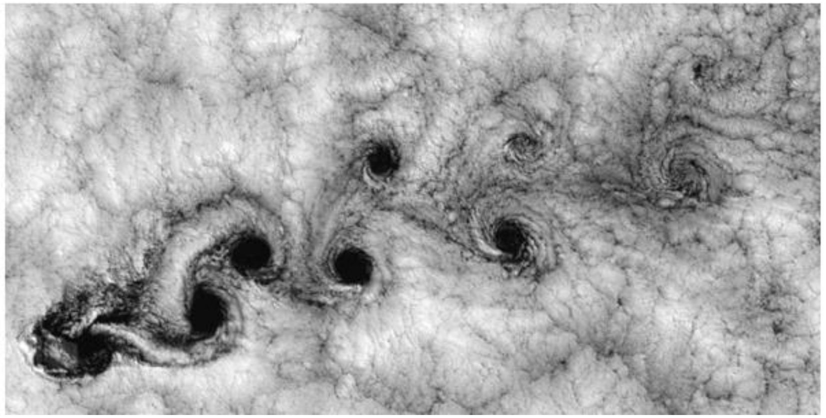

Kelvin-Helmholtz Instability

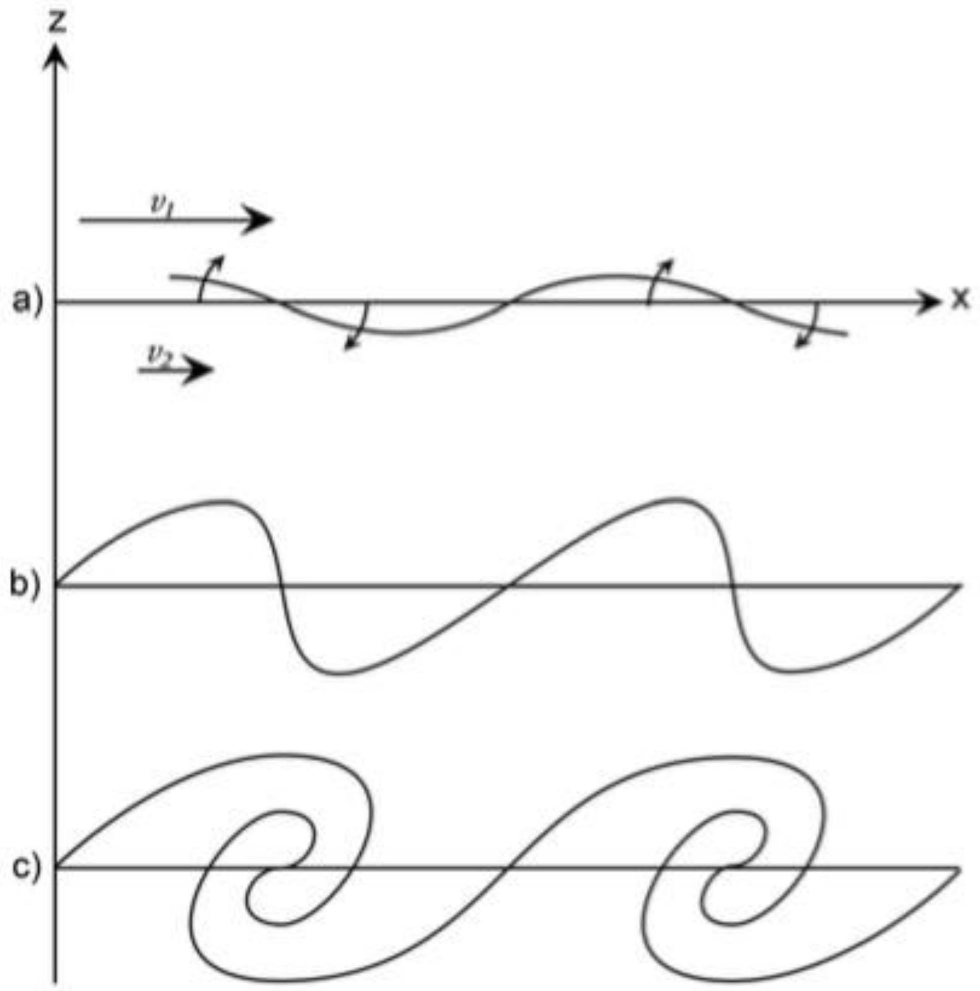

Lovelace & Hohlfeld 1978, Toomre 1981, Papaloizou & Pringle (1984), Hawley (1987), Lovelace et al (1999), Li et al. (2000), Varniere & Tagger (2005), Cheng & Youdin (2023).

Convection

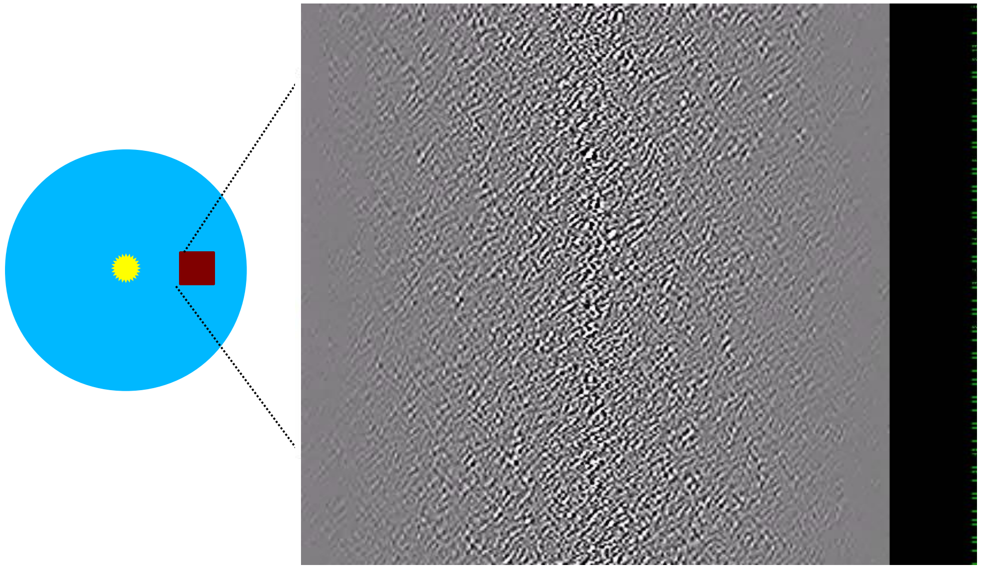

Lyra & Klahr (2011)
Klahr & Hubbard (2014)
Lyra (2014)
Latter (2016)
Volponi (2016)
Reed & Latter (2021)
Raettig et al. (2021)

Sketch of the
Convective Instability

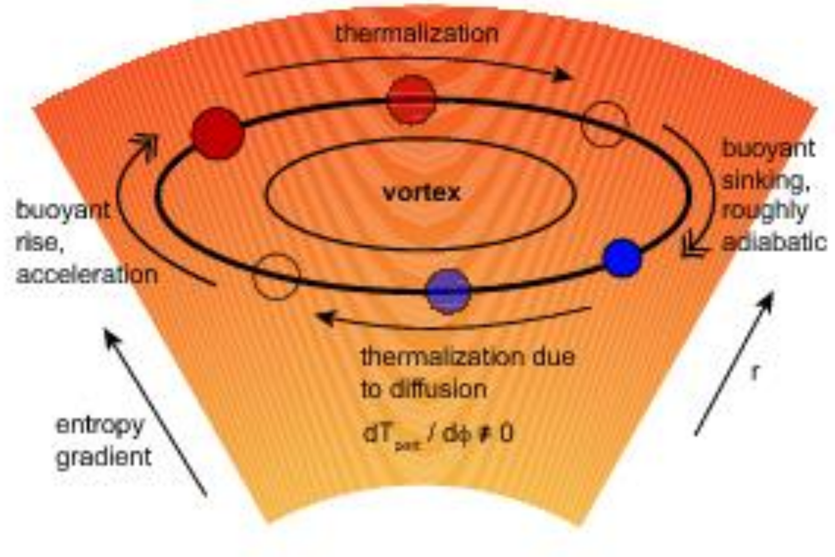

Armitage (2010)

Vortex Trapping

Geostrophic balance:

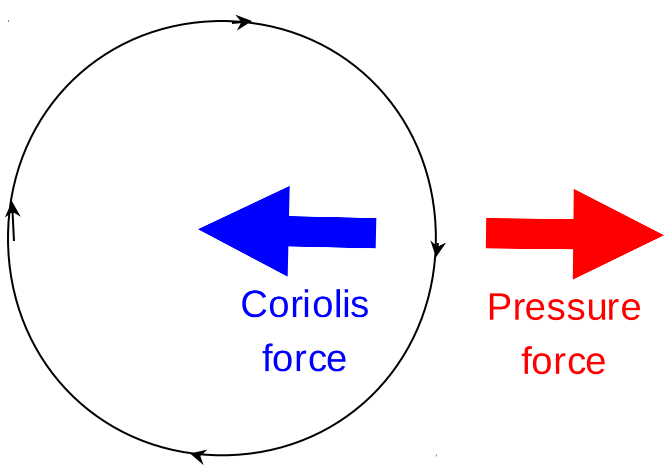

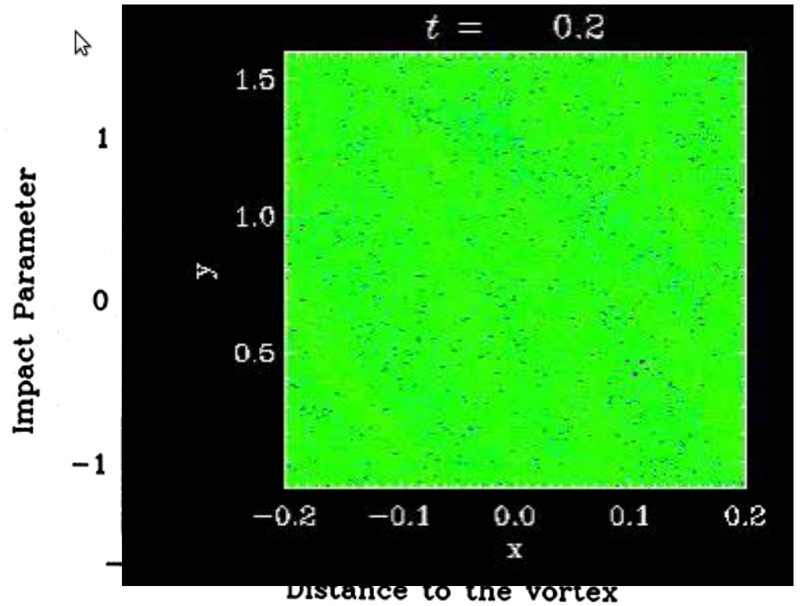

Barge & Sommeria (1995)

Grains do not feel the pressure gradient.

They sink towards the center, where they accumulate.

Aid to planet formation

(Barge & Sommeria 1995, Tanga et al. 1996, Adams et al. 1996)

Speeds up planet formation enormously

(Lyra et al. 2008b, 2009ab, Raettig et al. 2012, 2021)

Vortex Trapping

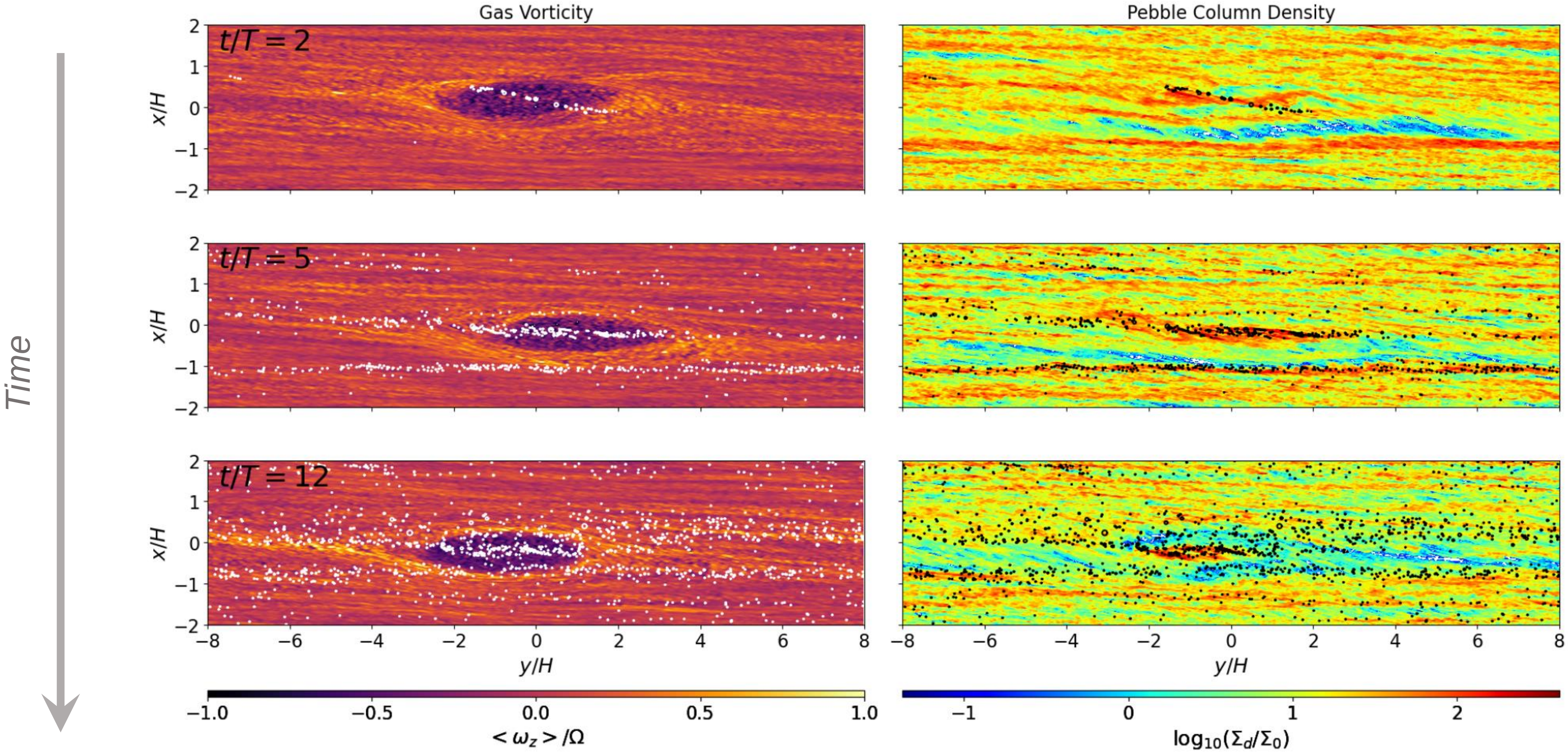

Lyra et al. (2024)

Vortex Trapping – Initial Mass Function

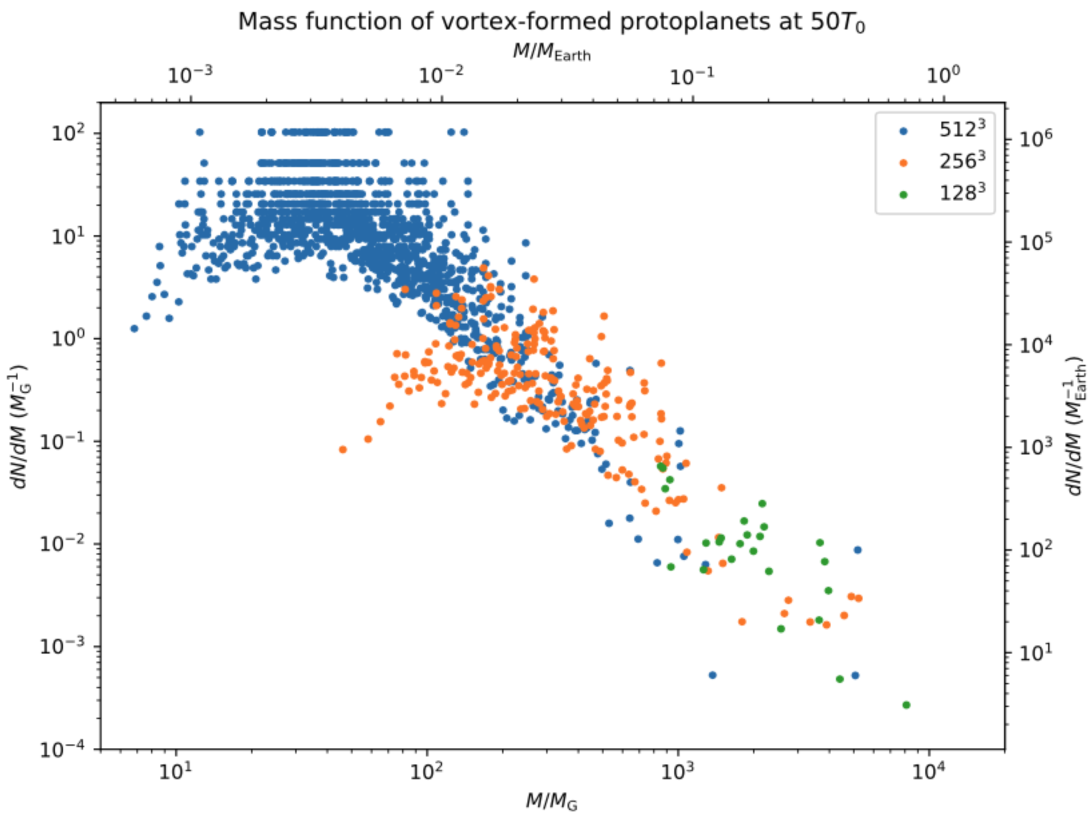

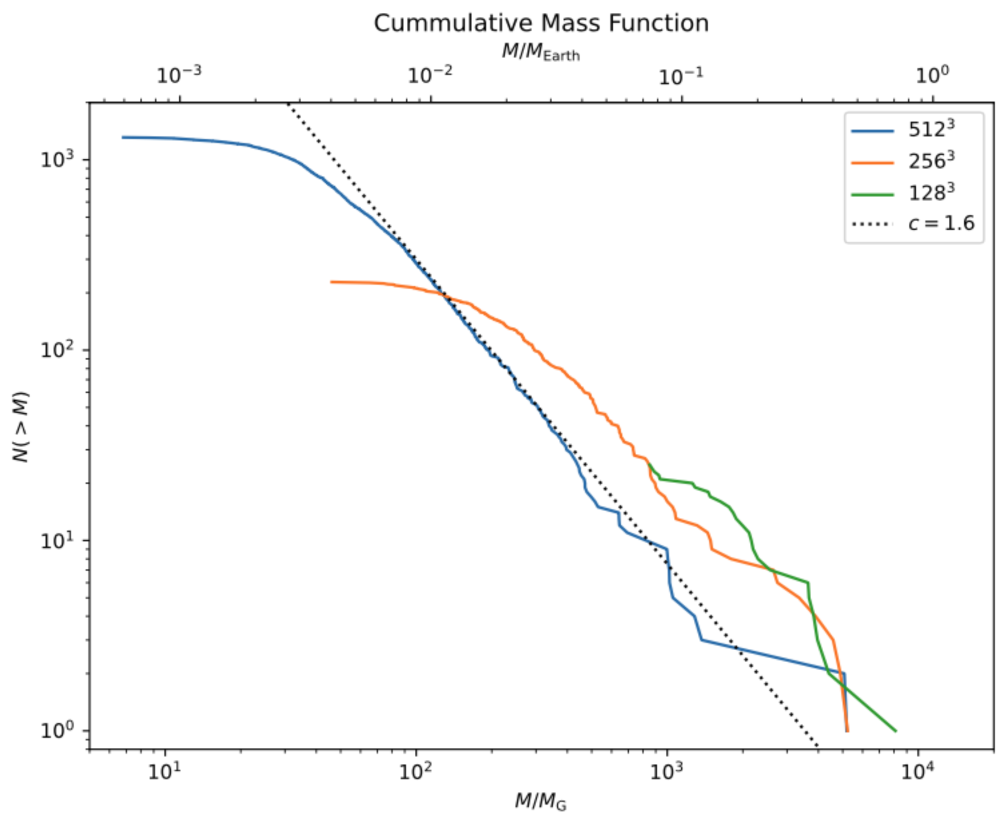

Lyra et al. (2024)

Disk Observations

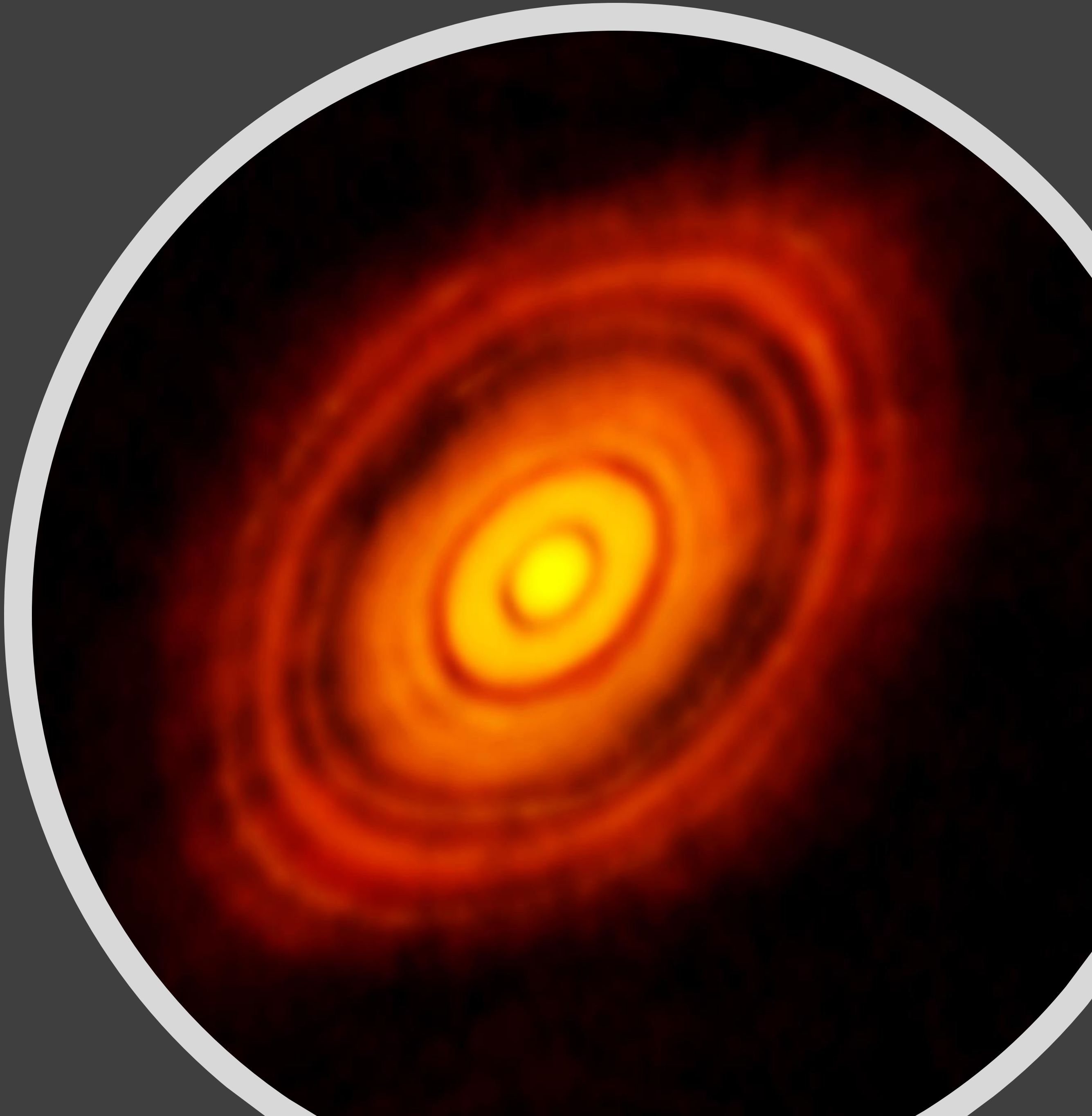

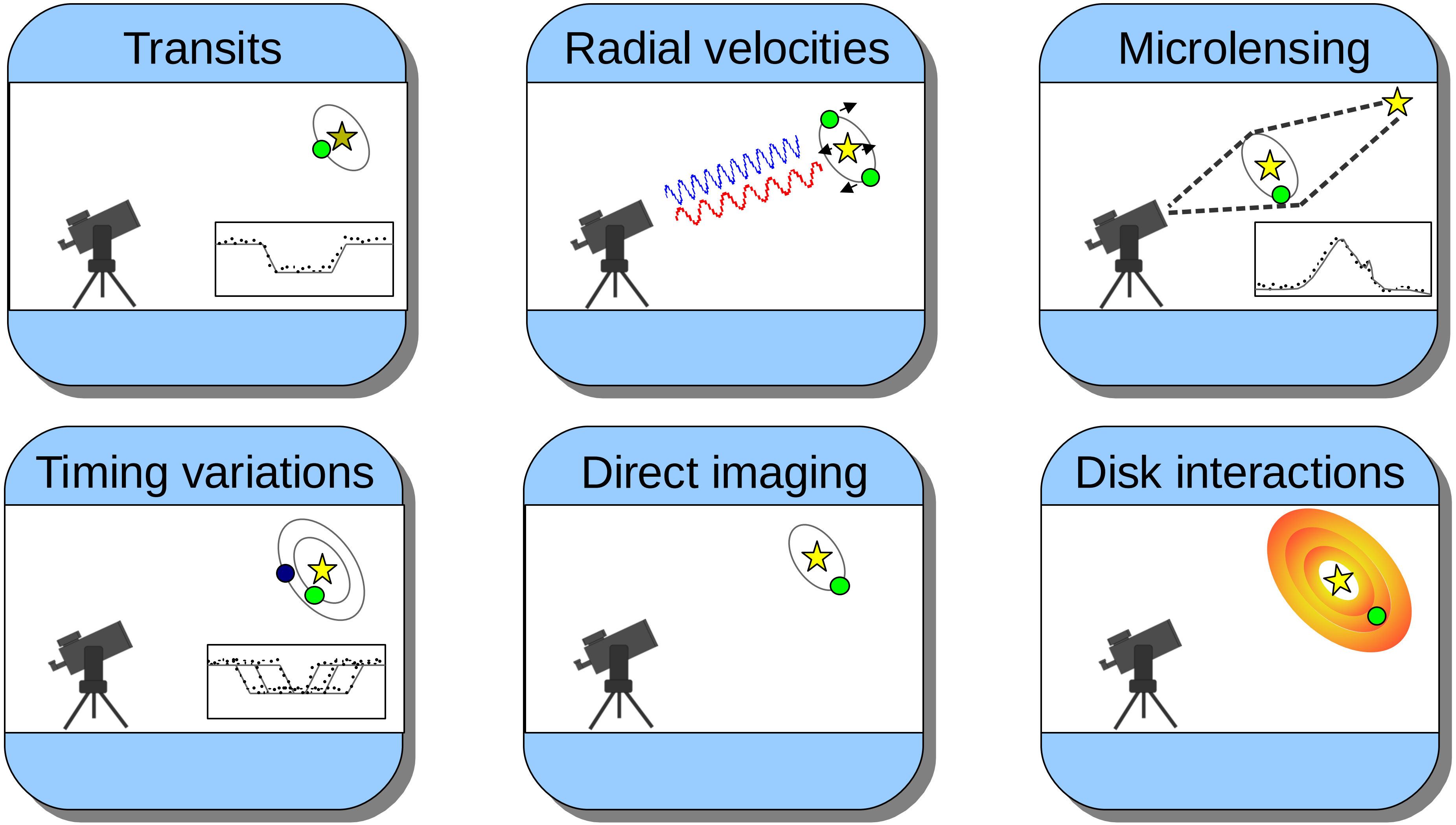

Slide by A. Richert

Disks are optically thick in infrared and optically thin in millimeter

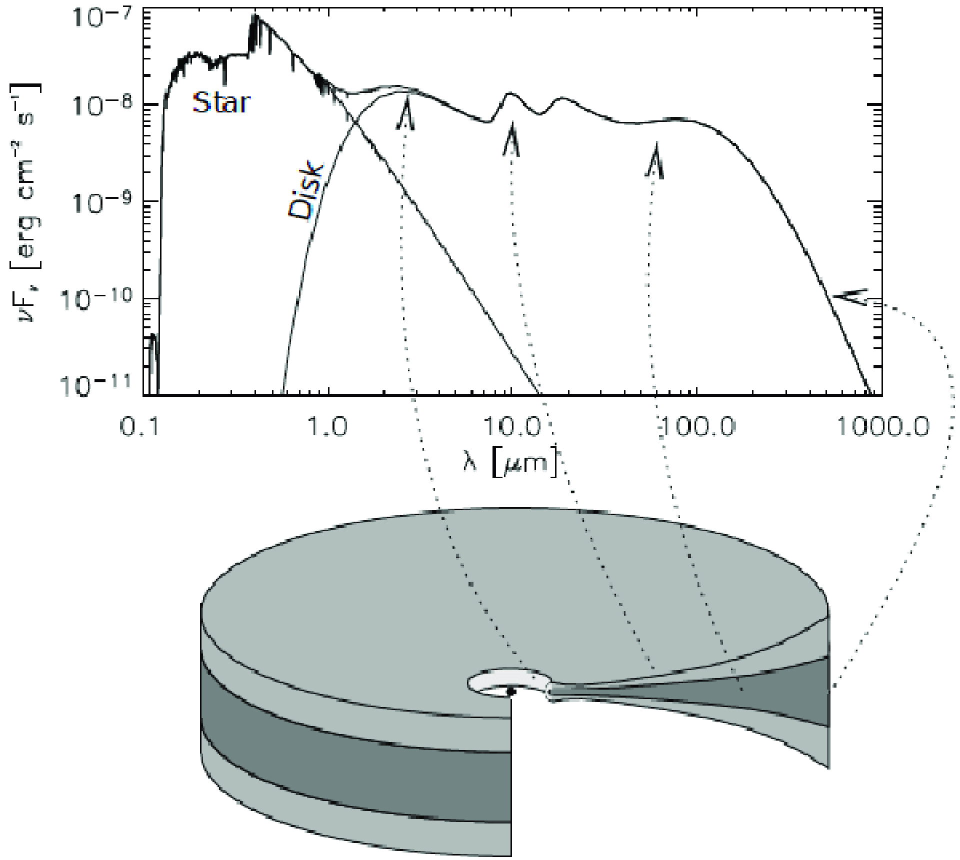

To witness planet formation we must observe in millimeter

A class of disks with missing hot dust.

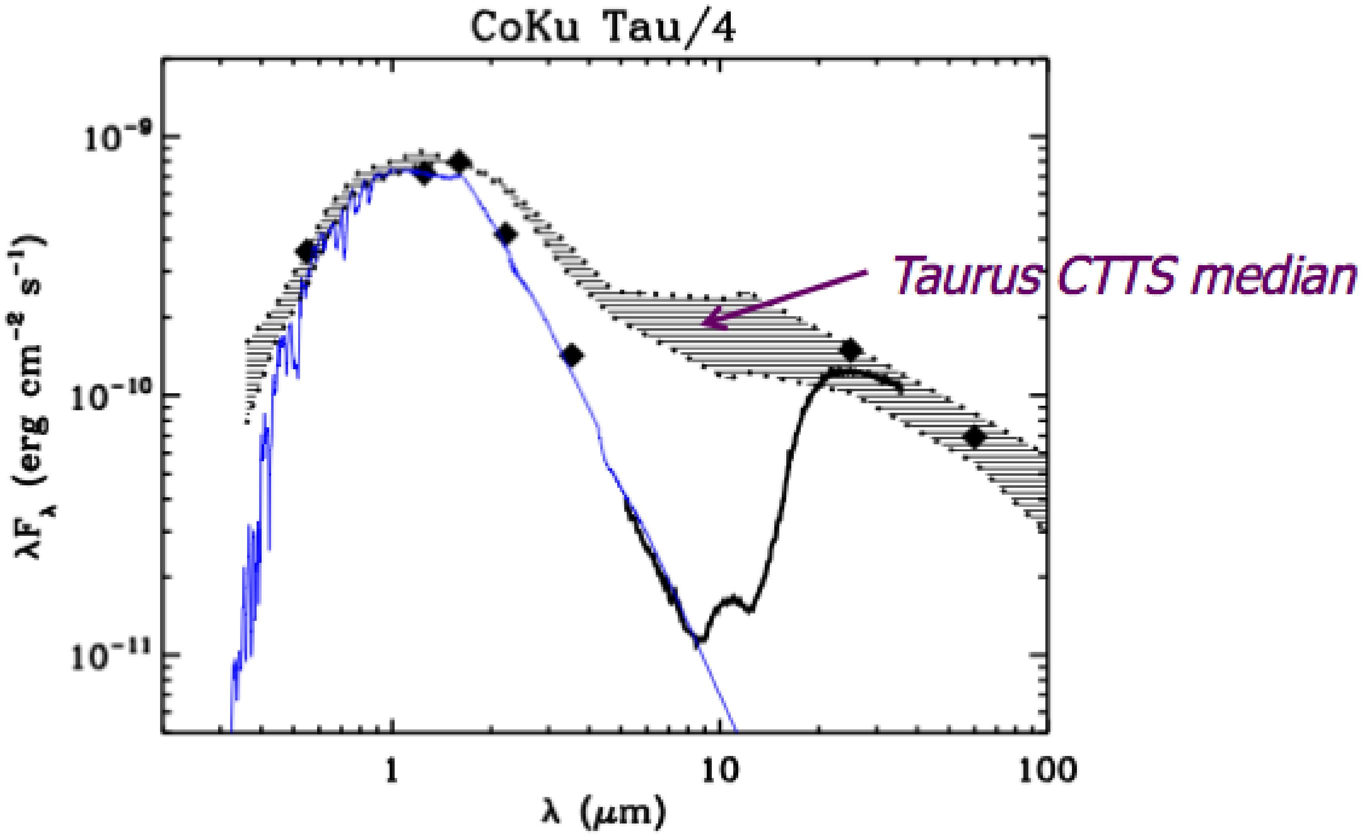

Disks with missing hot dust.

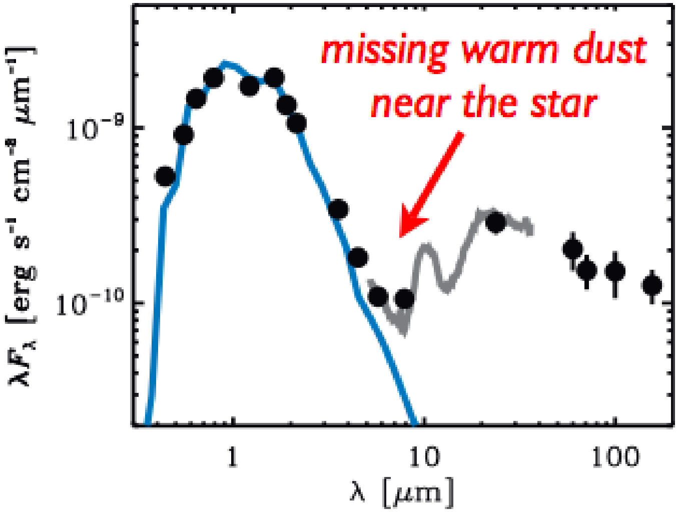

[e.g., Furlan et al. 2009]

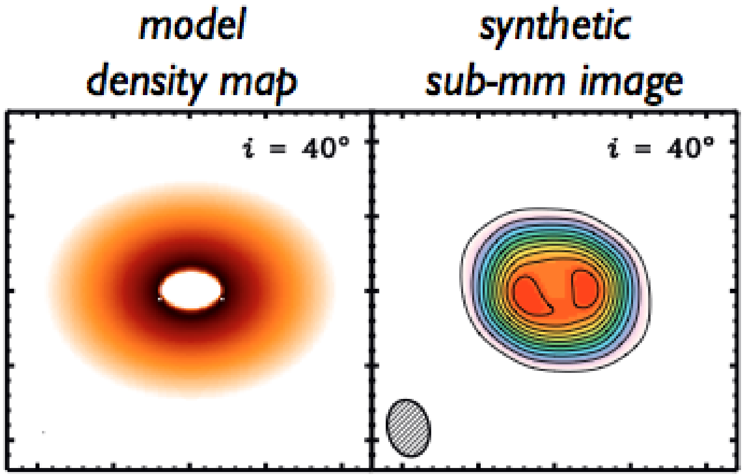

a disk with a large reduction
in optical depth near the star
(i.e., a "cavity" or "hole")

Planetary companion

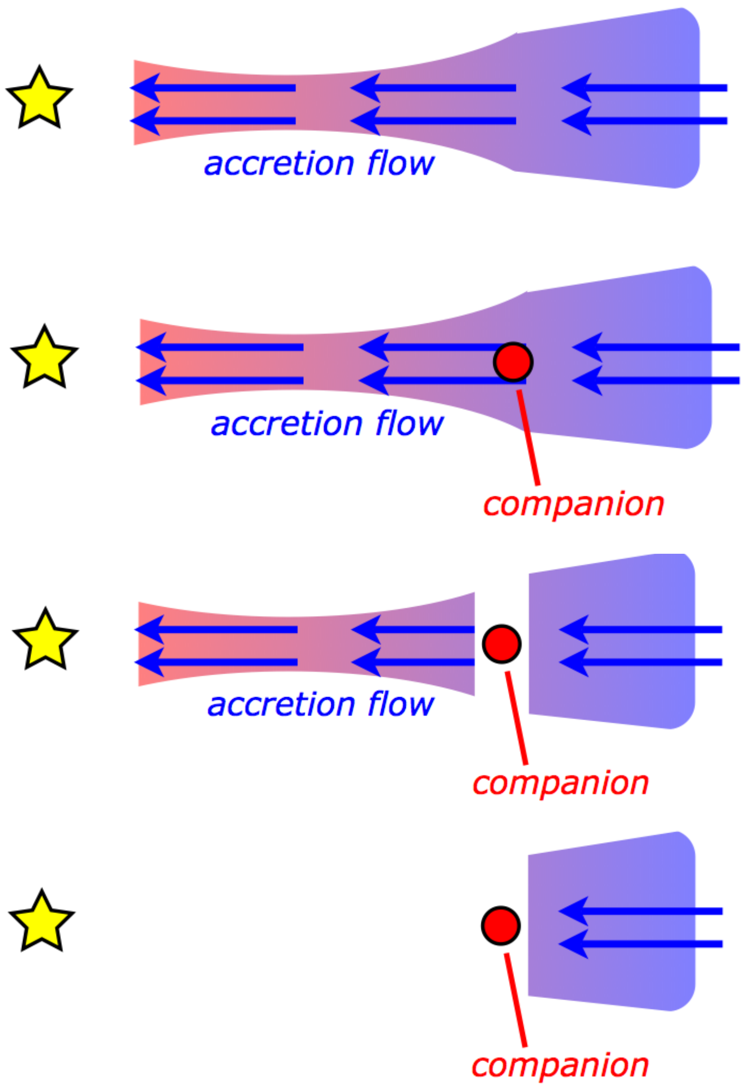

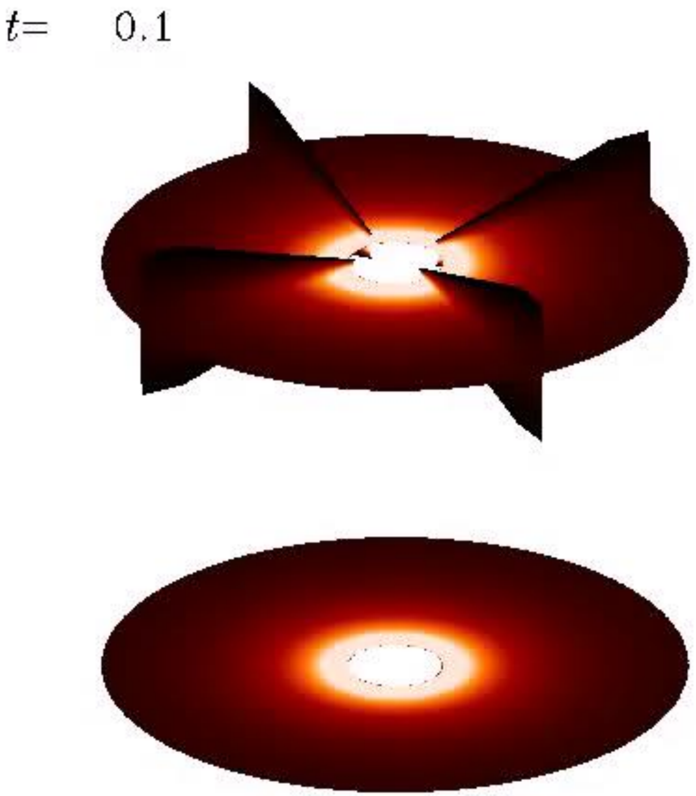

(Lyra 2009)

These cavities may be the telltale signature of forming planets

PDS 70 and PDS 70b

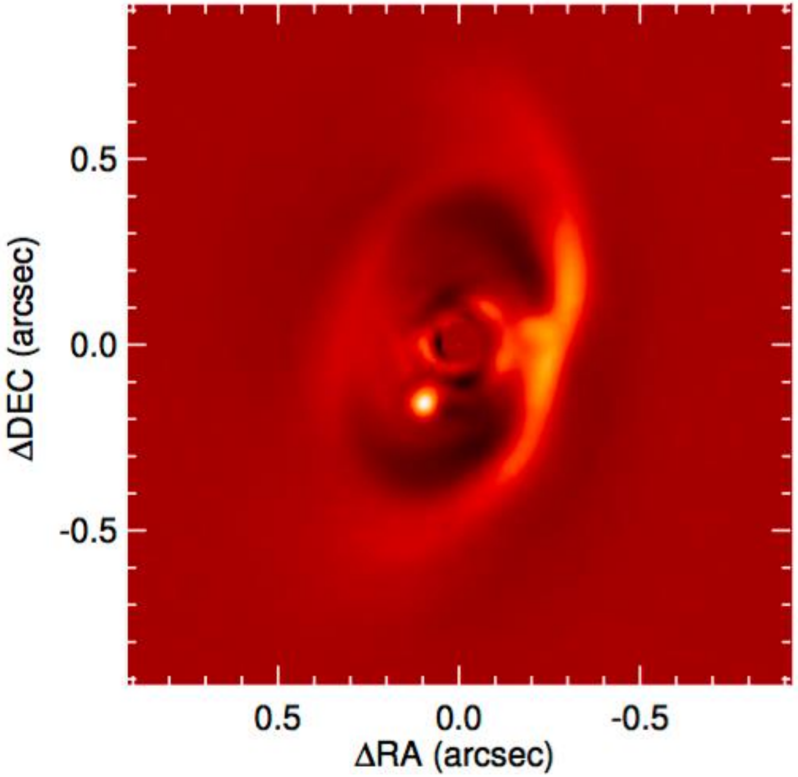

(Muller et al. 2018)

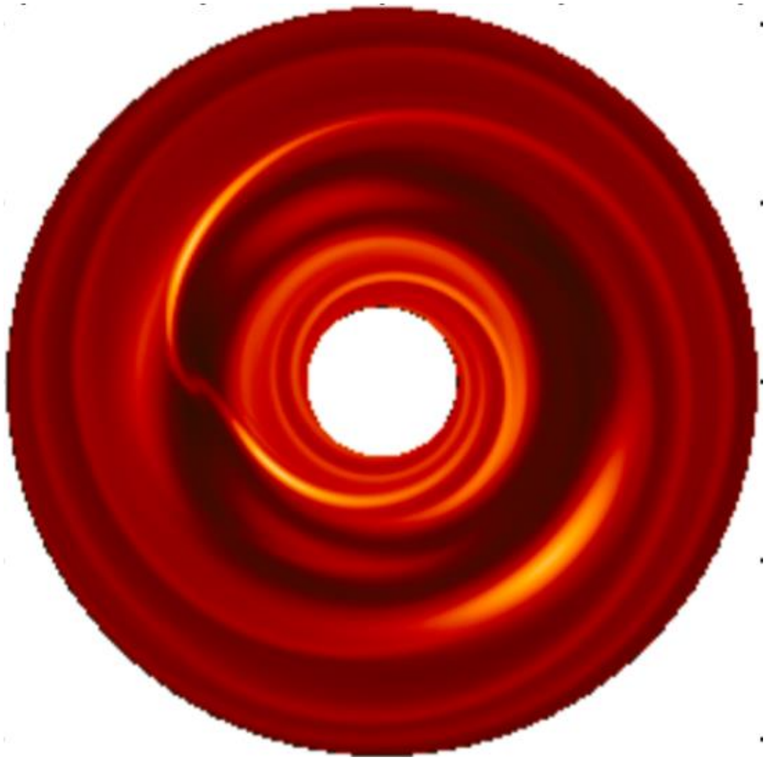

(Lyra et al. 2009b)

A way to directly study planet-disk interaction

Planet-disk interaction: gaps, spirals, and vortices.

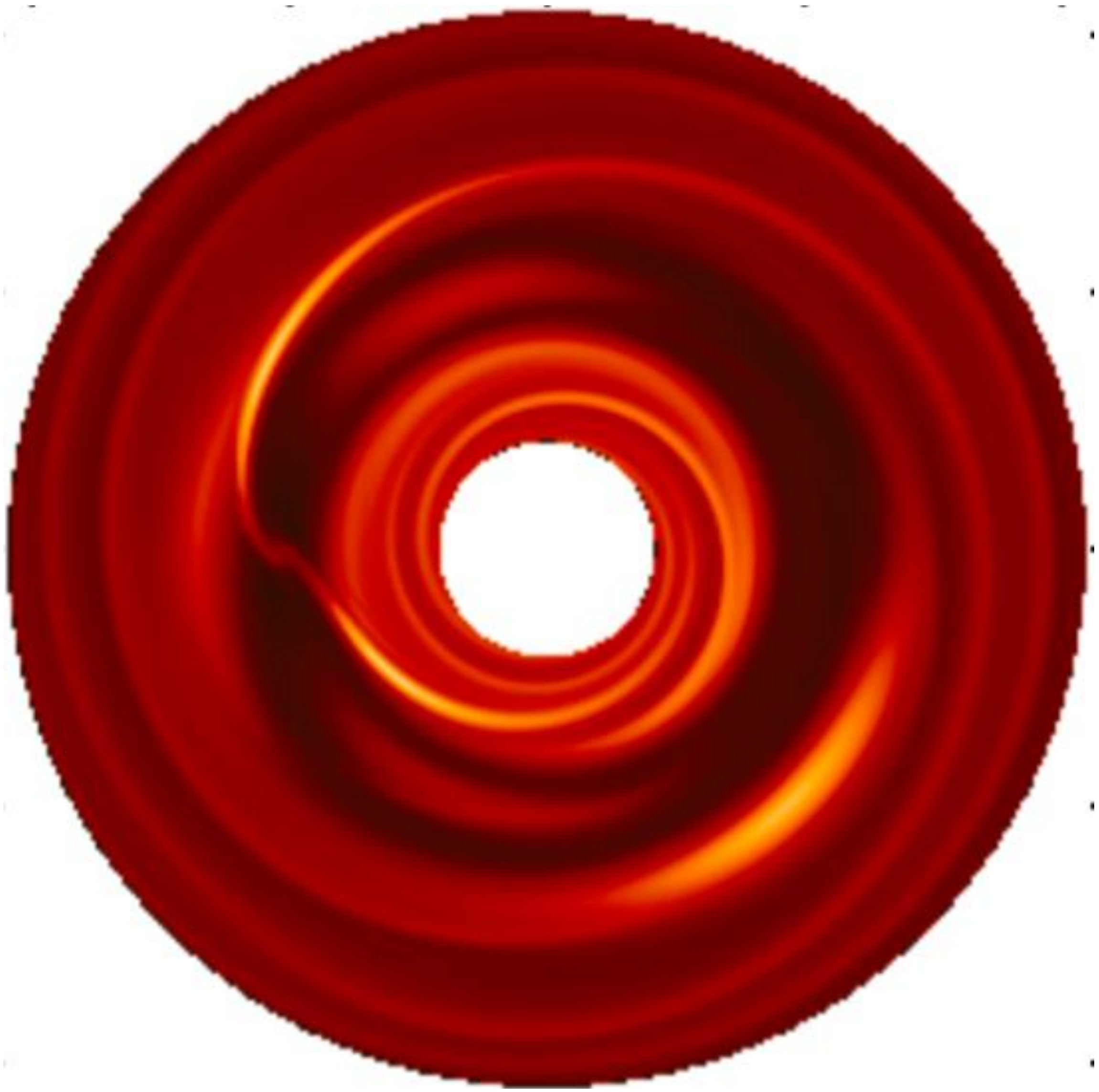

(Lyra et al. 2009b)

Observational evidence: gaps, spirals, and vortices

HL Tau

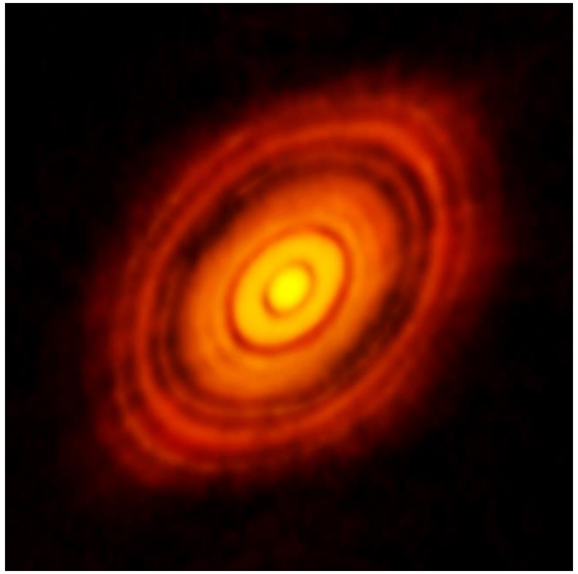

The ALMA Partnership et al. (2015)

SAO 206462

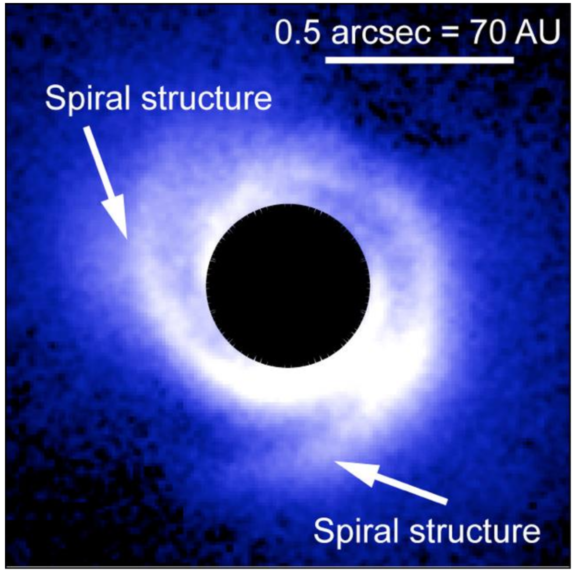

Muto et al. (2012)

Oph IRS 48

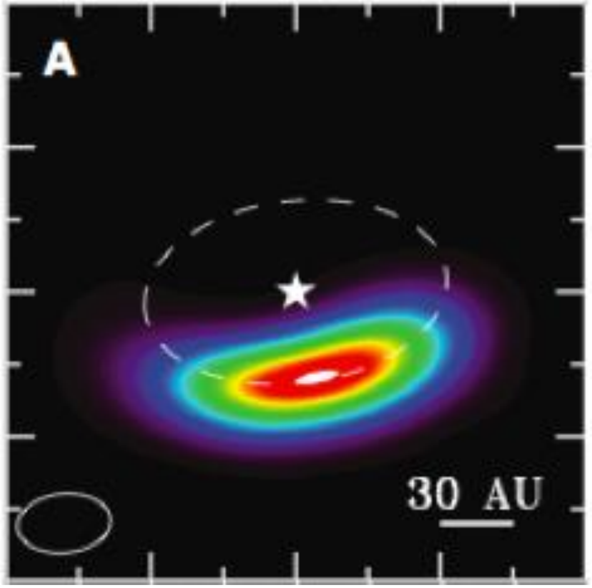

van der Marel et al. (2013)

The Atacama Large (sub-)Millimeter Array (ALMA)

The Very Large Array (VLA)

The ALMA Re~~v~~solution

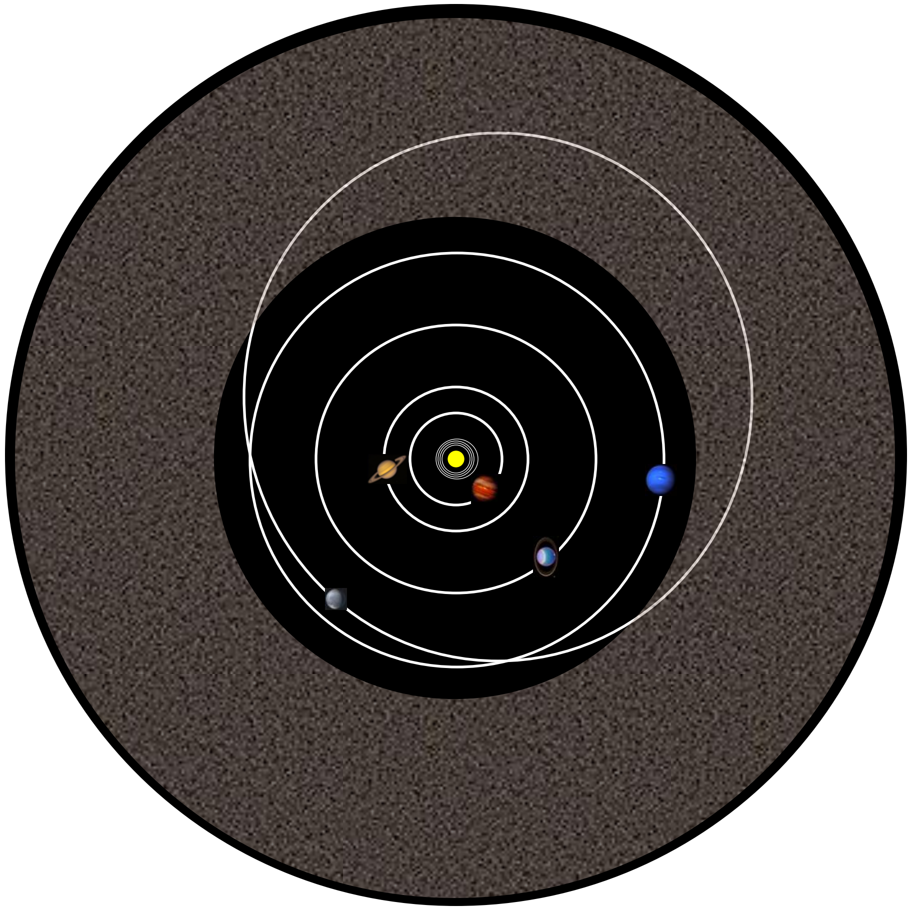

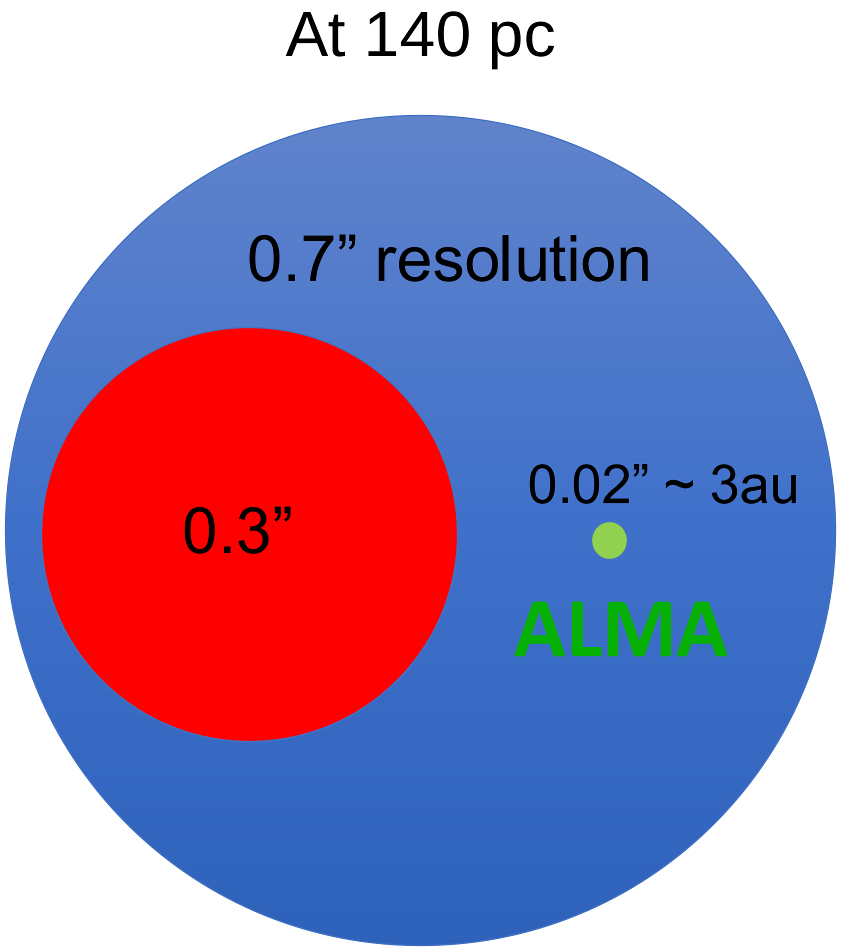

Before ALMA

ALMA

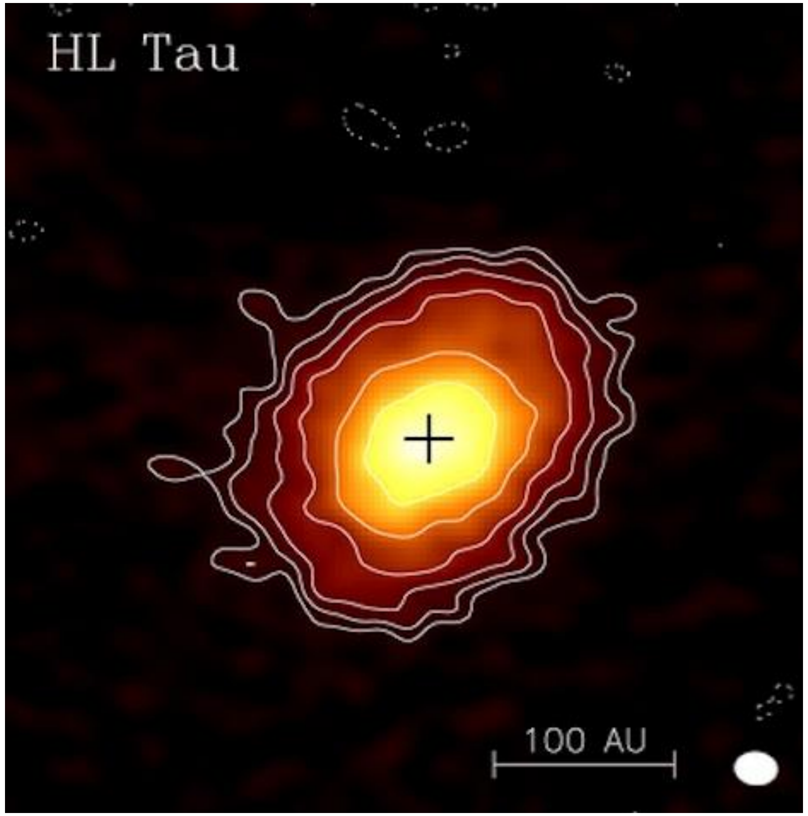

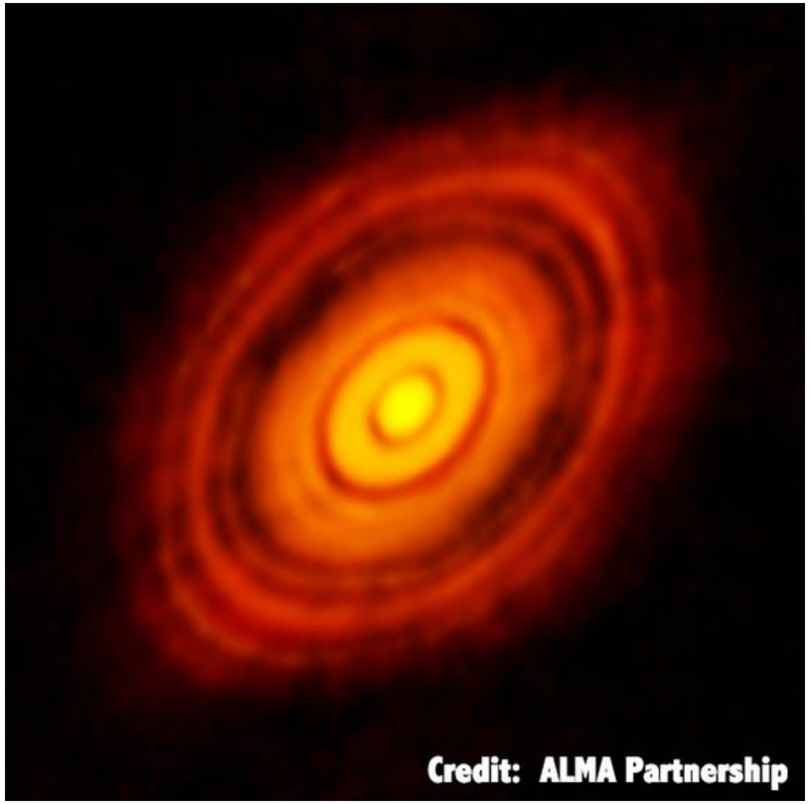

Dust traps in disks: ALMA Cycle 0 (2012)

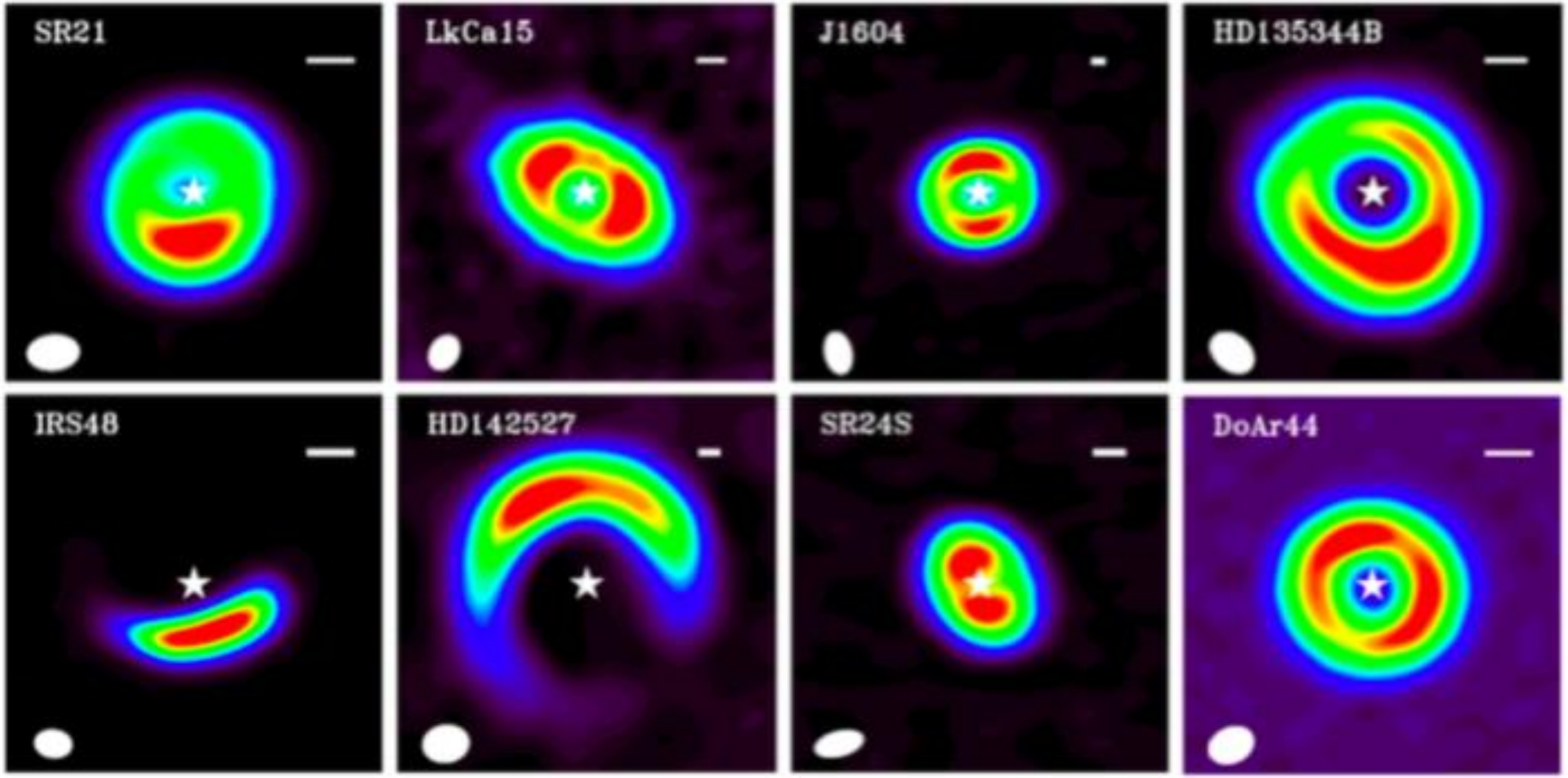

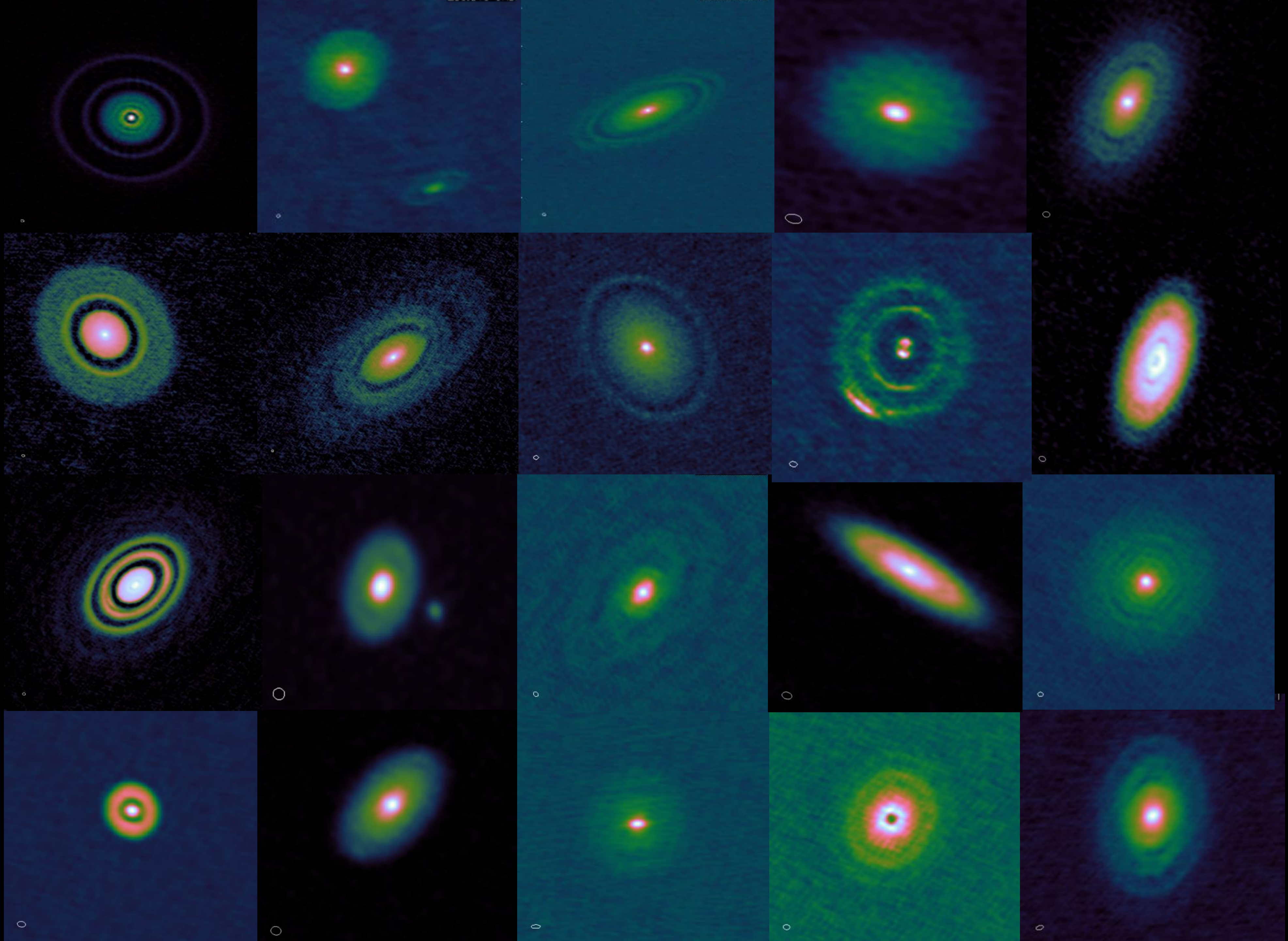

Oph IRS 48

A Major Asymmetric Dust Trap in a Transition Disk

Nienke van der Marel,[1*] Ewine F. van Dishoeck,[1,2] Simon Bruderer,[2] Til Birnstiel,[3] Paola Pinilla,[4] Cornelis P. Dullemond,[4] Tim A. van Kempen,[1,5] Markus Schmalzl,[1] Joanna M. Brown,[3] Gregory J. Herczeg,[6] Geoffrey S. Mathews,[1] Vincent Geers[7]

The statistics of discovered exoplanets suggest that planets form efficiently. However, there are fundamental unsolved problems, such as excessive inward drift of particles in protoplanetary disks during planet formation. Recent theories invoke dust traps to overcome this problem. We report the detection of a dust trap in the disk around the star Oph IRS 48 using observations from the Atacama Large Millimeter/submillimeter Array (ALMA). The 0.44-millimeter–wavelength continuum map shows high-contrast crescent-shaped emission on one side of the star, originating from millimeter-sized grains, whereas both the mid-infrared image (micrometer-sized dust) and the gas traced by the carbon monoxide 6-5 rotational line suggest rings centered on the star. The difference in distribution of big grains versus small grains/gas can be modeled with a vortex-shaped dust trap triggered by a companion.

Although the ubiquity of planets is confirmed almost daily by detections of new exoplanets (*1*), the exact formation mechanism of planetary systems in disks of gas and dust around young stars remains a long-standing problem in astrophysics (*2*). In

iencemag.org SCIENCE VOL 340 7 JUNE 2013 1199

Down

van der Marel+ ‘13

A huge vortex observed with ALMA

The Oph IRS 48 “comet formation factory”

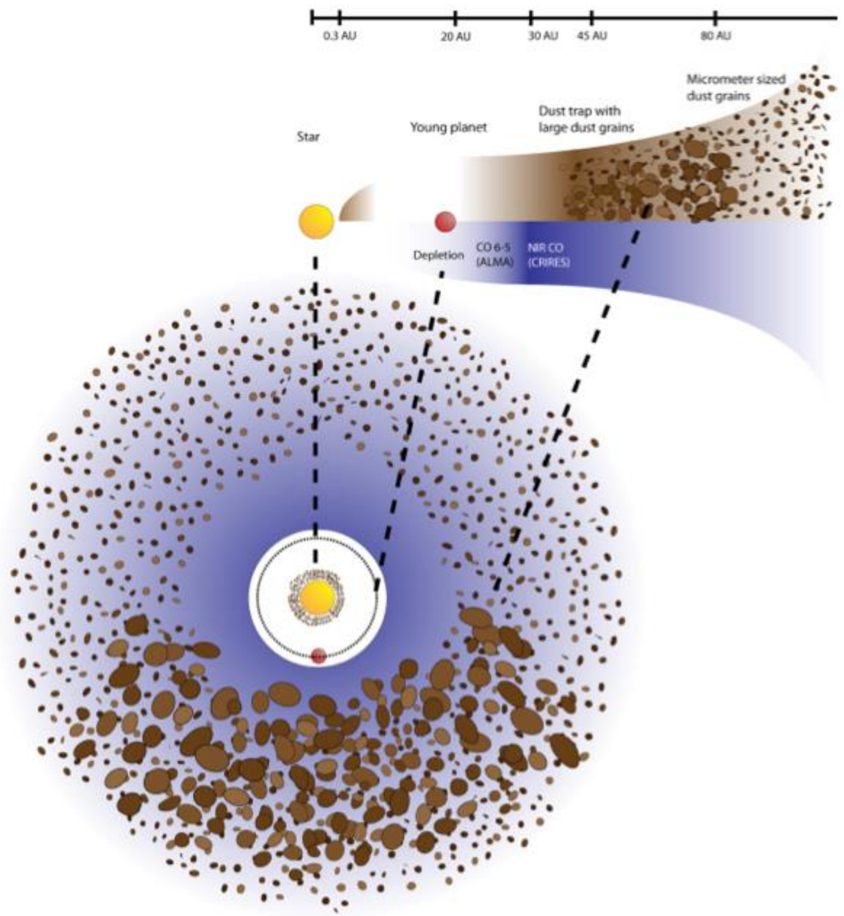

van der Marel+. ‘13

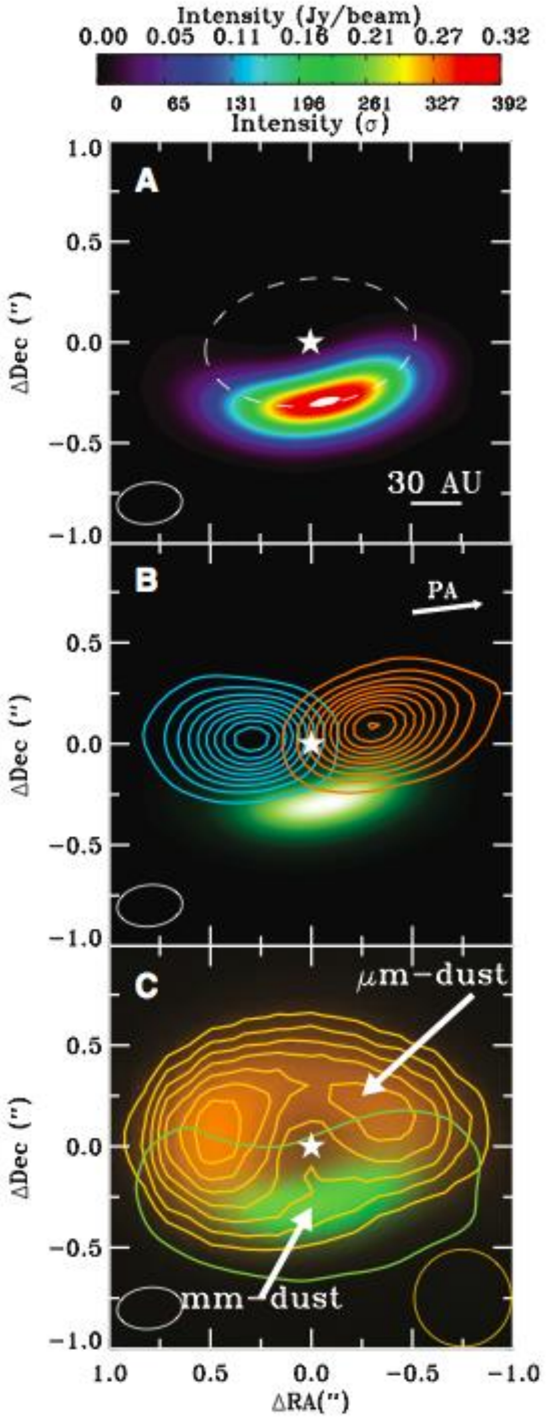

asymmetric mm dust at 63 AU

Gas detection: Keplerian rotation

Micron-sized dust follows gas

Drag-Diffusion Equilibrium

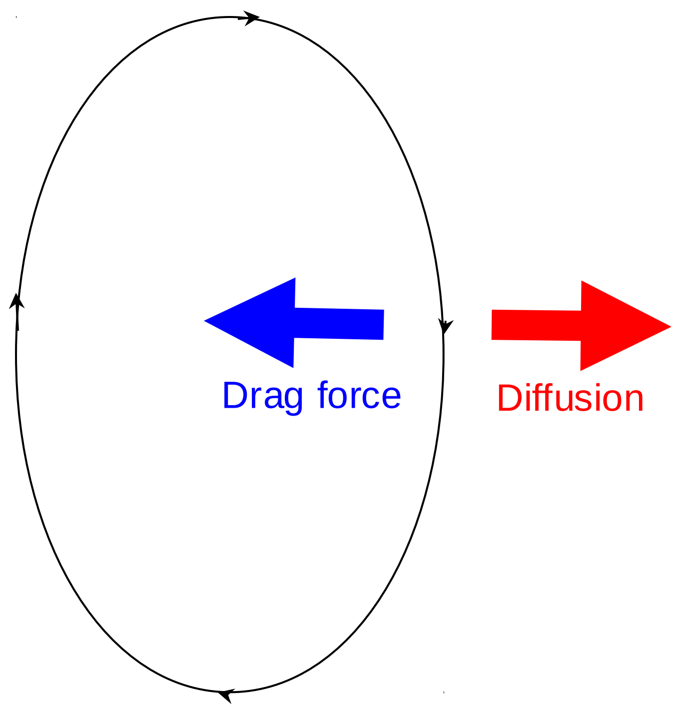

Trapped particle

Dust continuity equation

$$\frac{\partial \rho_d}{\partial t} = -(\boldsymbol{v} \cdot \boldsymbol{\nabla})\rho_d - \rho_d \boldsymbol{\nabla} \cdot \boldsymbol{v} + D\nabla^2 \rho_d,$$

advection **compression** **diffusion**

Analytical Solution for dust in Drag-Diffusion Equilibrium

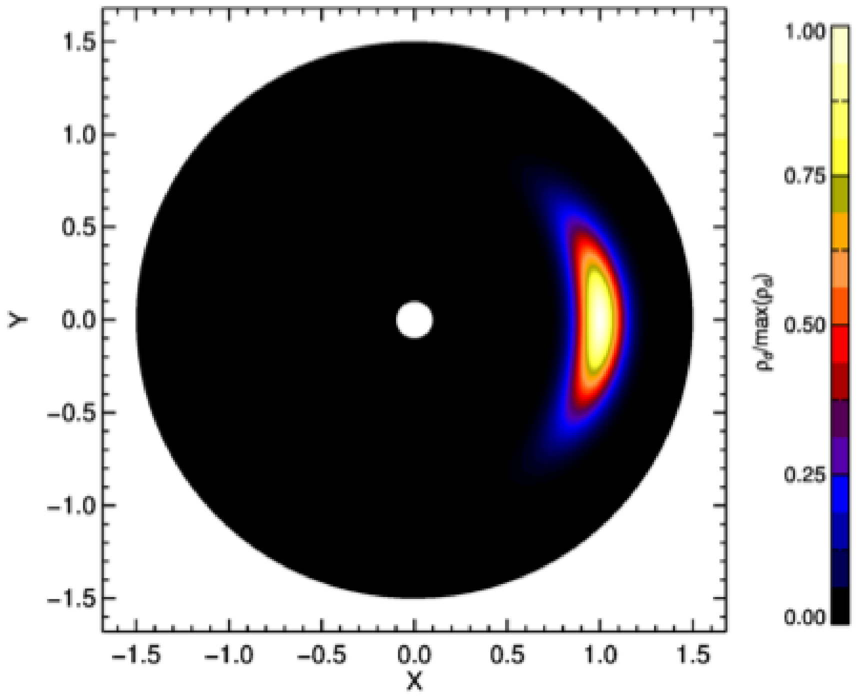

Solution for

H/r=0.1 χ*=4* *S*=1

Steady-state solution

$$\rho_d(a,z) = \varepsilon\rho_0 (S+1)^{3/2} \exp\left\{-\frac{[a^2 f^2(\chi) + z^2]}{2H^2}(S+1)\right\}$$

Lyra & Lin '13

$$S = \frac{St}{d}$$

$$\delta = v_{\rm rms}^2 / c_s^2,$$

a = vortex semi-minor axis
H = disk scale height (temperature)
χ = vortex aspect ratio
δ = diffusion parameter
St = Stokes number (particle size)
f(χ*)* = model-dependent scale function

Disk Tomography
SPHERE-ALMA-VLA overlay of MWC 758

SPHERE (μm)

ALMA (~ mm)

VLA (cm-m)

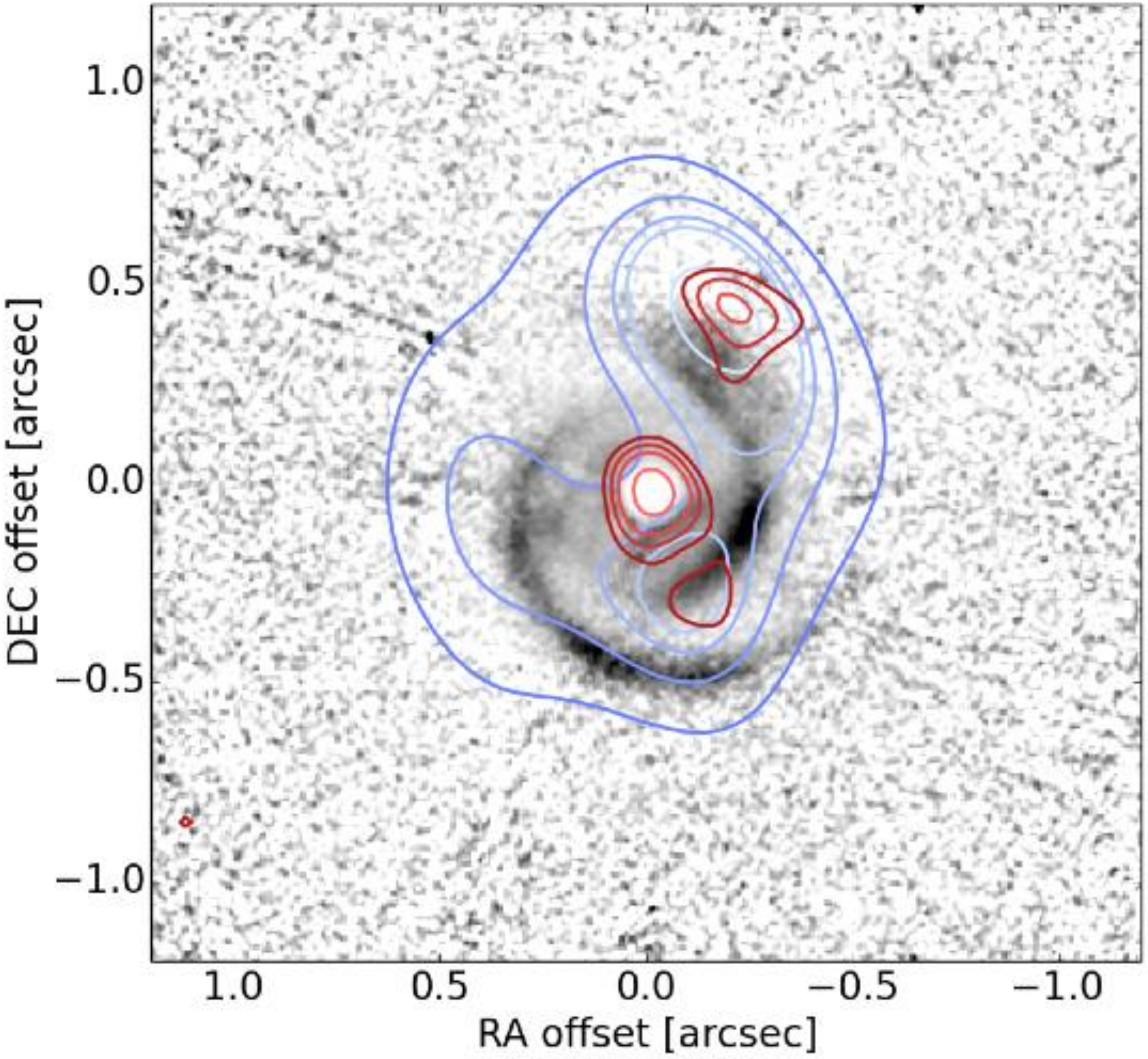

Marino+Lyra '15

ALMA

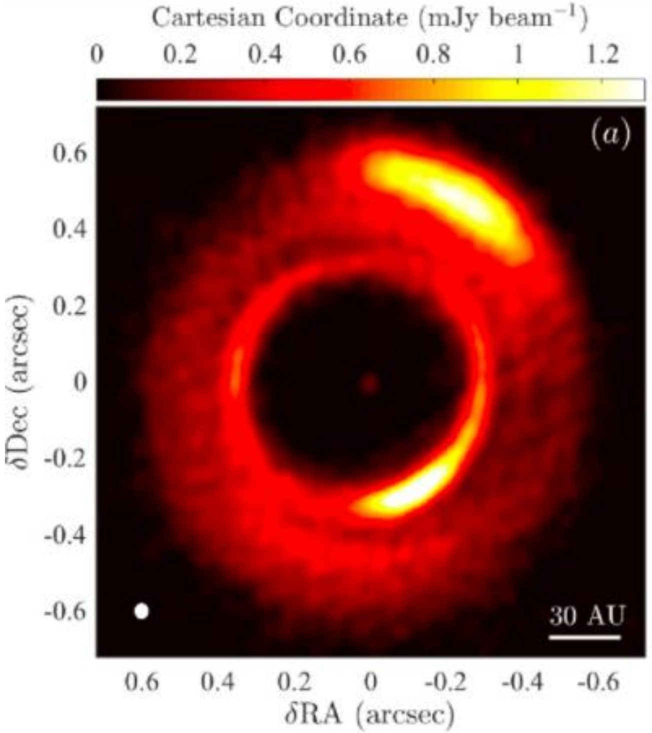

Dong+ '18

Pebble trapping

ALMA
(mm)

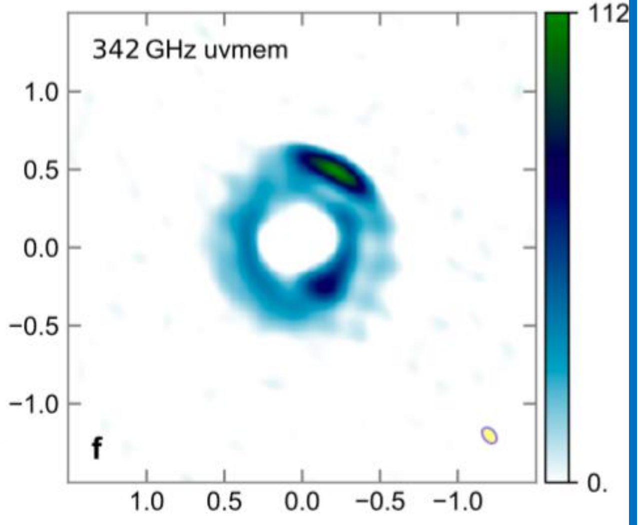

VLA
(cm-m)

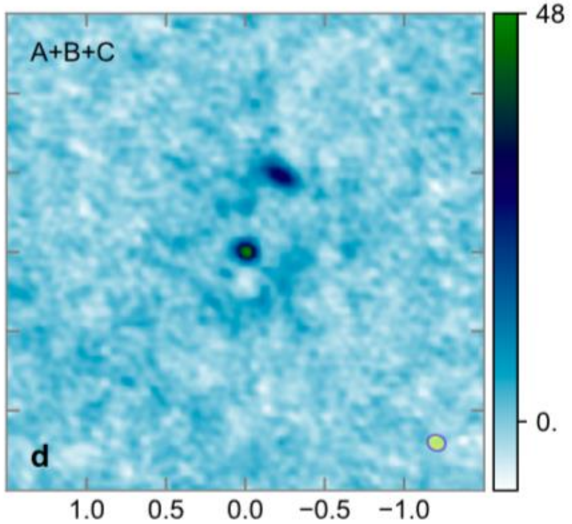

Overlay

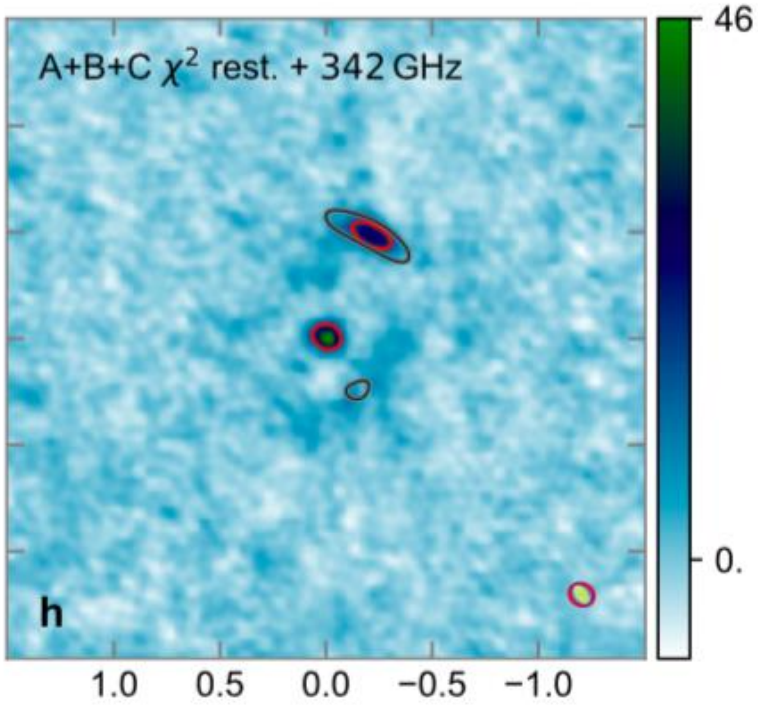

Casassus+Lyra ’19

Model vs Observation

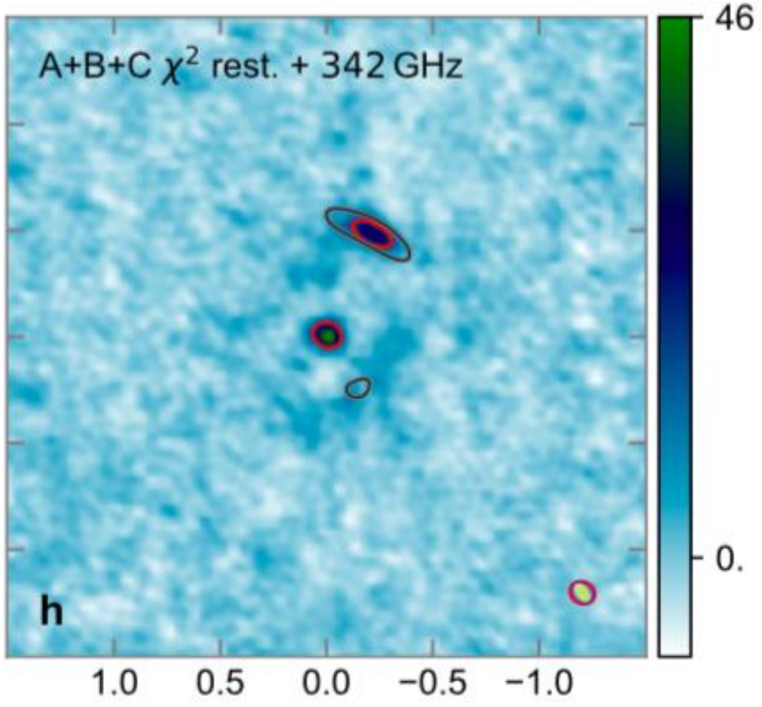

Casassus+Lyra ‘19

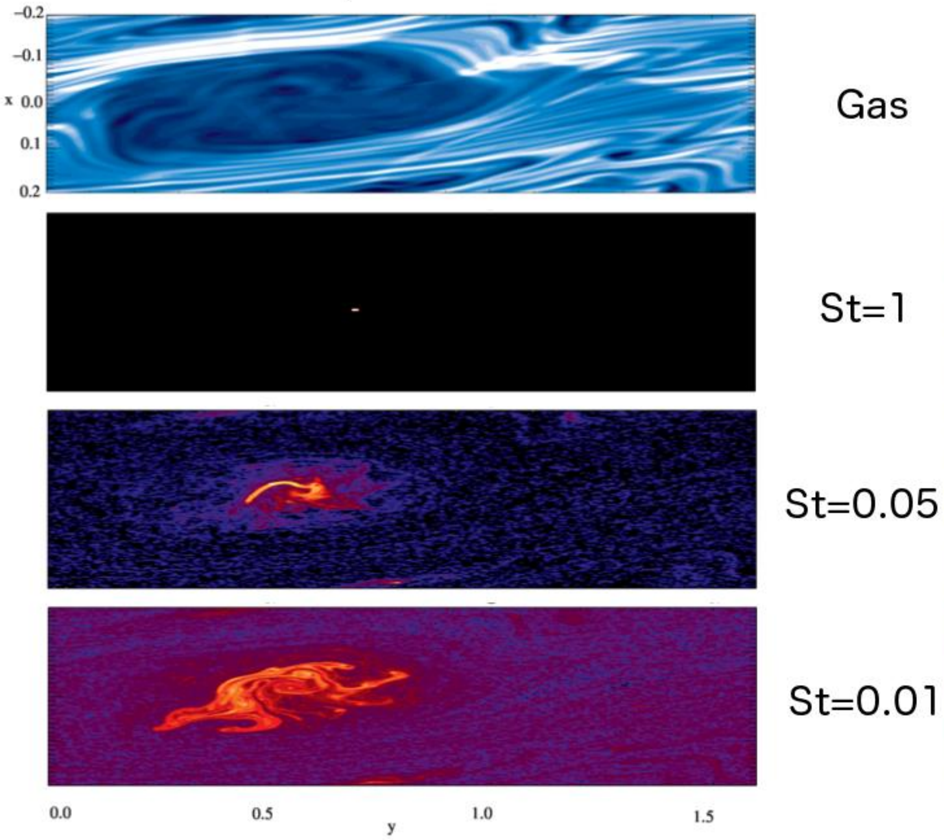

Raettig+Lyra ‘15

- Vortex-trapped dust in drag-diffusion equilibrium explains the observations

$$\rho_d(a,z) = \varepsilon\rho_0\,(S+1)^{3/2}\,\exp\left\{-\frac{[a^2 f^2(\chi)+z^2]}{2H^2}(S+1)\right\}$$

Lyra-Lin solution

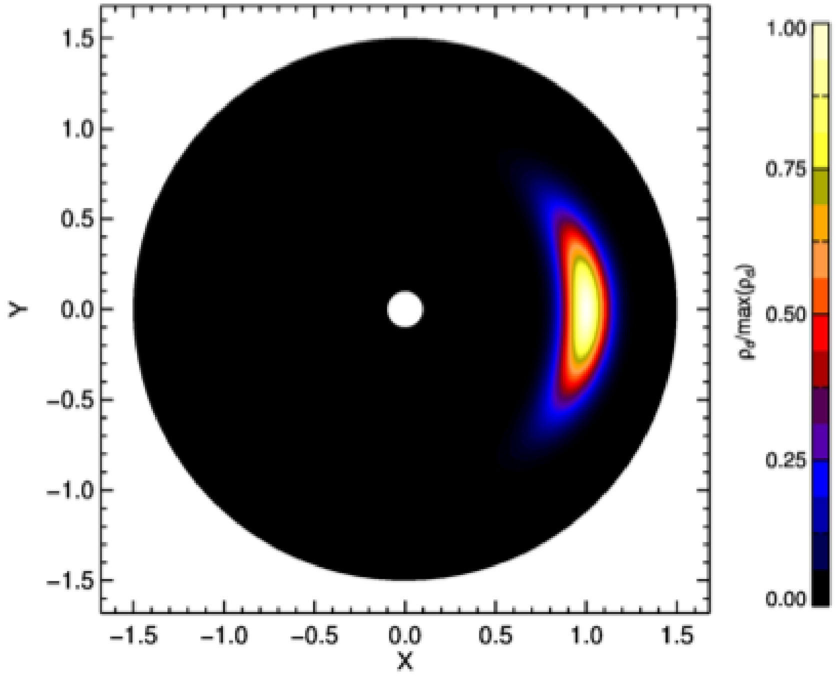

Observed Disk

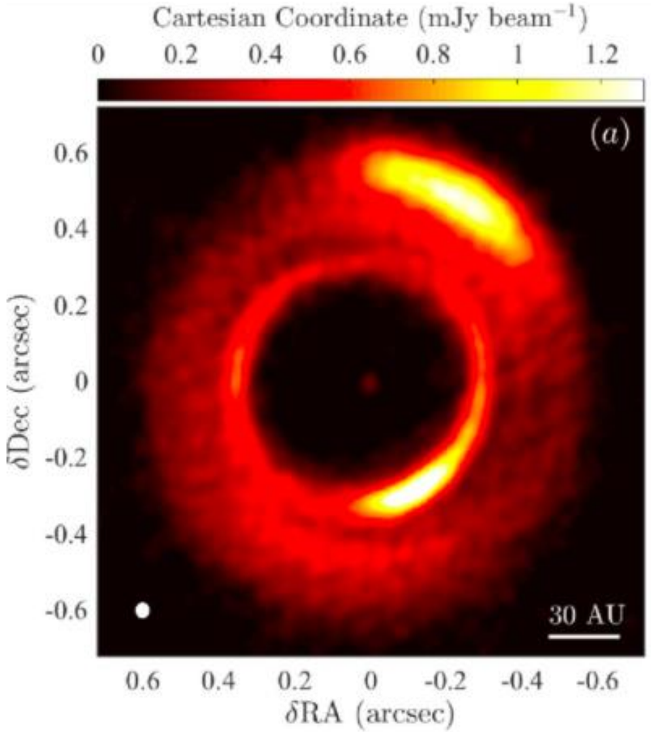

The future

After 10 years of ALMA…

Nearly all nearby disks observed at <0.1” (< 20-30AU) show substructures.

3 main types of substructures
- Crescent-shaped
- Spiral arms
- Rings/Gaps

Next Generation Very Large Array (ngVLA)

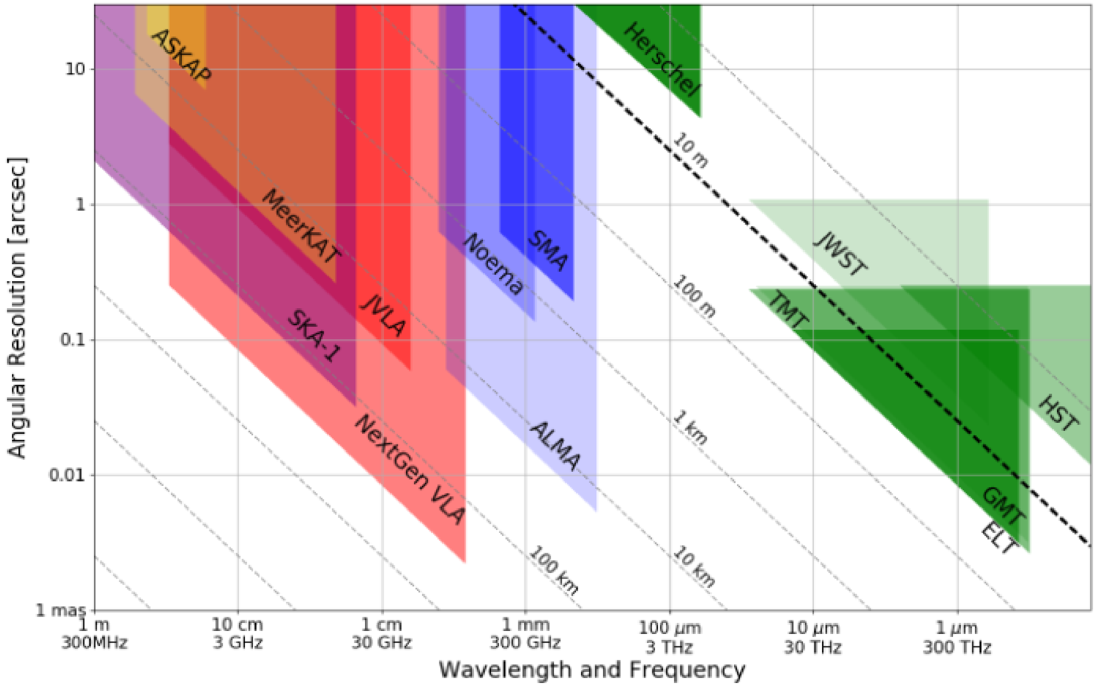

Planets at 5AU

ALMA @ 0.87mm

ngVLA @ 3mm

5 mas = 0.7 AU
rms = 5x10^{-7} Jy/beam

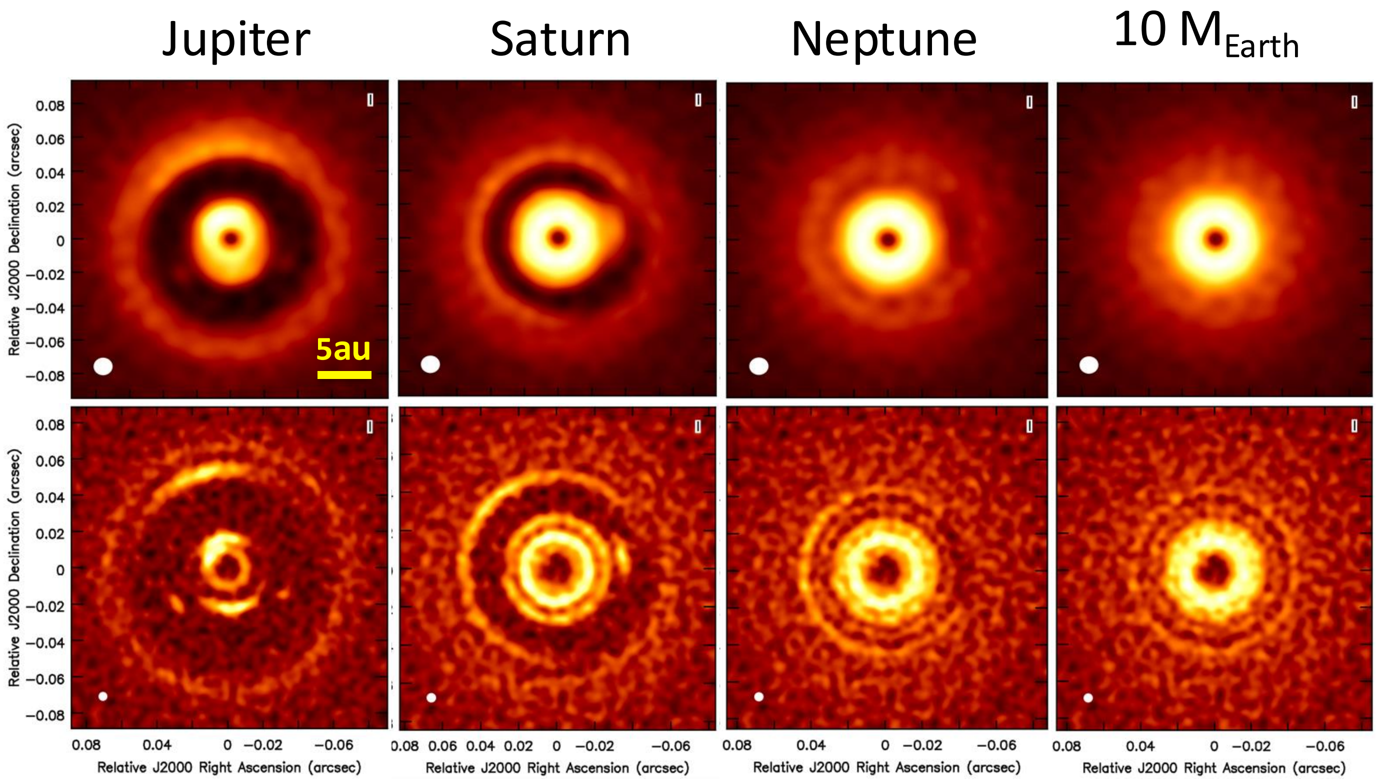

Ricci et al. 2018

ngVLA identifies gaps/substructures down to ~5-10 M_{Earth}

ngVLA: Proper motions

Jupiter at 5 AU

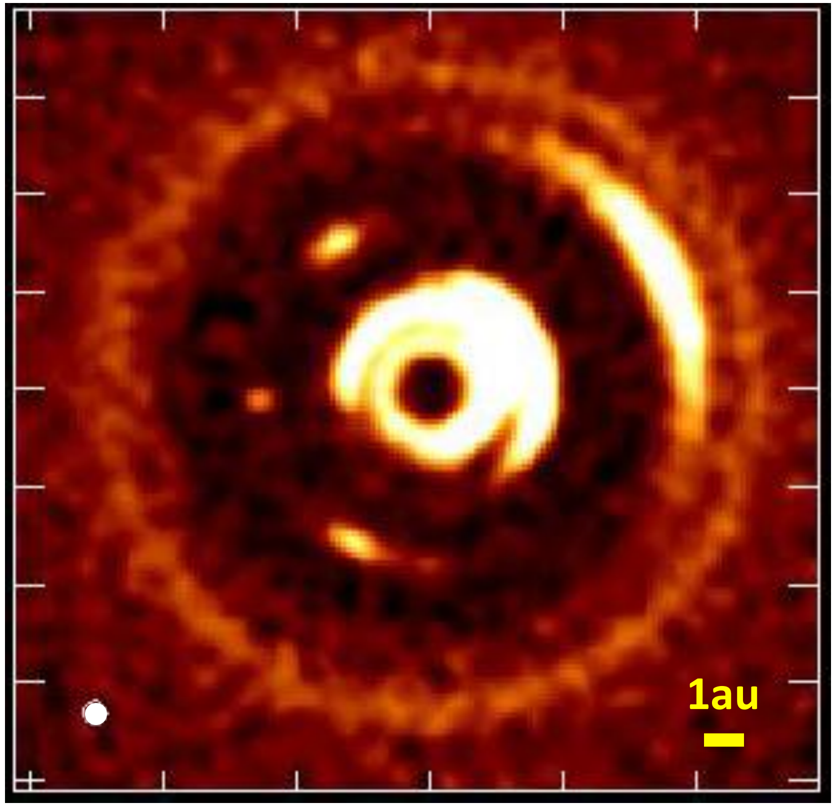

Planet Formation

"Planets form in disks of gas and dust"

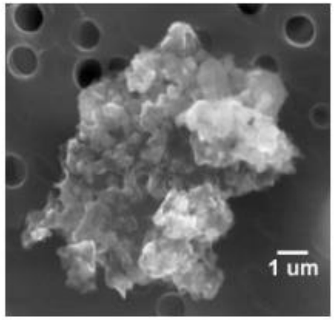

A miracle happens

Planet Formation

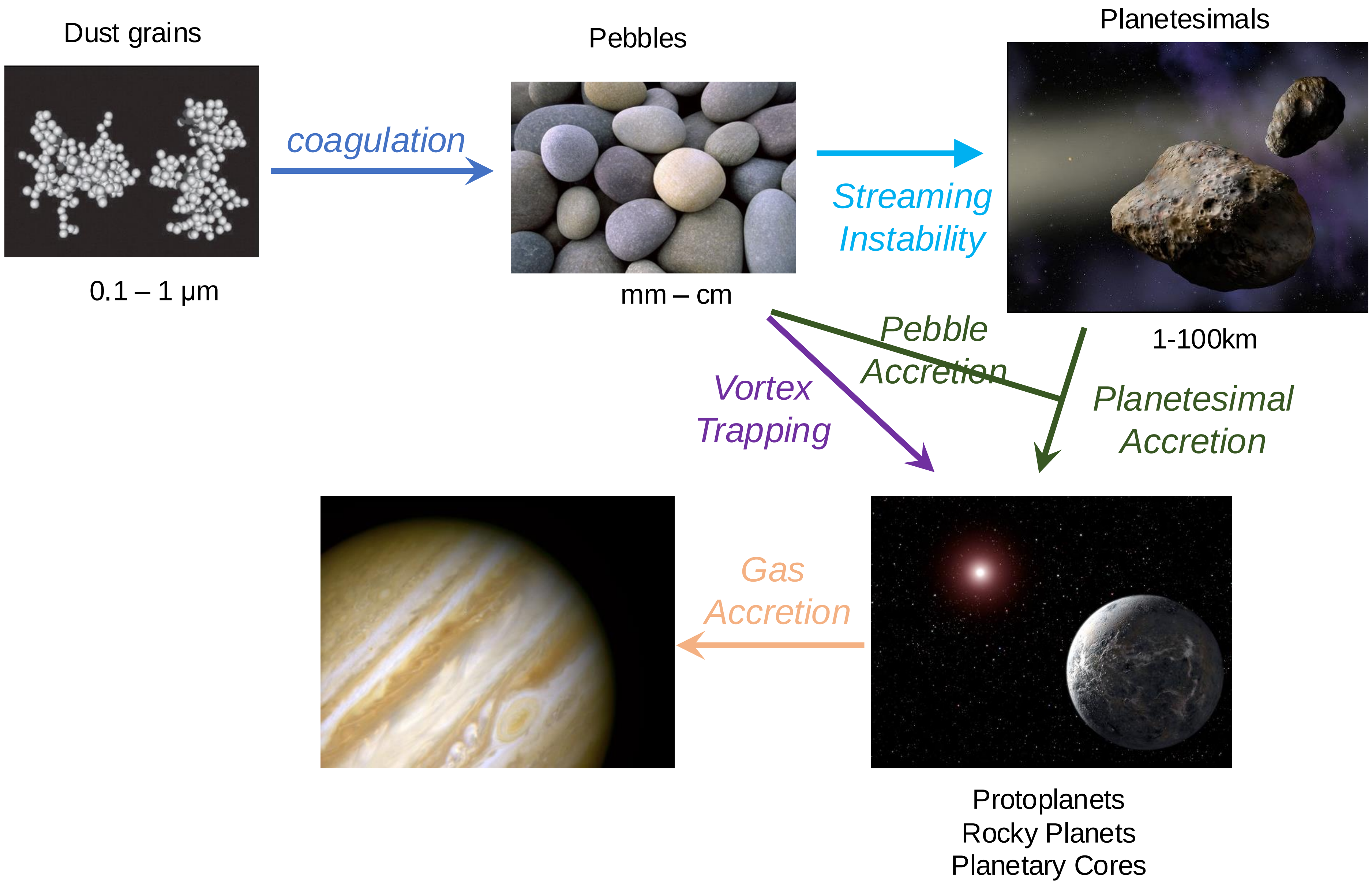

Conclusions

- Two routes for planet formation
  - Streaming instability
  - Vortex trapping

- Streaming Instability fits
  - slope of asteroid belt distribution,
  - prograde-retrograde distribution of Kuiper belt objects
  - Low density of small classical Kuiper belt objects

- Pebble accretion is a very efficient planetary growth mechanism
  - Polydisperse Bondi accretion 1-2 orders of magnitude more efficient than monodisperse
  - Silicate pebble accretion explains densities of high-mass Kuiper belt objects

- “Crescents” seen in observations of disks
  - Properties match those of vortices
  - Vortex-trapped dust in drag-diffusion equilibrium explains the observations